

Electronic Thesis and Dissertation Repository

---

4-13-2016 12:00 AM

## The Role of Sirtuin 6 in Maintaining Vascular Integrity

Sharon Z. Leung

*The University of Western Ontario*

Supervisor

Dr. J. Geoffrey Pickering

*The University of Western Ontario*

Graduate Program in Biochemistry

A thesis submitted in partial fulfillment of the requirements for the degree in Master of Science

© Sharon Z. Leung 2016

Follow this and additional works at: <https://ir.lib.uwo.ca/etd>



Part of the [Biochemistry Commons](#)

---

### Recommended Citation

Leung, Sharon Z., "The Role of Sirtuin 6 in Maintaining Vascular Integrity" (2016). *Electronic Thesis and Dissertation Repository*. 3676.

<https://ir.lib.uwo.ca/etd/3676>

This Dissertation/Thesis is brought to you for free and open access by Scholarship@Western. It has been accepted for inclusion in Electronic Thesis and Dissertation Repository by an authorized administrator of Scholarship@Western. For more information, please contact [wlsadmin@uwo.ca](mailto:wlsadmin@uwo.ca).

## Abstracts

Oxidative stress is an underlying cause for vascular pathologies including inflammation, hypertension, and atherosclerosis. Sirtuins (SIRT6) are a family of NAD<sup>+</sup> dependent deacetylases with pronounced roles in cellular metabolism and aging. SIRT6 is expressed in vascular smooth muscle cells (SMCs) and may offer protection from oxidative stress-induced damage. To study the role of SIRT6 in SMCs, we created a novel strain of SMC-specific SIRT6-deficient (SIRT6KO) mice with Cre-lox technology. Because no defects were observed in the aortas of SIRT6KO mice, they were then infused with angiotensin II (Ang II) to induce oxidative stress. Compared with vehicle controls, SIRT6KO mice developed aortitis, aortic hemorrhage, and aneurysms in response to Ang II. Therefore, we propose that SIRT6 has an anti-inflammatory role in aortic SMCs that is necessary for maintaining vessel wall integrity in the presence of oxidative stress.

## Keywords

SIRT6, vascular smooth muscle cell, angiotensin II, inflammation

## Acknowledgments

My thanks to everyone in the Pickering Lab and my advisory committee, Dr. Caroline Schild-Pouter and Dr. David O’Gorman, for their help and support throughout this project.

To Dr. Geoffrey Pickering, thank you for envisioning the project and sharing with me your passion for research, and particularly, the excitement that comes from looking down the microscope and appreciating the beauty of smooth muscle cells. I am very grateful for the opportunity to observe the logical way you approach problem solving in all projects in the lab.

To Dr. Hao Yin, thank you for your patience in teaching me all the lab techniques I had to acquire when I first started my project. Your guidance and encouragement has been invaluable in such a way that only other graduate students from the Pickering Lab can understand. Thank you Zengxuan Nong and Caroline O’Neil for the histological preparation of this mouse project. Also, thanks to Dr. Rob Gros for assisting with Ang II implantation surgeries. Thank you Alanna Watson, Brittany Balint, John-Michael Arpino, Sina Ghoreshi, Joshua Samsoundar, and my partner in crime, Krista Hawrylyshyn for your support and friendship during this whole experience.

Thanks to my parents, Gideon Leung, Serena Hsu, and all my friends from London and Toronto for their love and support. Thank you God for this chapter in my life, *Soli Deo gloria*.

# Table of Contents

Abstracts .....	i
Acknowledgments.....	ii
Table of Contents .....	iii
List of Figures .....	vi
List of Abbreviations .....	viii
Chapter 1 .....	1
1 Introduction .....	1
1.1 General Introduction .....	1
1.2 Vasculature and Cellular Composition of the Vessel Wall .....	1
1.2.1 Layers of the Arterial Wall .....	2
1.3 Oxidative Stress in the Vascular Wall .....	5
1.3.1 Angiotensin II Induces Oxidative Stress.....	6
1.3.2 Effects of Oxidative Stress in Vascular Inflammation and Atherosclerosis	7
1.3.3 Oxidative Stress-Induced DNA Damage in SMC .....	8
1.4 The Role of NAD <sup>+</sup> Consuming Enzymes in Managing Oxidative Stress.....	9
1.4.1 NAD <sup>+</sup> Biosynthesis and Consumption Pathways .....	9
1.4.2 PARPs .....	10
1.4.3 Sir2 and Sirtuin family .....	11
1.4.4 Sirtuin 1.....	12
1.4.5 Sirtuin 2.....	14
1.4.6 Sirtuin 3.....	15
1.4.7 Sirtuin 4.....	18
1.4.8 Sirtuin 5.....	19
1.4.9 Sirtuin 7.....	20

1.5 Sirtuin 6.....	21
1.5.1 SIRT6 Knockout and Transgenic Animal Models.....	21
1.5.2 SIRT6 in Lipid and Glucose Metabolism .....	22
1.5.3 SIRT6 in Genomic Stability.....	25
1.5.4 SIRT6 in Inflammation .....	25
1.5.5 SIRT6 in Cardiovascular Disease .....	26
1.6 Aims and Hypothesis .....	28
Chapter 2.....	30
2 Materials and Methods .....	30
2.1 Animals .....	30
2.2 Induction of SIRT6 Deficiency and Angiotensin II Treatment .....	32
2.2.1 Cre-Lox Recombination Induced by Tamoxifen .....	32
2.2.2 Angiotensin II Treatment.....	32
2.2.3 Blood Pressure Measurements .....	34
2.3 Qualitative Analysis of Aortic Media DNA .....	34
2.4 Quantitative Real-Time PCR Analysis for Gene Abundance.....	36
2.5 Immunoblotting.....	36
2.6 Histology.....	37
2.6.1 Characterization of Cell Infiltration and Aortic Wall Destruction .....	39
2.7 Immunohistochemistry .....	39
2.8 Statistical Analysis.....	39
Chapter 3.....	41
3 Results .....	41
3.1 Confirmation of SIRT6 Knockdown in Aortic Medial DNA, mRNA, and Protein in Novel Mouse Strain .....	41
3.2 SIRT6-Deficient Aortas Appear Healthy.....	45

3.3	Ang II-Infusion Induces Inflammatory Aortic Wall Destruction in SMC-specific SIRT6-Deficient Mice .....	49
3.3.1	Saline-Infused Corn Oil and Tamoxifen Injected Mice have Healthy Aortas .....	49
3.3.2	Ang II-Infusion causes Aortic Petechial Hemorrhage in SMC-specific SIRT6-Deficient Mice .....	51
3.3.3	Ang II-Infusion causes Aortic Aneurysms in SMC-specific SIRT6-Deficient Mice .....	54
3.3.4	Evidence of an Inflammatory Cell Infiltrate in Ang II-Infused SIRT6-Deficient Mice and Minor Cell Infiltration in the Vehicle Control .....	57
3.3.5	Ang II-Induced Hypertensive Response in Vehicles and SIRT6KO Mice	62
4	Discussion .....	64
4.1	Oxidative Stress Causes Aortic Wall Destruction in the Absence of SIRT6 .....	64
4.1.1	Petechial Hemorrhage and Aneurysm .....	64
4.1.2	Aortitis .....	66
4.1.3	Hypertension .....	68
4.1.4	Protective Effect of SIRT6 in SMCs .....	68
4.2	Reflections on Vascular Inflammation in Ang II-Infused Vehicle Controls and Cre-lox Technology .....	69
4.2.1	Hypotheses for Aortic Phenotype in Vehicle Controls .....	69
4.2.2	Creating SIRT6 <sup>f/f</sup> Cre-negative Controls .....	71
4.3	Conclusion .....	71
	References .....	72
	Appendices .....	93
	Curriculum Vitae .....	94

## List of Figures

Figure 1.1 Schematic of the three layers in the arterial wall: intima, media, adventitia.....	4
Figure 1.2 SIRT6 is expressed in cultured SMCs and may play a role in resistance to oxidative stress.....	29
Figure 2.1 SMC-specific SIRT6KD Mouse Breeding Strategy.....	31
Figure 2.2 Schematic of an inducible smooth muscle cell-specific SIRT6 knockdown using the Cre-Lox System. ....	33
Figure 2.3 Experimental timeline for Angiotensin II-induced aortic stress.....	35
Figure 2.4 Schematic diagram of aortic regional segments.....	38
Figure 2.5 Grading criteria for degree of cell infiltration and aortic wall destruction.....	40
Figure 3.1 Evidence of recombination allele present in the smooth muscle of SMMHC-CreERT2;SIRT6 <sup>f/f</sup> mice. ....	42
Figure 3.2 SIRT6 knockdown in mRNA expression and protein in aortic SMCs.....	44
Figure 3.3 Gross aortic morphology, aortic morphometry, and aortic histology appear normal after induction of SIRT6 knockdown. ....	48
Figure 3.4 Aortic morphometry and histology appear normal in the saline-infused in SIRT6KD mouse.....	50
Figure 3.5 Ang II-infusion causes petechial hemorrhage in SMC-specific SIRT6KO aortas.	53
Figure 3.6 Ang II-infusion causes aortic aneurysms in SMC-specific SIRT6KO mice. ....	56
Figure 3.7 Ang II-infusion of SIRT6KO mouse shows greater degree of inflammatory cell infiltration and aortic wall destruction compared to vehicle-control.....	61
Figure 3.8 Aortic mean arterial blood pressures of vehicle and tamoxifen-injected mice after saline/Ang II-infusion. ....	63

Figure 4.1 Diagram depicting the difference between aortic dissection and intramural  
hematoma..... 65



## List of Abbreviations

<b>Abbreviation</b>	<b>Meaning</b>
ACE	Angiotensin-converting enzyme
ADP	Adenosine diphosphate
Ang II	Angiotensin II
AMPK	AMP-activated protein kinase
ATM	Ataxia telangiectasia mutated
ATR	Ataxia telangiectasia and Rad3-related protein
AT <sub>1</sub> R and AT <sub>2</sub> R	Angiotensin type 1 and 2 receptor
BAT	Brown adipose tissue
BER	Base excision repair
CPS1	Carbamoyl phosphate synthetase 1
CtIP	C-terminal binding protein interacting protein
CVD	Cardiovascular disease
DDR	DNA damage response
DNA	Deoxyribonucleic acid
DNA-PKcs	DNA-dependent protein kinase catalytic subunit
DSB	Double-strand breaks
EC	Endothelial cell
ECM	Extracellular matrix
EGF	Epidermal growth factor
eNOS	Endothelial nitric oxide synthase
FAO	Fatty acid oxidation
FOXO	Forkhead box protein O
G6P	Glucose-6-phosphatase
GAPDH	Glyceraldehyde 3-phosphate dehydrogenase
GCN5	General control nonrepressed protein
GDH	Glutamate dehydrogenase
GH	Growth hormone
GK	Glucokinase
GLUT1, 4	Glucose transporter 1 and 4

HDAC	Histone deacetylase
HIF1 $\alpha$	hypoxia-inducible factor 1 $\alpha$
H <sub>2</sub> O <sub>2</sub>	Hydrogen peroxide
HMGCS2	3-hydroxy-3-methylglutaryl-CoA synthase 2
HR	Homologous recombination
ICAM-1	Intercellular cell adhesion molecule-1
IDE	Insulin-degrading enzyme
IDH2	Isocitrate dehydrogenase 2
IGF1	Insulin-like growth factor 1
IL1	Interleukin-1
IL1B	Interleukin-1 beta
IL6	Interleukin-6
IFN $\gamma$	Interferon- $\gamma$
LCAD	Long-chain acyl coenzyme A dehydrogenase
LDH	Lactate dehydrogenase
LDL	Low-density lipoprotein
LPK	Liver pyruvate kinase
MCD	Malonyl CoA decarboxylase
MEF	Mouse embryonic fibroblast
MMP-9	Matrix metalloproteinase-9
NAM	Nicotinamide
NAD <sup>+</sup>	Nicotinamide adenine dinucleotide
NAD(P)H	Nicotinamide adenine dinucleotide (phosphate)
NAMPT	Nicotinamide phosphoribosyltransferase
NBS1	Nijmegen Breakage Syndrome-1
NDUFA9	NADH dehydrogenase [ubiquinone] 1 alpha subcomplex subunit 9
NHEJ	Non-homologous end joining
NF- $\kappa$ B	Nuclear factor kappa B
NO	Nitric oxide
NR	Nicotinamide riboside
OAADPr	<i>O</i> -acetyl-ADP ribose

OH <sup>•</sup>	Hydroxyl radical
O <sub>2</sub> <sup>•-</sup>	Superoxide anion
OTC	Ornithine transcarbamoylase
PAF53	Polymerase-associated factor 53
PAR	Poly(ADP-ribose)
PARP	Poly (ADP-ribose) polymerase
PCK1	Phosphoenolpyruvate carboxykinase
PCSK9	Proprotein convertase subtilisin kexin type 9
PDC	Pyruvate dehydrogenase complex
PDGF	Platelet-derived growth factor
PDHA1	Pyruvate dehydrogenase alpha 1
PDP	Pyruvate dehydrogenase phosphatase
PFK-1	Phosphofructokinase-1
PGC-1 $\alpha$	Peroxisome proliferator-activated receptor gamma coactivator 1-alpha
PI3K	Phosphoinositide 3-kinase
Pol I	RNA polymerase I
PPAR $\alpha$	Peroxisome proliferator-activated receptor alpha
PPAR- $\gamma$	Peroxisome proliferator-activated receptor gamma
rDNA	Ribosomal DNA
ROS	Reactive oxygen species
SA- $\beta$ -gal	Senescence-associated beta-galactosidase
SdhA	Succinate dehydrogenase flavoprotein
SIPS	Stress-induced premature senescence
SIR	Silent information regulator
SIRT	Sirtuin
SMC	Smooth muscle cell
SMMHC	Smooth muscle-myosin heavy chain
SOD	Superoxide dismutase
SREBP1/2	Sterol regulatory element binding proteins 1 and 2
SSB	Single-strand breaks
TCA	Tricarboxylic acid

TG	Triglycerides
TGF- $\beta$	Transforming growth factor- $\beta$
TNF- $\alpha$	Tumor necrosis factor- $\alpha$
TPI	Triose phosphate isomerase
UBF	Upstream binding factor
VCAM-1	Vascular cell adhesion molecule-1
WAT	White adipose tissue
XO	Xanthine oxidase

## Chapter 1

### 1 Introduction

#### 1.1 General Introduction

Cardiovascular disease (CVD) remains the leading cause of death worldwide, a fact that drives ongoing research towards its prevention and intervention. To many, CVD such as coronary artery disease, hypertension, congestive heart failure, and stroke have become household terms. Overall cardiovascular well-being is dependent on the condition of our blood vessels, which ultimately points toward the health of cells comprising the vasculature, including endothelial cells (ECs), vascular smooth muscle cells (SMCs), and other cell types resident in the vascular wall. It is fundamental to understand the biology of the vascular wall and the cellular constituents for the prevention and treatment of CVDs.

#### 1.2 Vasculature and Cellular Composition of the Vessel Wall

The vasculature is an intricate network of blood vessels that transports blood between the heart and peripheral parts of our body. Oxygen, nutrients, and other circulating factors, such as hormones, are carried through the blood. Of the three main types of vessels—arteries, veins, and capillaries—arteries carry oxygenated blood away from the heart, veins carry deoxygenated blood to the heart, and capillaries are responsible for delivering all the aforementioned components of blood flow to end organs. Exceptions are found in the pulmonary vasculature with pulmonary arteries carrying deoxygenated blood away from the heart and pulmonary veins carrying oxygenated blood to the heart.

The vessel wall is made up of three distinct layers that are comprised of different cell types and have unique characteristics that contribute to the overall functionality of the blood vessel. The innermost layer, tunica intima, is made up of a single layer of endothelial cells. The middle layer, tunica media, has many concentric layers of vascular SMC and elastin fibers. The outer and most diverse layer, tunica adventitia, is comprised of a collagen-rich extracellular matrix (ECM) containing fibroblasts, progenitor cells, nerves, adipocytes, immune cells, and a microvascular network known as the vasa vasorum [1].

Although veins and arteries have the same three layers, arterial walls have a substantially thicker media to withstand direct pressure from cardiac output as well as high oxygen content. An overall decrease in wall thickness, elastin, and collagen result in veins that are less stiff than arteries [2]. In contrast, capillaries are comprised of a one cell layer thick endothelium wrapped with pericytes. There are three types of capillary EC structure: continuous, fenestrated, and discontinuous. These differences are indispensable for simultaneously producing continuous capillaries in the blood brain barrier to block out toxic substances and fenestrated capillaries in the glomerulus to allow for the filtration of blood [3].

## 1.2.1 Layers of the Arterial Wall

### 1.2.1.1 Intima

Vascular ECs in the intima regulate blood flow through the production of nitric oxide (NO), a vasodilator that controls the tone of vascular SMC [4]. Direct contact with the lumen allows ECs to act as border guards that control wall permeability. ECs prevent unwanted plasma proteins from moving into the wall through their tight junctions as well as facilitate leukocyte extravasation in cases of injury or damage [4].

### 1.2.1.2 Media

In large arteries such as the aorta, the media is by far the thickest layer, therefore, making vascular SMCs the major constituents of the aortic wall and the cell type of interest for this project. In mice, there are 3-6 concentric layers of SMCs and elastin fibers depending on which aortic region is under observation. The greatest number of layers are found in aortic root media with progressively fewer layers the more distal it is to the heart.

The media exclusively consists of SMCs and the associated ECM during embryonic development (i.e. collagen, elastin fibers, proteoglycans). The primary role of SMCs is to mediate contraction and relaxation of the arterial wall, which is indispensable for efficient regional distribution of blood flow into different tissues. Compared to smaller arteries, aortas have increased collagen content for vessel wall strength [5]. This combined with

higher quantities of elastin give the aorta the ability to simultaneously stretch and also withstand the highest levels of blood pressure coming directly out of the heart [5].

Of greater interest to this project, the other main responsibility of SMCs is its response to injury and repair of the vessel wall. Both roles are realized due to the profound phenotypic plasticity of SMCs, setting them apart from striated (skeletal or cardiac) muscle cells.

Normal “contractile” SMCs are characterized by a very low rate of proliferation and expression of proteins and signaling molecules necessary for contraction. These include proteins such as SM  $\alpha$ -actin, smooth muscle-myosin heavy chain (SMMHC), h<sub>1</sub>-calponin, SM22 $\alpha$ , and smoothelin [6]. Morphologically, they appear long and spindle-shaped [7]. Being the only protein found exclusively in SMCs, SMMHC is currently the most specific marker protein for identifying contractile SMC. Other contractile proteins mentioned previously are also expressed in cardiomyocytes, myofibroblasts, and endothelial cells during vascular remodeling [6,7]. In the event of vascular damage, SMCs respond to either acute or chronic stimuli with a phenotypic change in protein expression. The switch is facilitated via ligand-receptor interactions and epigenetic modifications, respectively. Platelet-derived growth factor-BB (PDGF-BB) is a key repressor of vascular SMC-specific gene expression while TGF- $\beta$  a major promoter of it [8]. These rhomboid-shaped “synthetic” SMCs have an increased ability to synthesize ECM components, proliferate, and migrate [6].

### 1.2.1.3 Adventitia

Because the adventitia is home to such a variety of cell types, its function is expectedly complex. The adventitia serves as a storehouse for many types of progenitor cells (e.g. endothelial, mesenchymal, SMC, pericyte) [1]. A large population of fibroblasts, macrophages, and dendritic cells allows the adventitia to have one of the first inflammatory responses to vascular stressors.

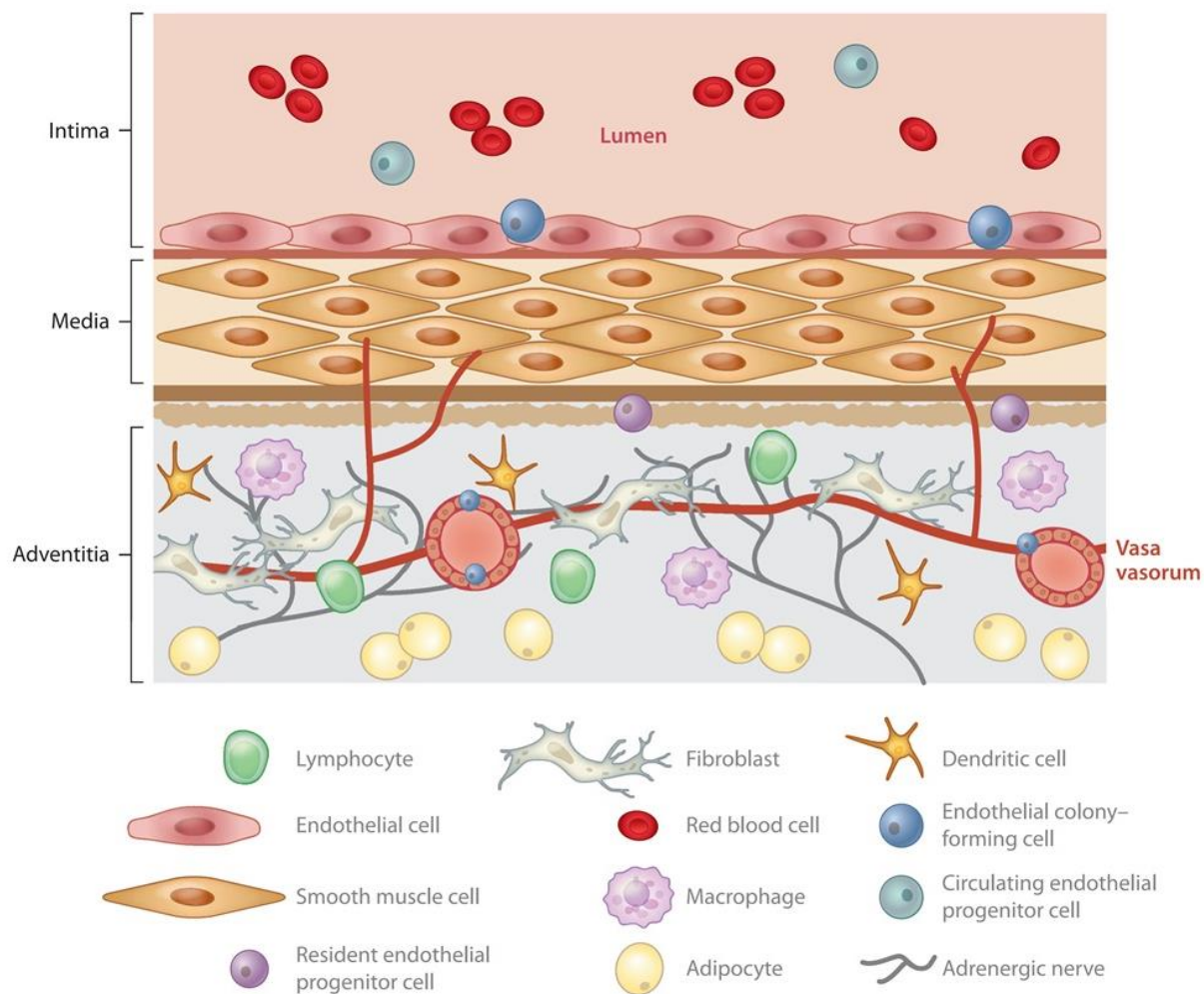


**Figure 1.1 Schematic of the three layers in the arterial wall: intima, media, adventitia.**

The intima and media are comprised of endothelial cells and smooth muscle cells, respectively. The adventitia is host to a variety of cell types and the wall's main blood source, the vasa vasorum. (Image adapted from Stenmark 2013 [1])



### 1.3 Oxidative Stress in the Vascular Wall

Of the various insults that can threaten the integrity of the vascular wall, oxidative stress is a common denominator among vascular diseases. Vascular cells naturally produce reactive oxygen species (ROS) such as hydroxyl radicals ( $\text{OH}^\bullet$ ), superoxide anion ( $\text{O}_2^{\bullet-}$ ), and hydrogen peroxide ( $\text{H}_2\text{O}_2$ ). During aerobic metabolism, low levels of ROS are formed as a byproduct from the reduction of oxygen and used to regulate SMC contraction [9]. Oxidant enzyme systems that facilitate these reactions include nicotinamide adenine dinucleotide phosphate hydrogen (NAD(P)H) oxidase, xanthine oxidase (XO), myeloperoxidase, and endothelial nitric oxide synthase (eNOS) [10]. ROS generation as a consequence of oxidative phosphorylation also makes the mitochondria a major source of ROS [11]. However, the aforementioned enzymes have been implicated in the development of vascular pathologies that make them of particular interest to this project. In particular, NAD(P)H oxidase accounts for the majority of ROS in all vascular cells [9]. Different isoforms of this multi-subunit protein are found in ECs, vascular SMCs, and adventitial fibroblasts [10] and activated by vascular injury (e.g. cytokines, hormones, and hemodynamic forces) [12]. Consequently, an increase in intracellular ROS results in impaired vessel tone; an exaggerated inflammatory response; and SMC hypertrophy, hyperplasia, and apoptosis [13]. To protect against accumulation of ROS, endogenous antioxidants such as superoxide dismutase (SOD) convert superoxide radicals into  $\text{H}_2\text{O}_2$  [10]. From that point on, catalase and glutathione peroxidase further catalyze  $\text{H}_2\text{O}_2$  into water and oxygen [14].

Whether caused by increased oxidase activity or deficient removal by antioxidants, excess ROS exert their detrimental effects through uncontrolled oxidation of deoxyribonucleic acid (DNA), proteins, and lipids [10]. Structural changes in such biological molecules result in defective DNA replication and transcription, decreased enzymatic activity, and loss of membrane permeability. Accordingly, oxidative stress is the term given for collective ROS-induced damage in cells. In vascular cells, oxidative stress has a role in the advancement of various cardiovascular pathologies that will be discussed in the following sections.

### 1.3.1 Angiotensin II Induces Oxidative Stress

A diverse range of molecules activate NAD(P)H oxidase and increase ROS production: growth factors (e.g. platelet-derived growth factor (PDGF), epidermal growth factor (EGF), transforming growth factor- $\beta$  (TGF- $\beta$ ), thrombin), cytokines (e.g. angiotensin II (Ang II), interferon- $\gamma$  (IFN $\gamma$ ), interleukin-1 (IL1), tumor necrosis factor- $\alpha$  (TNF- $\alpha$ )), lipids (e.g. low-density lipoprotein (LDL) cholesterol, oxidized LDL), and even ROS (i.e. H<sub>2</sub>O<sub>2</sub>) [14].

Ang II is one of the most potent and well-studied stimuli of NAD(P)H oxidase. It is the most important effector of the blood pressure-regulating renin angiotensin system. Through a series of cleavage reactions, angiotensinogen is converted to angiotensin I, which is then converted to Ang II through angiotensin-converting enzyme (ACE). Ang II can then be further cleaved by ACE2 into Ang-(1-7) [15]. As a result, ACE and ACE2 are potential targets for diminishing the potential harmful effects of Ang II by controlling the production and degradation of the peptide. This peptide hormone carries out its effects through angiotensin type 1 and 2 receptor, AT<sub>1</sub>R and AT<sub>2</sub>R, respectively [16]. However, Ang II's harmful effects are predominantly carried out through AT<sub>1</sub>Rs expressed in liver, adrenals, brain, lung, kidney, heart, and vasculature. In vascular SMCs, Ang II binding to AT<sub>1</sub>R initiates a G-protein-dependent signaling pathway that triggers an influx of Ca<sup>2+</sup> from the sarcoplasmic reticulum into the cell [17]. This increases the interaction of actin and myosin filaments, resulting in vasoconstriction and elevated blood pressure over time. Prolonged Ang-II infusion was shown to induce hypertension in mice, rats, rabbits, and humans [18].

The AT<sub>1</sub>R-initiated G-protein-dependent pathway also serves to activate NAD(P)H oxidase [16]. This is mediated through intracellular signaling molecules upstream of NAD(P)H (e.g. phospholipase D, protein kinase C, c-Src, phosphoinositide 3-kinase (PI3K), Rac) [15]. Moreover, Ang II increases the abundance of essential NAD(P)H oxidase subunits (e.g. gp91phox, p22phox, p47phox) [19]. There are many studies that confirm the association between Ang II, NAD(P)H, oxidative stress, and hypertension. Ang II-infusion increased both blood pressure and vascular O<sub>2</sub><sup>-</sup> levels in mice. p47phox deficiency was enough to blunt the hypertension and eliminate increases in O<sub>2</sub><sup>-</sup> [20].

Another mouse study generated similar decreases in Ang II-induced hypertension and  $O_2^{\cdot-}$  production using a peptide that inhibited interaction between NAD(P)H subunits, gp91phox and p47phox [21]. Two different rat models of hypertension showed that increased NAD(P)H activity was correlated with elevated Ang II levels [22] or was brought down by treatment with an AT<sub>1</sub>R antagonist [23].

### 1.3.2 Effects of Oxidative Stress in Vascular Inflammation and Atherosclerosis

Atherosclerosis is a disease characterized by chronic inflammation that begins as a local response to endothelial damage. As the disease progresses, oxidized LDLs, inflammatory cells, and SMCs form a plaque comprised of a lipid core protected by a fibrous cap [24]. The presence of increased ROS and upregulation of NAD(P)H oxidase subunits in all layers of the diseased wall indicate a positive correlation between oxidative stress and atherosclerosis [14]. One of the initial effects of ROS is the oxidization of LDL particles that have invaded the subendothelium. A proinflammatory environment is created as ECs secrete signals such as TNF- $\alpha$  and Ang II. Both cytokines induce the expression of vascular cell adhesion molecule-1 (VCAM-1) and intercellular cell adhesion molecule-1 (ICAM-1), thereby drawing leukocytes into the vascular wall [13].

Once in the wall, monocytes mature into macrophages that generate even more ROS [24]. Macrophages that take up oxidized LDL become foam cells which eventually aggregate and form the core of an atherosclerotic plaque. In addition to those processes,  $O_2^{\cdot-}$  inactivates EC-secreted NO; therefore, disrupting its important vasodilatory and anti-inflammatory effects of on both ECs and vascular SMCs [13]. In the course of plaque development, SMCs proliferate and are recruited in an attempt to stabilize the lesion with ECM that they produce. PDGF triggers SMC proliferation and migration in a ROS-dependent manner [10].

In summary, ROS are extensively involved in all phases of atherosclerosis. Oxidative stress is crucial in initiating the inflammatory response as well as propagating it throughout the vascular wall.

### 1.3.3 Oxidative Stress-Induced DNA Damage in SMC

In addition to attacking proteins and lipids, free radicals have the ability to oxidize DNA. Because hydroxyl radicals react readily with both purines and pyrimidines, it has the potential to form DNA adducts with all bases. This leaves DNA susceptible to single strand breaks (SSBs), double-strand breaks (DSBs), and base modifications [25]. An example of a common site of hydroxyl radical attack is carbon 8 on guanine (8-oxo-guanine). This base modification has received special attention because of its ability to avoid detection by the DNA repair system and high mutagenicity (i.e. 8-oxo-G mis-pairs with adenine; therefore, causing a guanine to thymine mutation) [26]. The consequences of DNA damage in a cell can be devastating: mis-pairings of bases during replication, interruption of transcription, and overall increased mutagenesis [26].

Accumulation of oxidative stress-induced DNA damage can cause cellular senescence, a state of permanent cell cycle arrest. Cells naturally lose the ability to divide as they age and telomere lengths shorten from multiple rounds of replication [27]. As telomeres are tandem repeats of nucleotide sequences at the ends of chromosomes, they protect the cell from losing important coding and noncoding sequences during replication. Therefore, shortened telomeres signal cell cycle arrest as a defensive measure against the malignant transformation that is seen in cancer cells [28]. Cells remain viable until eventually succumbing to apoptosis through activation of the tumor suppressor, p53 [27].

Aside from replicative senescence, cells exposed to external stimuli such as irradiation and oxidative stress undergo stress-induced premature senescence (SIPS) that is largely independent of telomere status [27]. The senescence is considered premature because cells of similar age that are not exposed to such insults have normal proliferation rates. DNA damage from ROS triggers the DDR mentioned earlier; therefore, causing the cell to stop dividing until repairs can be made. An unsuccessful attempt results in senescence and inevitably, apoptosis through p53 signaling [29]. Relatedly, ROS are implicated in telomere-based senescence because of their ability to induce DNA strand breaks in telomeres [30]. This can exacerbate the DDR already triggered by telomere shortening during replication and further accelerate telomere loss.

The association of oxidative stress with both telomere-based senescence and SIPS demonstrates the connection between the two different types of cellular senescence. Cultured aortic SMCs from aged mice produced higher levels of ROS with decreased proliferation compared to cells from younger mice [31]. Another study showed that expression of telomerase, an enzyme that facilitates telomere extension, delayed SMC senescence *in vitro* [32]. Furthermore, vascular SMCs in an *in vivo* atherosclerotic model show this overlap particularly well. Plaque vascular SMC showed a positive correlation between markers of senescence (i.e. senescence-associated beta-galactosidase (SA- $\beta$ -gal) and p16) and oxidative stress-induced DNA damage (i.e. 8-oxo-guanine) and had shorter telomere lengths compared to normal vessel SMC [32].

## 1.4 The Role of NAD<sup>+</sup> Consuming Enzymes in Managing Oxidative Stress

Nicotinamide adenine dinucleotide (NAD<sup>+</sup>) and its reduced form NADH were first discovered as electron carriers in cellular oxidation/reduction reactions. For many decades, NAD<sup>+</sup> was mainly known as a cofactor for enzymes in energy metabolism pathways such as glycolysis and oxidative phosphorylation [33]. In contrast to its usage in redox reactions where it can be recycled over and over again, NAD<sup>+</sup> has only recently been discovered to be consumed as a cosubstrate in biochemical reactions.

### 1.4.1 NAD<sup>+</sup> Biosynthesis and Consumption Pathways

There are three major classes of enzymes that deplete cellular NAD<sup>+</sup> levels: cyclic adenosine diphosphate (cADP)-ribose synthases, adenosine diphosphate (ADP)-ribose transferases, and sirtuins (SIRTs) [34]. Therefore, NAD<sup>+</sup> deficiency disrupts the many crucial pathways that these enzymes participate in. cADP-ribose synthase is involved in calcium signaling. It uses NAD<sup>+</sup> to make cADP-ribose, a second messenger that triggers the release of calcium from intracellular stores [35]. The poly (ADP-ribose) polymerase (PARP) family of proteins are the most prevalent ADP-ribose transferases. PARPs detect DNA damage, bind to those sites, and form poly (ADP)-ribose (PAR) chains using NAD<sup>+</sup>. These chains recruit other DNA repair factors to initiate a cascade of DNA repair events [35]. Out of the three classes of enzymes mentioned previously, SIRTs were the last NAD<sup>+</sup>

consumers to be discovered. This family of deacetylases requires NAD<sup>+</sup> to catalyze the removal of acetyl groups from proteins. SIRT6s have been considered regulators of mammalian healthspan because of their impact on energy metabolism, cellular stress resistance, genomic stability, aging, and tumorigenesis [36].

Naturally, discovery of NAD<sup>+</sup> consumption pathways stemmed renewed interest in enzymes of NAD<sup>+</sup> biosynthesis. NAD<sup>+</sup> is synthesized *de novo* from the amino acid L-tryptophan that comes from dietary intake. The majority of NAD<sup>+</sup>, however, is generated from the salvage pathway which uses other NAD<sup>+</sup> precursors from our diet (e.g. nicotinamide (NAM), nicotinamide riboside (NR), nicotinic acid) [34]. Nicotinamide phosphoribosyltransferase (NAMPT) is a key enzyme in the salvage pathway because it catalyzes the first, rate-limiting step in the conversion of NAM into NAD<sup>+</sup> [34]. The ability of NAMPT to influence PARP and SIRT activity underscores their reliance on NAD<sup>+</sup> [37]. In cultured human SMCs, overexpression of NAMPT protected cells from NAD<sup>+</sup>-dependent oxidative stress-induced damage [38]. Decreased expression of NAMPT prompted premature senescence while conversely, its overexpression postponed senescence. A corresponding increase in SIRT1 activity indicates a role for SIRT6s in resisting oxidative stress [38]. This study by our lab demonstrates the association between NAD<sup>+</sup> bioavailability and oxidative stress-induced damage.

### 1.4.2 PARPs

DNA lesions from free radicals or other sources of damage are often categorized as either SSBs or DSBs because of the distinct repair mechanisms associated with them. Base excision repair (BER) and nucleotide excision repair mend SSBs, while homologous recombination (HR) and non-homologous end joining (NHEJ) process DSBs [39]. Common to all repair mechanisms is the DDR, a cascade of damage sensing and signal amplifying enzymes (e.g. PI3K-related kinase family, PARPs, MRE11-RAD50-NBS1 complex) that regulate recruitment of DNA repair factors [40].

The PARP family, most notably PARP1, plays an important role in sensing DNA damage and is recruited prior to all SSB and DSB repair mechanisms [41]. Although PARP1 in itself does not have any intrinsic DNA repair activity, it binds DNA lesion sites and

catalyzes the addition of adenosine diphosphate (ADP)-ribose units onto a target protein (e.g. histones H1 and H2B, PARP1 itself) [42]. This ADP-ribosylation reaction involves NAD<sup>+</sup> hydrolysis and produces poly(ADP-ribose) (PAR) chains that are linked via glycosidic ribose-ribose bonds [43]. Although there is some baseline PARP1 activity, DNA breaks increase the level of PAR chains by 10- to 500-fold. At more than 200 PAR units on each target protein, this makes PARP1 a major consumer of NAD<sup>+</sup> [44]. PAR chains continue to advance the DDR by recruiting ataxia telangiectasia mutated (ATM) and ataxia telangiectasia and Rad3-related protein (ATR), major signaling factors in the PI3K-related kinase family [41]. Additionally, the presence of PAR chains on histones interferes with transcription factors and loosens chromatin structure [42]. This further facilitates the DDR or activates apoptosis in cases of damage too extensive to be repaired efficiently.

### 1.4.3 Sir2 and Sirtuin family

Through mutation studies, the silent information regulator (SIR) family of genes were first discovered as negative regulators of mating type loci in *Saccharomyces cerevisiae* [45–48]. In addition, *SIR* gene products are required for silencing at telomeres and ribosomal DNA (rDNA) [49–53]. *SIR2* is distinct from the remaining family members in two notable areas: it is highly conserved from lower organisms like *S. cerevisiae* and *Caenorhabditis elegans* to humans [54]; its gene product, Sir2, is necessary for all three areas of silencing previously mentioned. Enzymatically, Sir2 was initially identified as an ADP-ribosyltransferase, an enzyme that uses NAD<sup>+</sup> to transfer an ADP-ribose group to a protein carrier [55]. However, further studies showed that Sir2's role as a chromatin silencer is predominately mediated through its role as a NAD<sup>+</sup>-dependent histone deacetylase (HDAC) [56]. While a classical HDAC mechanism uses metal ions and water molecules, Sir2 couples NAD<sup>+</sup> hydrolysis with deacetylation [57]. This reaction results in the production of a deacetylated substrate and NAM. Interestingly, the expected ADP-ribose was replaced by *O*-acetyl-ADP ribose (OAADPr), a novel product comprised of the ADP-ribose moiety of NAD<sup>+</sup> and the transferred acetyl group [58]. Interest in Sir2 took a big leap when it was found to promote longevity in *S. cerevisiae* by repressing rDNA recombination. This is thought to happen by reducing production of extrachromosomal

rDNA circles that cause aging in yeast [59]. As a result, more effort was put into understanding the role of Sir2-like proteins in mammals.

Sir2-like proteins are found in prokaryotes and eukaryotes and given the name, sirtuins. There are seven mammalian SIRT, SIRT1-7, that have conserved catalytic core domains with Sir2 and varying N- and C-terminals [60,61]. Although SIRTs are phylogenetically classified into four classes, they are more practically organized by their typical cellular localizations: SIRT1, 6, 7 in the nucleus, SIRT2 in the cytoplasm, and SIRT3-5 in the mitochondria [61,62]. SIRT mRNA is ubiquitously expressed in all human organs tested, although each SIRT has its own unique expression profile [62]. SIRTs make up the class III family of HDACs based on their unique mechanism of deacetylation as described previously with Sir2. All SIRTs are deacetylases with the exception of SIRT4 which only functions as an ADP-ribosyltransferase [63]. Deacetylation targets are unique to each SIRT—with some overlap—which give rise to different physiological functions.

#### 1.4.4 Sirtuin 1

Since its discovery, the majority of sirtuin-related studies have focused on SIRT1, the family member with the greatest sequence similarity to SIR2 [61]. Although predominantly located in the nucleus [62], it can also travel to and from the cytoplasm [64]. SIRT1-deficient mice models generated different phenotypes based on varying strain backgrounds. Inbred 129/Sv SIRT1KO mice showed gross signs of developmental defects (i.e. eye abnormalities), were consistently smaller than the WT, and seldom survived postnatally [65,66]. In an outbred background, SIRT1KO mice survive to adulthood but are sterile and smaller than WT [66]. As SIR2's closest homolog, there was great interest in a possible role for SIRT1 in lifespan extension. Lack of SIRT1 in mice decreased their median lifespan [67]. Though, transgenic mice overexpressing SIRT1 exhibited delayed progression of age-associated diseases (e.g. cancer, metabolic syndrome), overall longevity was not extended [68]. Interestingly, brain-specific SIRT1 overexpression increased lifespan through SIRT1-dependent activation of the hypothalamus. This resulted in enhanced physiological functions such as physical activity, body temperature, oxygen consumption, and quality of sleep compared to control mice [69].



As a major regulator of metabolism, SIRT1 deacetylates important metabolic targets in skeletal muscle and the liver including peroxisome proliferator-activated receptor alpha (PPAR $\alpha$ ), peroxisome proliferator-activated receptor gamma coactivator 1-alpha (PGC-1 $\alpha$ ). PPAR $\alpha$  belongs to a family of lipid-sensing receptors that activate genes involved in fatty acid homeostasis [70]. Particularly activated during prolonged periods of fasting, PPAR $\alpha$  acts to conserve energy via its role in fatty acid catabolism (i.e. ketogenesis). SIRT1 stimulates fatty acid oxidation (FAO) by deacetylating and activating hepatic PPAR $\alpha$  [71]. Another layer of SIRT1-dependent FAO regulation comes from activation of the PPAR $\alpha$  transcriptional coactivator PGC-1 $\alpha$  in skeletal muscle and the liver [71,72]. Interaction with PGC-1 $\alpha$  also gives SIRT1 control over the initiation of gluconeogenesis during fasting [73]. In white adipose tissue (WAT), SIRT1 deacetylation of PPAR $\gamma$  represses its function as a promoter of adipogenesis [74]. In addition, deacetylation of PPAR $\gamma$  at Lys268 and Lys 293 allows for recruitment of coactivators that simultaneously induce brown adipose tissue (BAT) genes and repress WAT genes in white adipocytes [75]. This “browning” of WAT is thought to increase energy expenditure. Therefore, SIRT1-dependent PPAR $\gamma$  deacetylation in adipocytes is hypothesized to protect against obesity-related diseases.

#### 1.4.4.1 Sirtuin 1 in Vascular Smooth Muscle Cells

Our lab was one of the first groups to study the importance of SIRT1 in vascular SMCs. We found that NAMPT overexpression extends lifespan in SMCs by increasing SIRT1 deacetylation of p53 [38]. SMCs overexpressing SIRT1 are senescence-resistant, provided there are adequate NAD<sup>+</sup> levels to sustain SIRT1 activity [76]. Furthermore, SIRT1 levels decline with age, making SMCs more vulnerable to genomic stress and cellular senescence [77]. SIRT1's role in DNA repair has been a focal point for its importance in atherosclerosis. In the event of oxidative stress, SIRT1 deacetylates and activates the DNA repair protein Nijmegen Breakage Syndrome-1 (NBS1). As a result of reduced SIRT1 levels in atherosclerotic plaques, these diseased vascular SMCs have increased rates of DNA damage and apoptosis [78]. SIRT1's beneficial effects also extend toward possible complications of atherosclerosis such as calcification and neointima formation. SIRT1 prevents hyperphosphatemia-induced-calcification in SMCs, a pathology that is associated

with increased cellular senescence [79]. Using carotid artery ligation and wire injury models, SIRT1 overexpression was shown to reduce neointima thickening. SIRT1 inhibited SMC proliferation and migration via downregulation of cyclin D1 and matrix metalloproteinase-9 (MMP-9) [80].

*In vitro* and *in vivo* Ang II models have been used to elucidate SIRT1's role in vascular SMCs. One of the many negative effects of Ang II is increased ROS levels in the vasculature. In particular, Ang II activation of the NAD(P)H oxidase isoform, Nox1, induces vascular hypertrophy. Accordingly, SIRT1 inhibits hypertrophy in SMCs by suppressing Nox1 mRNA expression, and thereby, reducing oxidative stress [81]. As discussed previously, Ang II-induction of hypertension and oxidative stress is predominantly mediated via AT<sub>1</sub>R. In vascular SMCs, overexpression of SIRT1 downregulated both AT<sub>1</sub>R mRNA expression and AT<sub>1</sub>R signaling via ERK phosphorylation. Resveratrol, an activator of SIRT1, reduced aortic AT<sub>1</sub>R protein abundance and reduced Ang II-induced hypertension in mice [82]. A separate group created SMC-specific SIRT1 transgenic mice that were also resistant to Ang II-induced hypertension. Aortas from these mice had reduced ROS levels, inflammation, and collagen accumulation. These beneficial effects of SIRT1, however, were not because of changes in AT<sub>1</sub>R levels. It was proposed that SIRT1 decreases TGF- $\beta$ 1 expression via inhibition of p65/RelA binding on its promoter [83]. Lastly, a recent SMC-specific SIRT1KO mouse model demonstrated the protective effect of SIRT1 against aortic dissection. After a 14-day course of Ang II infusion, mice lacking SIRT1 in aortic SMCs had increased mortality rates. The manifestation of aortic dissection was attributed to increased MMP2 and MMP9 expression in SMCs. Interestingly, aortic dissection was not a result of increased hemodynamic stress because SMC-specific SIRT1-deficiency attenuated Ang II-induced hypertension [84].

#### 1.4.5 Sirtuin 2

SIRT2 is deacetylase that is ubiquitously expressed in mouse tissues and predominantly cytoplasmic, but also found in the nucleus [85]. The first deacetylation target identified was  $\alpha$ -tubulin [86], important in regulating oligodendrocyte cytoskeleton myelination and maturation [87]. During mitosis, SIRT2 will migrate to the nucleus and ultimately help

maintain genomic stability [85]. SIRT2 regulation of chromatin condensation is associated with histone H4 lysine 16 deacetylation [88]. Interestingly, SIRT2's role in cell cycle control via deacetylation of the mitotic checkpoint kinase, BubR1, links SIRT2 with aging. Overexpression of SIRT2 increases BubR1 abundance, which was shown to increase median lifespan in BubR1-deficient male mice [89]. SIRT2-dependent genomic stability is also believed to be the reason why SIRT2-deficient mice develop tumorigenesis [90].

SIRT2 is also involved in lipogenesis, glucose metabolism, and inflammation. Forkhead box protein O1 (FOXO1) is a transcription factor that initiates transcription of gluconeogenic genes (i.e. glucose-6-phosphatase (G6P)) and inhibits peroxisome proliferator-activated receptor gamma (PPAR- $\gamma$ ), a nuclear receptor that activates adipocyte maturation [91]. SIRT2 deacetylation of FOXO1 results in its activation; therefore, promoting gluconeogenesis and preventing adipogenesis [92,93]. Nuclear factor kappa B (NF- $\kappa$ B) is a major transcription factor that induces expression of inflammatory genes. SIRT2 exhibits an anti-inflammatory role by directly deacetylating NF- $\kappa$ B, hindering transcription, and weakening any resultant inflammatory response [94]. SIRT2-deficient mice are more susceptible to dextran sulfate sodium-induced colitis and have increased levels of pro-inflammatory cytokines (e.g. TNF- $\alpha$ , interleukin-1 beta (IL1B), interleukin 6 (IL-6)) compared to wildtype (WT) mice [95].

SIRT2 also contributes towards oxidative stress resistance via interactions between FOXO3a and SOD. Deacetylation of FOXO3a increases FOXO3a binding and activation of SOD, thus, decreasing ROS levels [96]. However, one study found contradicting results where inhibition of SIRT2 protected ECs from H<sub>2</sub>O<sub>2</sub>-induced cell death [97]. SIRT2 is also necessary in ECs, mediating Ang II-induced cell migration. SIRT2 deacetylates tubulin in the aortic intima of mice and promotes microtubule reorganization. Therefore, SIRT2 mediates Ang II-induced vascular remodeling [98].

#### 1.4.6 Sirtuin 3

SIRT3 is a mitochondrial SIRT expressed in all tissues with higher levels in the liver, kidney, and heart [99,100]. SIRT3KO mice are healthy with no observable differences compared to controls. Mitochondrial hyperacetylation in these mice identified SIRT3 as a

major mitochondrial protein deacetylase [101]. Because SIRT3 target proteins are involved in almost all mitochondrial functions, loss of SIRT3 has been shown to accelerate a wide range of diseases.

With respect to energy homeostasis, SIRT3 regulates mitochondrial oxidative phosphorylation by deacetylating proteins involved in the electron transport chain. SIRT3 deacetylates and activates the Complex I subunit, NADH dehydrogenase [ubiquinone] 1 alpha subcomplex subunit 9 (NDUFA9), and the Complex II subunit, succinate dehydrogenase flavoprotein (SdhA) [99,102]. Consequently, SIRT3KD causes a decrease in basal ATP levels and oxygen consumption *in vitro* [99,103]. In nitrogen metabolism, SIRT3 activates glutamate dehydrogenase (GDH), a mitochondrial enzyme that converts glutamate into  $\alpha$ -ketoglutarate [104]. The nitrogen from glutamate is released as the byproduct ammonia and is removed via the urea cycle. The second step in this cycle is catalyzed by ornithine transcarbamoylase (OTC), another SIRT3 protein target. SIRT3 deacetylation and activation of OTC promotes amino acid catabolism and ammonia detoxification [105].

SIRT3's role in glucose metabolism is a mechanism through which it acts as a tumor suppressor. An early clue came from oncogene expressing SIRT3KO MEFs that had increased metabolic activity from sources besides mitochondrial oxidative phosphorylation [106]. Indeed SIRT3 regulates the Warburg effect, typical metabolic reprogramming in cancer cells that favors aerobic glycolysis, through deacetylation of hypoxia-inducible factor-1 $\alpha$  (HIF1 $\alpha$ ). SIRT3 suppresses the Warburg effect by destabilizing HIF1 $\alpha$ , a transcription factor that upregulates glycolytic genes [107]. Pyruvate dehydrogenase phosphatase (PDP) and pyruvate dehydrogenase alpha 1 (PDHA1), a subunit of the pyruvate dehydrogenase complex (PDC), are also deacetylation targets of SIRT3. These actions work to activate PDC and promote oxidative phosphorylation; thereby, possibly oppose the Warburg effect [108].

SIRT3's capacity as a tumor suppressor via glucose metabolism regulation is dependent on its ability to modulate ROS levels. SIRT3 deacetylation reduces oxidative stress by activating SOD2 and isocitrate dehydrogenase 2 (isocitrate dehydrogenase 2 (IDH2) [109–

112]. The previously discussed SOD2 neutralizes  $O_2^{\cdot-}$ , while IDH2 supports regeneration of glutathione, the antioxidant that breaks down  $H_2O_2$  [110]. In a study mentioned earlier, increased ROS levels were observed in SIRT3KO MEFs and supplementing SOD2 was enough to stop immortalization of SIRT3-deficient MEFs expressing an oncogene [106]. SIRT3 attenuates HIF1 $\alpha$  activity via reducing ROS production [107,113].

#### 1.4.6.1 Sirtuin 3 in Cardiovascular Disease

As the most well-defined mitochondrial SIRT, studies have revealed protective roles for SIRT3 in cardiovascular disease. SIRT3 drives the FAO pathway by deacetylating and activating long-chain acyl coenzyme A dehydrogenase (LCAD). Under fasting conditions, SIRT3-deficient mice displayed metabolic stress symptoms consistent with defective FAO such as lower ATP levels and intolerance to cold exposure [114]. SIRT3KO mice on a high-fat diet demonstrate an accelerated metabolic syndrome that coincides with global mitochondrial hyperacetylation. Diet-induced obesity, insulin resistance, hepatic steatosis, and hyperlipidemia are all exacerbated in SIRT3-deficient mice compared to WT [115].

In cardiomyocytes, SIRT3 levels increase in response to stress and is required for cell viability [116]. SIRT3 suppresses cardiac hypertrophy by regulating the activation of mitochondrial permeability transition pores. In addition to cardiac hypertrophy, SIRT3KO mice develop fibrosis and have increased signs of aging in their hearts [117]. SIRT3 also inhibits cardiac hypertrophy by lowering cellular ROS levels. By deacetylating and stabilizing FOXO3, SIRT3 facilitates upregulation of FOXO3-dependent mitochondrial antioxidant enzymes, SOD2 and catalase [118]. The anti-oxidant properties of SIRT3 also play a role in protecting ECs. In response to hypoxic stress, SIRT3 mediates ROS detoxification through the same FOXO3 pathway [119]. SIRT3-null hypercholesterolemic (i.e. LDL receptor-KO) mice fed a high-fat diet had elevated ROS levels, accelerated weight gain, and impaired metabolic adaptation to changes in nutrient intake. Surprisingly, SIRT3 deficiency did not exacerbate advanced atherosclerotic lesions when compared to controls [120]. Lastly, SIRT3-dependent mitochondrial function is necessary for pulmonary artery SMCs and preventing spontaneous pulmonary arterial hypertension in SIRT3KO mice [121].

### 1.4.7 Sirtuin 4

This second mitochondrial SIRT is expressed in all tissues with higher levels in the kidney, heart, brain, liver, and pancreatic  $\beta$  cells [63]. Little is known about SIRT4's enzymatic function; it is the only SIRT that cannot carry out NAD<sup>+</sup>-dependent deacetylation. Initial studies implicate SIRT4 in glucose metabolism, cancer, and lipid metabolism.

Though SIRT4KO mice were developmentally normal and did not show any gross defects compared to WT littermates, SIRT4KO pancreatic  $\beta$  cells had higher GDH activity. SIRT4 was first described to ADP-ribosylate, and thus, inhibit GDH activity [63]. In addition to its role in nitrogen waste disposal, GDH metabolizes glutamate to generate more ATP and ultimately promote insulin secretion [122]. So, SIRT4 blocks insulin secretion in pancreatic  $\beta$  cells. Another study affirmed SIRT4 expression in  $\beta$  cells and proposed negative regulation of insulin through interactions with insulin-degrading enzyme (IDE) [123]. Because some cancer cells need glutamine to survive [124], inhibition of glutamine metabolism by SIRT4 gives it a tumor-suppressive role. With genomic instability being a characteristic of all cancers, DNA damage was shown to induce SIRT4 expression [125]. SIRT4 repressed both tumor proliferation *in vitro* and tumor formation *in vivo* [125,126]. SIRT4 expression was found to be significantly lower in human bladder, breast, colon, gastric, ovarian, and thyroid carcinomas compared to normal tissue [127]. Lastly, SIRT4 has a role in hepatic lipid metabolism that contrasts the functions of other SIRTs. SIRT4 represses FAO in primary mouse hepatocytes and *in vivo* [128,129]. Malonyl -oA decarboxylase (MCD) deacetylation by SIRT4 results in elevated levels of malonyl-CoA [129]. This metabolite's levels are closely regulated because of its important role in simultaneously promoting fat synthesis and inhibiting FAO [129]. Interestingly, this effect of SIRT4 seems to be dependent on SIRT1-repression [128].

With respect to vascular health, SIRT4 appears to have an anti-inflammatory role in protecting ECs from cigarette smoke-induced inflammatory responses. Overexpression of SIRT4 in the cigarette smoke-activated endothelium helped decrease monocyte adhesion to ECs by inhibiting adhesion molecules VCAM-1 and E-selectin. Moreover, SIRT4 reduces NF- $\kappa$ B activity and its downstream cytokines TNF $\alpha$ , IL-1 $\beta$ , and IL-6 [130].

### 1.4.8 Sirtuin 5

SIRT5 is primarily located in the mitochondria but also found in the cytosol [131]. In mice, SIRT5 protein is expressed in all tissues with higher levels in brain, heart, liver, and kidney [132]. Upon gross inspection, SIRT5-deficient mice are normal and healthy [101,133,134]. SIRT5 was originally identified as a deacetylase with carbamoyl phosphate synthetase 1 (CPS1) as its target *in vitro* and *in vivo* [132,135]. SIRT5 deacetylation activates CPS1, the rate-limiting step in the urea cycle that is necessary for removing potentially toxic buildup of ammonia from the body [132]. Though this finding established SIRT5's role in ammonia detoxification, the underlying mechanism was brought into question when SIRT5 was shown to remove succinyl and glutaryl moieties from CPS1 in a NAD<sup>+</sup>-dependent manner [136,137]. The physiological function of SIRT5-dependent deacetylation is unclear because the catalytic efficiencies of desuccinylation and demalonylation were 29- to >1000-fold higher than deacetylation [136]. SIRT5 also desuccinylates and inhibits glutaminase, an enzyme that generates ammonia. By lowering glutaminase activity, SIRT5 protects against ammonia-induced autophagy and mitophagy [138].

SIRT5 also targets enzymes involved in mitochondrial metabolism. High percentages of proteins in the amino acid degradation pathway, tricarboxylic acid (TCA) cycle, and fatty acid metabolism were succinylated. Specifically, SIRT5-dependent succinylation of pyruvate dehydrogenase complex (PDC) and succinate dehydrogenase suppresses their activity in MEFs [139]. SIRT5 may play a role in FAO, the pathway with the highest percentage of succinylation target proteins and SIRT5 target proteins [133]. SIRT5 is also proposed to regulate ketone body production because there was evidence of 3-hydroxy-3-methylglutaryl-CoA synthase 2 (HMGCS2) desuccinylation under fasting conditions *in vivo* [133]. A recent study highlighted a new role for SIRT5 in glucose metabolism. Pathway analysis revealed glycolysis as the foremost SIRT5-regulated pathway via demalonylation of a plethora of proteins including, glyceraldehyde 3-phosphate dehydrogenase (GAPDH) [140]. Though SIRT5 is associated with many different metabolic pathways, the biological significance of its various enzymatic functions remains unclear. Multiple normal SIRT5-deficient mouse lines imply the dispensable nature of SIRT5's role in metabolic homeostasis under basal conditions [134]. Thus far, SIRT5's

only relevance to cardiovascular health is an association between single nucleotide polymorphisms in the *Sirt5* gene and risk of carotid plaques [141].

#### 1.4.9 Sirtuin 7

SIRT7 is one of the least studied SIRT and uniquely located in the nucleolus [62]. It is found in all mouse tissue with higher expression in metabolically active tissues (e.g. liver, spleen, testis) and lower expression in non-proliferating tissues (e.g. muscle, heart, brain) [142]. With rDNA transcription as the foremost activity of the nucleolus [143], SIRT7 has been found to increase rRNA synthesis by promoting RNA polymerase I (Pol I)-mediated transcription [142]. SIRT7 is involved via direct interaction with the rDNA transcription factor, upstream binding factor (UBF) [144]), and deacetylation of Pol I subunit, polymerase-associated factor 53 (PAF53) [145]. Following the pattern of other SIRTs, SIRT7 is a specific histone deacetylase. SIRT7-mediated H3K18 deacetylation represses transcription at promoters of tumor suppressor genes [146]. The physiological significance of this interaction is that SIRT7 is required for maintaining a cell's cancerous phenotype. SIRT7's potential as an oncogene is helped by evidence of its upregulation in all cancers that have been studied so far (e.g. thyroid, breast, bladder, colorectal) [143]. With respect to metabolic regulation, two separate SIRT7-deficient models revealed contrasting results. One study reported that SIRT7 prevents the development of hepatic steatosis by suppressing endoplasmic reticulum stress [147]. Another study showed that SIRT7-deficient mice were resistant to high-fat diet-induced fatty liver. SIRT7 promoted hepatic steatosis via regulation of the ubiquitin-proteasome pathway [148].

Thus far, only one study has described a role for SIRT7 in cardiovascular health. In the first SIRT7KO model, SIRT7 was shown to protect mice from a decreased lifespan due to heart hypertrophy and inflammatory cardiomyopathy. SIRT7-deficient myocardium revealed inflammatory infiltrations paralleled with higher levels of cytokines IL-12 and IL-13. SIRT7 also protects cardiomyocytes from apoptosis by deacetylating, and therefore, decreasing p53 activity [149].



## 1.5 Sirtuin 6

SIRT6's core domain is flanked by an N-terminal important for histone deacetylation and chromatin association and a C-terminal necessary for nuclear localization [150]. Mouse mRNA and protein expression is highest in the brain, heart, and liver [151]. Primarily characterized as an NAD<sup>+</sup>-dependent HDAC, SIRT6 uses the same mechanism as Sir2 to remove acetyl groups from lysines [152,153]. Solving its crystal structure led to the discovery that SIRT6 is uniquely able to bind NAD<sup>+</sup> in absence of an acetylated substrate [153]. SIRT6 targets histones H3K9, H3K56, and also directly deacetylates proteins [154–157]. In addition to deacetylation, SIRT6 has deacylase and weak mono-ADP-ribosylase activity [151,158]. Surprisingly, *in vitro* measurements of deacetylase activity were 300-fold lower than deacylation of a myristoyl group [158]. *In vivo*, this low intrinsic deacetylation is activated by long-chain fatty acids [159] and SIRT6's association with the nucleosome complex [160]. In addition to fatty acid activation, only a few mechanisms of SIRT6 regulation have been discovered. At the transcriptional level, c-FOS binds the promoter to induce expression [161]. SIRT6 is negatively regulated post-transcriptionally via micro RNA (miR)-766, -33a, and -33b [162,163]. Post-translationally, the ubiquitin ligase CHIP ubiquitinates SIRT6 to increase protein stability and prevent proteasome-mediated degradation [164].

### 1.5.1 SIRT6 Knockout and Transgenic Animal Models

Three week-old 129Sv SIRT6-deficient mice developed an acute degenerative aging-like phenotype and died shortly after postnatal day 24. Defects included reduced body size, severe lymphopenia, hypoglycemia, acute loss of subcutaneous fat, lordokyphosis, and osteopenia. At the cellular level, MEFs from these mice showed enhanced sensitivity to DNA damage agents. SIRT6KO-induced genomic instability was attributed a role in base excision repair [165]. A separate SIRT6KO mouse line demonstrated a similar premature aging phenotype, hypoglycemia, and early lethality in 60% of mice [166]. Interestingly, early lethality was circumvented by feeding mice with glucose containing water; therefore, identifying hypoglycemia as the main cause of death. This was due to enhanced insulin dependent and independent glucose uptake from increased levels of both glucose transporter 1 and 4 (GLUT1, 4) [166]. The mice that survived past 4 weeks of age went on

to develop chronic liver inflammation starting at 2 months of age [167]. In addition to SIRT6KO models, transgenic mice overexpressing SIRT6 were also created. Lifespan was extended in male, but not female, SIRT6 transgenic mice. This male-specific phenomenon was associated with lower insulin-like growth factor 1 (IGF1) signaling in WAT, an observation that has been linked to prolonged lifespan in rodent models [168]. Transgenic mice overexpressing SIRT6 are also less prone to high fat diet-induced metabolic damage [169].

Tissue-specific SIRT6KO models have also been created for brain, liver, and heart. Neural-specific deletion of SIRT6 led to growth retardation at 4 weeks of age [170]. However, not only did the mutant mice eventually reach normal size, they showed increased adiposity and became obese by 6-8 months of age. Modified growth hormone (GH)/IGF1 signaling and obesity-related neuropeptides were the likely causes of this phenotype [170]. Liver-specific SIRT6KO mice have fatty livers from an accumulation of triglycerides (TGs) [171]. With respect to heart-specific models, both SIRT6KO and transgenic SIRT6 overexpressing mice were created. Both models showed that SIRT6 protects against cardiac hypertrophy and heart failure [172].

In conclusion, SIRT6 mouse KO models have been crucial in elucidating SIRT6's various biological functions: glucose and lipid metabolism, genomic stability/DNA repair, and inflammation. The following sections will further discuss the mechanisms behind these functions and how they impact disease.

### 1.5.2 SIRT6 in Lipid and Glucose Metabolism

SIRT6 protects against the physiological damage of obesity through the regulation of TG and cholesterol homeostasis. SIRT6 silences glycolytic and lipogenic genes in the liver via H3K9 deacetylation [171]. In the absence of hepatic SIRT6, genes involved in TG synthesis were overexpressed while expression of genes for  $\beta$ -oxidation were reduced. Liver-specific SIRT6KO mice developed fatty livers as a result of TG accumulation [171]. SIRT6 also represses sterol regulatory element binding proteins 1 and 2 (SREBP1/2) expression by deacetylating H3K56 at their promoters [163,173]. SREBP1/2 are transcription factors that control expression of key genes in FA and TG biosynthesis and

cholesterol synthesis, respectively. In addition to reducing their transcription levels, SIRT6 regulates SREBP1/2 via two other mechanisms: inhibiting the formation of their active cleaved forms and increasing the inactive phosphorylated form of SREBP. SIRT6 promotes the latter event by activating another enzyme with a major role in inhibiting TG and cholesterol synthesis, AMP-activated protein kinase (AMPK) [163]. SIRT6 also lowers LDL-cholesterol levels by suppressing proprotein convertase subtilisin kexin type 9 (PCSK9)-dependent degradation of LDL-receptor. Similar to SREBP1/2, deacetylation of H3K56 at the PCSK9 promoter decreases its expression [163]. As mentioned previously, transgenic SIRT6 mice were protected from fat accumulation, impaired glucose tolerance, and impaired insulin secretion. That study found reduced expression of PPAR $\gamma$ -regulated genes and DGAT1, an important enzyme in TG synthesis [169]. Neural-specific SIRT6KO triggered obesity in adult mice by reducing hypothalamic expression of *Pomc*, *Sim1*, *Bdnf*. In humans, decrease in any one of those neuropeptides can result in obesity [170]. With such a large range of targets, SIRT6 is an important regulator of lipid metabolism.

Lethal hypoglycemia in SIRT6-deficient mice was the first piece of evidence that indicated an important role for SIRT6 in glucose metabolism [165,166]. As discussed, this resulted from increased insulin dependent (GLUT4) and independent (GLUT1) glucose uptake [166]. Since then, SIRT6 has been described as a central regulator of glycolysis and gluconeogenesis [36]. Hypoxia-inducible factor 1 alpha (HIF1 $\alpha$ ) is a transcription factor that mediates the shift from aerobic to anaerobic metabolism in cells under hypoxic or low nutrient environments. SIRT6 directly interacts with HIF1 $\alpha$  and represses transcription at the promoters of HIF1 $\alpha$  target genes. In addition, SIRT6 directly inhibits expression of important glycolytic genes such as lactate dehydrogenase (LDH), triose phosphate isomerase (TPI), adolase, and phosphofructokinase-1 (PFK-1), glucokinase (GK), and liver pyruvate kinase (LPK) [171,174]. With respect to gluconeogenesis, SIRT6 directly deacetylates general control nonrepressed protein (GCN5) to enhance its activity. GCN5 in return acetylates and deactivates PGC-1 $\alpha$ , a potent stimulator of gluconeogenic enzymes including FOXO1 [157]. FOXO1 plays a prominent role in gluconeogenesis by upregulating expression of the rate-limiting enzymes phosphoenolpyruvate carboxykinase (PCK1) and glucose-6-phosphatase (G6P). SIRT6 exerts yet another layer of control as it promotes FOXO1 deacetylation and subsequent nuclear exclusion [175]. Therefore, SIRT6

a negative regulator of hepatic glucose production. Furthermore, SIRT6 overexpression in mice prevented a high caloric diet-induced hyperglycemia and glucose intolerance. Transgenic mice had enhanced insulin sensitivity in skeletal muscle and liver, making SIRT6 a possible target for treatment of type 2 diabetes mellitus [176].

### 1.5.2.1 Cancer

The interaction here between SIRT6 and HIF1 $\alpha$  was an early clue concerning a possible role for SIRT6 in cancer. SIRT6-deficient cells favored glycolysis and lactate production in the presence of oxygen, a metabolic shift usually reserved for anaerobic conditions [174]. This finding was reminiscent of the “Warburg effect” in cancer and exceedingly proliferative cells. Also known as aerobic glycolysis, cancer cells undergo metabolic reprogramming that generates a surplus of glycolytic intermediates for cell growth and proliferation [177]. Further studies showed that indeed, SIRT6 suppresses tumor formation *in vivo* by repressing aerobic glycolysis. SIRT6 also co-represses c-Myc, a key regulator of cell proliferation that is often constitutively activated in cancer cells [178].

The tumor-suppressing ability of SIRT6 has been observed in different cancers. In hepatocellular carcinoma, c-Fos induces SIRT6, which then reduces expression of the tumor initiation protein survivin. Expression of SIRT6 is enough to prevent liver tumorigenesis in wild-type mice compared to mice carrying a malfunctioning SIRT6 [161]. SIRT6 inhibition of survivin also suppresses endometrial cancer by inducing apoptosis and suppressing proliferation [179]. The breast cancer drug Trastuzumab inhibits cancer cell proliferation through the induction of SIRT6. In addition, the oncoprotein AKT1 promotes proteasome degradation of SIRT6 in breast cancer cell lines [180]. Recently, eight point mutation in SIRT6 were observed to be selected for in a variety of tumor types including non-small-cell lung cancer, renal clear cell carcinoma, cervical carcinoma, and melanoma. The mutations inhibited SIRT6 deacetylase activity, affecting its repression of glycolytic genes [181].

### 1.5.3 SIRT6 in Genomic Stability

SIRT6 plays a vital role in maintaining genomic stability, interacting with many different DDR factors. The necessity of SIRT6 has been implicated in both SSB and DSB repair pathways. In the first knockout mouse study, SIRT6-deficient MEFs were hypersensitive to DNA damage agents due to defective BER [165]. However, most studies have focused on SIRT6's role in DSB repair processes. As one of the first factors recruited during the DDR, SIRT6 acts as a scaffold protein and recruits the chromatin remodeler SNF2H to DSBs. This, combined with H3K56 deacetylation promotes chromatin relaxation and further recruitment of DNA repair factors [40]. In NHEJ, SIRT6 is needed to mobilize DNA-dependent protein kinase catalytic subunit (DNA-PKcs) to DNA ends [182]. Moreover, SIRT6 directly deacetylates C-terminal binding protein interacting protein (CtIP) and promotes DSB end resection in HR [156]. Overexpressing SIRT6 was able to prevent the decline in HR efficiency observed in presenescent cells [183]. As discussed previously, the DDR factor PARP1 is recruited to both SSBs and DSBs. Accordingly, SIRT6's interaction with PARP1 allows for additional control over DNA repair via BER, NHEJ, and HR. Decreasing efficiency of BER in aging cells is rescued by SIRT6 overexpression in a PARP1-dependent manner [184]. In cells exposed to oxidative stress, SIRT6 overexpression increased the efficiency of NHEJ and HR. This was attributed to SIRT6 activation of PARP1 by mono-ADP-ribosylation [185].

The protective effect of SIRT6 for DNA damage extends towards telomeres as well. SIRT6 deacetylation of H3K9 at telomeric chromatin inhibits chromosomal end-to-end fusions from forming and causing genomic instability. The hypothesis is that hypoacetylated telomeres makes it easier for WRN binding, a protein involved in telomere maintenance and replication [152].

### 1.5.4 SIRT6 in Inflammation

Depending on its surroundings, SIRT6 has been shown to be both proinflammatory and anti-inflammatory. SIRT6 positively regulates inflammation in human monocytic cells via two different modifications of TNF- $\alpha$ , the proinflammatory cytokine. As a deacylase,

SIRT6 removes myristoyl groups from lysine 19 and 20 of TNF- $\alpha$  and promotes its secretion [158]. SIRT6 increases TNF- $\alpha$  mRNA translational efficiency when it is overexpressed in cells [186]. In pancreatic cancer cells, the byproduct of SIRT6's deacetylase activity, OAADPr, triggers a Ca<sup>2+</sup> response that results in enhanced expression of inflammatory cytokines in addition to TNF- $\alpha$ : IL1 $\alpha$ , IL6, IL8, and CSF1 [187].

SIRT6's anti-inflammatory role is mediated through the NF- $\kappa$ B signaling pathway, a transcription factor necessary for the expression of many proinflammatory genes. SIRT6 binds the NF- $\kappa$ B subunit, RELA, and deacetylates H3K9 at the promoters of target genes to repress transcription. TNF- $\alpha$ , an upstream activator of NF- $\kappa$ B, induces the interaction between SIRT6 and RELA [188]. In a rheumatoid arthritis mouse model, SIRT6 overexpression helped to block TNF- $\alpha$ -induced NF- $\kappa$ B target gene expression. Mice had lesser incidence and severity of collagen-induced arthritis with lower levels of inflammatory cytokines [189]. Similarly, attenuation of NF- $\kappa$ B-dependent inflammatory genes by SIRT6 overexpression was shown to prevent osteoarthritis in mice [190]. As previously discussed, SIRT6 has an anti-inflammatory role in the liver. SIRT6KO mice develop chronic liver inflammation because of SIRT6 deficiency in lymphocytes and myeloid-derived cells, as opposed to in hepatocytes. Further analysis revealed that SIRT6 represses inflammatory cytokine production in macrophages by inhibiting c-JUN signaling [167].

### 1.5.5 SIRT6 in Cardiovascular Disease

In cardiomyocytes, SIRT6 offers protection from cardiac hypertrophy and heart failure. Global SIRT6KO mice given hypertrophic agonists have hearts with increased cardiomyocyte size and fibrosis compared to WT. Consistent results were found in cardiac-specific SIRT6KO mice, while SIRT6 overexpression in cardiac-specific transgenic mice were protected from developing hypertrophy. Because continued hyperactivation of IGF-Akt signaling induces hypertrophy, SIRT6 represses c-JUN transcriptional activity at the promoters of those signaling genes [172]. A separate study confirmed the anti-hypertrophic properties of SIRT6 with a different cardiomyocyte model. Ang II-induced hypertrophy was inhibited via SIRT6 suppression of NF- $\kappa$ B transcriptional activity [191]. SIRT6 also

protects cardiomyocytes from hypoxic damage including ROS production, apoptosis, and inflammation [192].

Though SIRT6 is expressed in both aortic ECs and vascular SMCs, very little is known about its role in the vessel wall. SIRT6-deficient ECs have decreased rates of proliferation and are prone to premature senescence. Mechanistically, these ECs are more susceptible to DNA damage and have higher levels of p21, a cyclin-dependent kinase inhibitor that promotes growth arrest and senescence [193]. In vascular SMCs, SIRT6 mediates contractile to synthetic phenotypic switching associated with cyclic mechanical strain from arterial blood flow. Cyclic strain is thought to upregulate SIRT6 via TGF- $\beta$  signaling [194].

From the human internal thoracic aorta, our lab isolated the first line of adult SMCs that can convert between a synthetic and contractile state [195]. We show that SIRT6 is abundantly expressed in the nuclei of human vascular SMCs (Figure 1.2, A). A preliminary experiment was conducted to investigate a potential protective role for SIRT6 in response to oxidative stress in vascular SMCs. We found that SIRT6-deficient SMCs were particularly susceptible to cell death after exposure to oxidative stress in the form of H<sub>2</sub>O<sub>2</sub> (Figure 1.2, B).

In summary, oxidative stress underlies many pathological conditions that are important in the development of vascular diseases [24]. The majority of ROS in vascular SMCs are generated by NAD(P)H oxidases. Ang II is a potent physiological activator of NAD(P)H oxidase which then results in increased production of ROS in SMCs [15]. Through this signaling pathway, Ang II both initiates and propagates vascular pathologies such as vascular remodeling, inflammation, and DNA damage. In time, these manifest into diseases such as hypertension, atherosclerosis, and aortic aneurysms [17]. Our lab has studied the importance of NAD<sup>+</sup> bioavailability in conjunction with NAD<sup>+</sup> consuming enzymes in SMCs. We were particularly interested in Sirtuins, a family of NAD<sup>+</sup> dependent deacetylases implicated in a plethora of biological functions. Our lab found that increased SIRT1 activity in vascular SMCs resulted in increased replicative lifespan and resistance to oxidative stress [76]. Moreover, SMC SIRT1 protects mice from Ang II-induced aortic

dissections [84]. This, together with our preliminary *in vitro* experiments with SIRT6 in SMCs led us to the following hypothesis.

## 1.6 Aims and Hypothesis

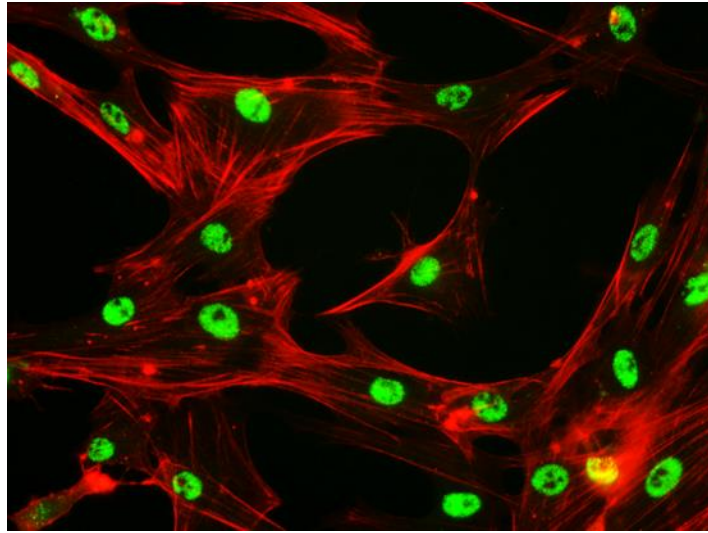
I hypothesize that SIRT6 in vascular smooth muscle cells is required to maintain blood vessel wall integrity.

To test this hypothesis, I will address two aims:

1. To generate a mouse model with SIRT6-deficient smooth muscle cells
2. To characterize the SMC-specific SIRT6-deficient aorta at baseline and following persistent oxidative stress



A



B

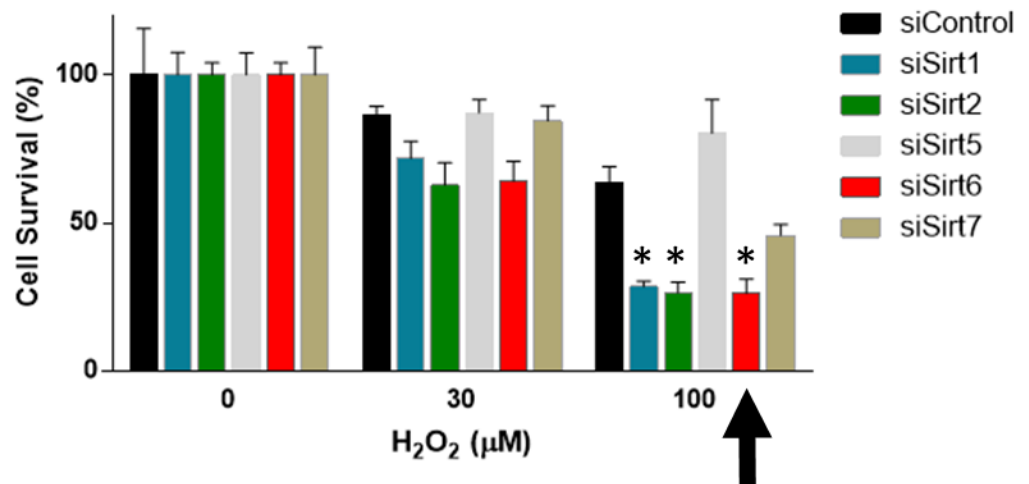


**Figure 1.2 SIRT6 is expressed in cultured SMCs and may play a role in resistance to oxidative stress**

A) Cultured human vascular SMC show nuclear expression of SIRT6. Cells were immunostained for SIRT6 (green) and smooth muscle-actin (red). B) SIRT6-deficient cells are particularly susceptible to cell death in response to oxidative stress via hydrogen peroxide.

## Chapter 2

### 2 Materials and Methods

#### 2.1 Animals

All animals were cared for in accordance with the Canadian Guide for the Care and Use of Laboratory Animals, and all experimental procedures were approved by the Animal Care Committee at the University of Western Ontario. FVB/NJ floxed mutant mice with loxP sites flanking exons 2-3 of SIRT6 targeted gene (SIRT6<sup>f/f</sup>) (Figure 2.1) were purchased from Jackson Laboratory (Bar Harbor, ME) [171]. C57BL/6 smooth muscle-specific Cre transgenic males were obtained from our collaborator, Dr. S. Offermanns (Heidelberg, Germany). Only males were used because the construct containing a smooth muscle myosin heavy chain (SMMHC) promoter and Cre recombinase fused to a G400V/M543A/L544A triple mutation of the human estrogen receptor ligand binding domain (ER<sup>T2</sup>) is located on the Y chromosome [196]. Mice were fed *ad libitum*, a phytoestrogen-free rodent chow diet (Harlan Teklad Global Soy Protein-Free Extruded Rodent Diet 2020X, Madison WI) and housed with littermates in standard cages at 23°C.

To create SMC-specific SIRT6 KO mice, we first generated mice that had floxed SIRT6 alleles and expressed SMMHC-CreER<sup>T2</sup>. SIRT6<sup>f/f</sup> FVB females were crossed with SMMHC-CreER<sup>T2</sup> C57BL/6 males to produce male offspring that were heterozygous for floxed SIRT6 (SIRT6<sup>f/+</sup>) with Cre expression. These males were then backcrossed with SIRT6<sup>f/f</sup> FVB females to generate SMMHC-CreER<sup>T2</sup>;SIRT6<sup>f/f</sup> mice on a 75% FVB and 25% C57BL/6 background (Figure 2.1, B). To identify SIRT6<sup>f/f</sup> from SIRT6<sup>f/+</sup> mice, animals were anesthetized with isoflurane and tail samples were obtained at 21 days of age. SIRT6 WT and mutant alleles are amplified using primers P1: 5' AGT GAG GGG CTA ATG GGA AC 3' and P2: 5' AAC CCA CCT CTC TCC CCT AA 3' (Figure 2.1, A).

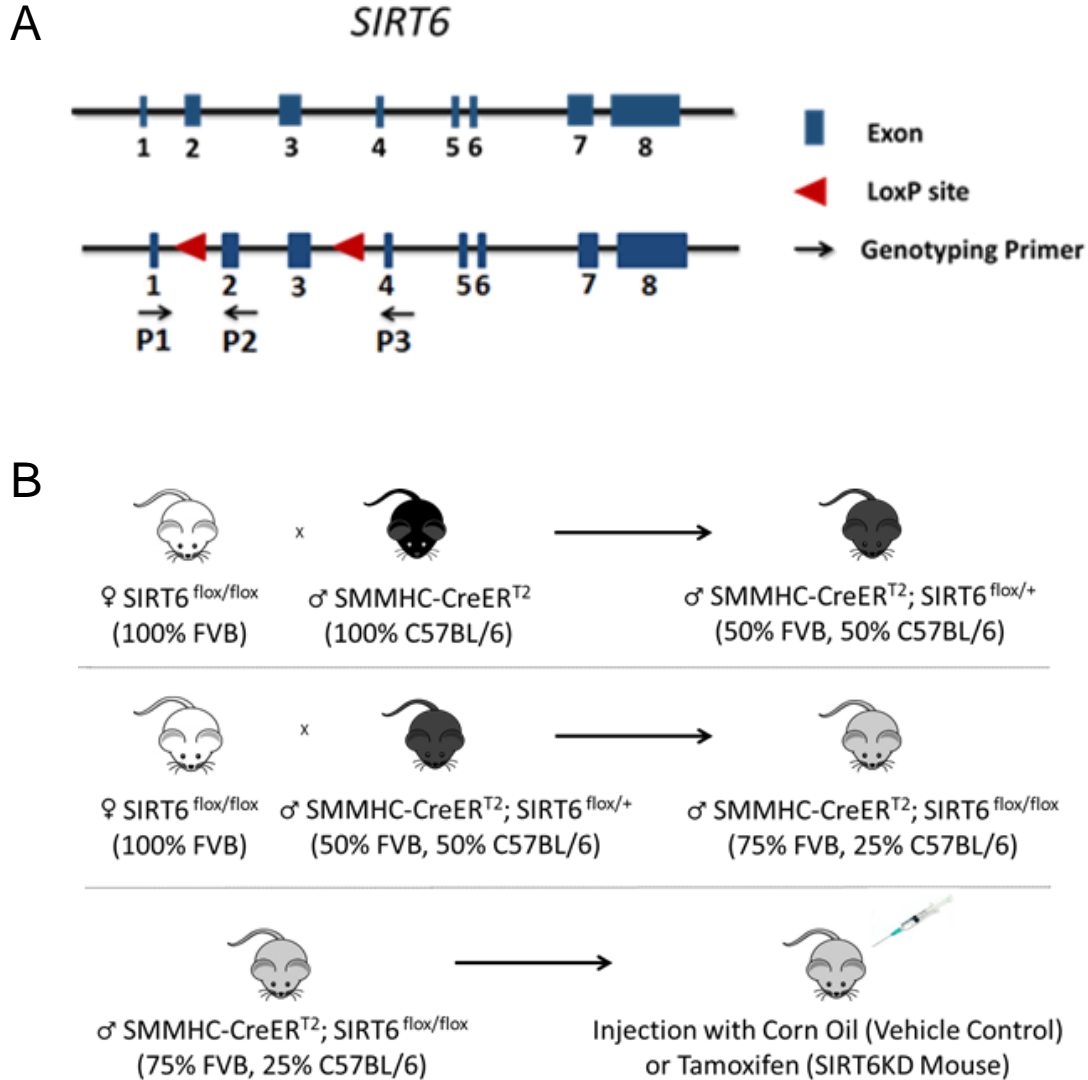


**Figure 2.1 SMC-specific *SIRT6*KD Mouse Breeding Strategy.**

A) Schematic diagram of *SIRT6* gene with loxP sites and primers. B) Mice homozygous for the floxed *SIRT6* allele on a FVB background (*SIRT6*<sup>f/f</sup>) were crossed with mice C57BL/6 mice expressing *SMMHC-CreER*<sup>T2</sup> supplied by Dr. Offermanns' laboratory. Only male offspring were used because in the initial creation of *SMMHC-CreER*<sup>T2</sup> mice, the bacterial artificial chromosome containing *SMMHC-CreER*<sup>T2</sup> inserted onto the Y chromosome. Resultant males heterozygous for the wildtype and floxed *SIRT6* allele (*SIRT6*<sup>f/+</sup>) were crossed with *SIRT6*<sup>f/f</sup> to produce mice homozygous for floxed *SIRT6* allele that simultaneously expresses *SMMHC-CreER*<sup>T2</sup>. Experimental mice on a 75% FVB and 25% C57BL/6 background received intraperitoneal injections of corn oil as the vehicle control or tamoxifen (dissolved in corn oil) for 5 days at 8 weeks of age to induce *SIRT6* deficiency.

## 2.2 Induction of SIRT6 Deficiency and Angiotensin II Treatment

### 2.2.1 Cre-Lox Recombination Induced by Tamoxifen

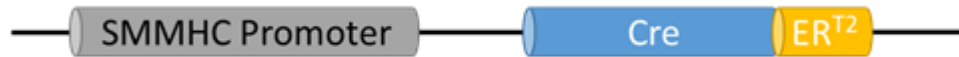
SMMHC is expressed exclusively in SMCs; therefore, using this promoter allows for spatial control of CreER<sup>T2</sup> expression. The modified estrogen receptor on CreER<sup>T2</sup> provides temporal control over Cre-mediated recombination by specifically binding the synthetic estrogen antagonist, 4-hydroxy-tamoxifen, as opposed to endogenous estrogen. Moreover, CreER<sup>T2</sup> is a second-generation inducible Cre recombinase that is ten times more specific to 4-hydroxy-tamoxifen than the original CreERT [197]. After 4-hydroxy-tamoxifen binds CreER<sup>T2</sup>, Cre recombinase translocates into the nucleus and facilitates recombination at the floxed SIRT6 alleles (Figure 2.2).

The experimental timeline is illustrated in Figure 2.3. Eight-week old SMMHC-CreER<sup>T2</sup>;SIRT6<sup>f/f</sup> mice were given tamoxifen, which is metabolized into 4-hydroxy-tamoxifen by the liver [198], administered via 1.5mg/20g body weight intraperitoneal injections per day for five consecutive days, to induce SIRT6 deficiency in SMCs. SMMHC-CreER<sup>T2</sup>;SIRT6<sup>f/f</sup> mice administered the vehicle alone, corn oil, were used as littermate controls.

### 2.2.2 Angiotensin II Treatment

At 6 weeks after initial administration of corn oil or tamoxifen, mice were anesthetized with isoflurane. Osmotic minipumps (Alzet M-1004) were surgically implanted subcutaneously to allow infusion of angiotensin II (A9525, Sigma-Aldrich) at a rate of 1.44 mg/kg/day or saline for 28 days.

A



B

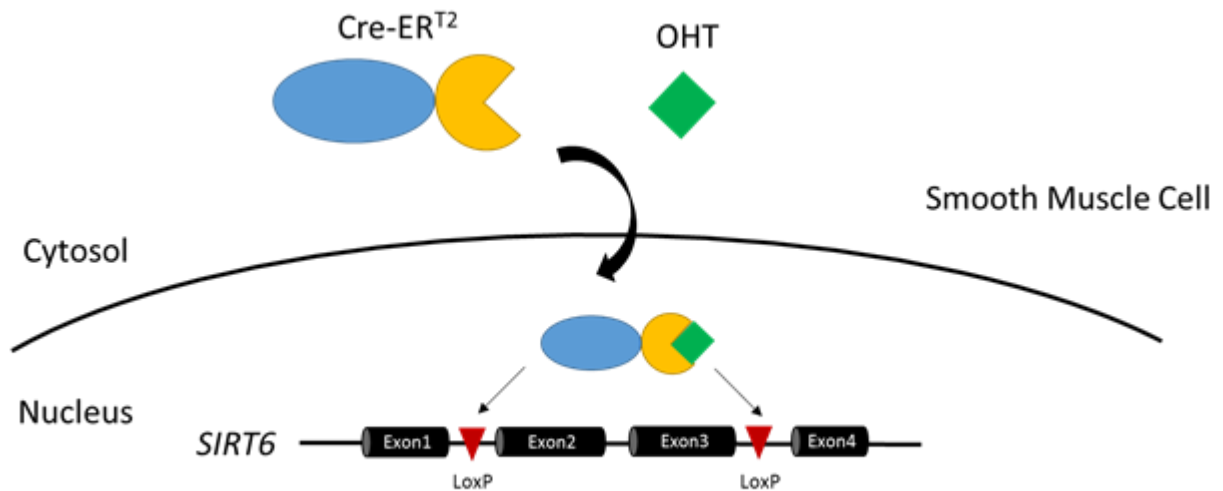


**Figure 2.2 Schematic of an inducible smooth muscle cell-specific SIRT6 knockdown using the Cre-Lox System.**

A) DNA construct containing a smooth muscle myosin heavy chain (SMMHC) promoter controlling Cre recombinase fused with a modified estrogen receptor-binding domain (ER<sup>T2</sup>). SMMHC is a contractile protein expressed exclusively in SMCs during embryogenesis. B) Under the control of the SMMHC promoter, Cre-ER<sup>T2</sup> is specifically expressed in SMCs. After the administration of tamoxifen, the liver metabolizes it into 4-hydroxytamoxifen (OHT). Binding of OHT to ER<sup>T2</sup> enables the translocation of Cre to the nucleus where it can catalyze the recombination at loxP sites on the modified SIRT6 allele.

### 2.2.3 Blood Pressure Measurements

Blood pressure was measured using a non-invasive CODA tail-cuff system (Kent Scientific, Torrington). To avoid effects of environmental stress on blood pressure, mice were transported to the experimental room 1 hour before measurements were taken to ensure that mice were calm. Prior to minipump implantation, mice were trained on the blood pressure machine for at least 5 days to accustom them to the procedure. The measurements on the final 3 days were averaged to obtain a baseline blood pressure before surgery. Over the course of the 28-day Ang II or saline-infusion, blood pressure was measured twice a week (Figure 2.3). The two measurements were averaged to represent the weekly blood pressure.

## 2.3 Qualitative Analysis of Aortic Media DNA

Genomic DNA was isolated from medial SMCs in descending aorta of mice at 8 weeks of age (i.e. 2 weeks after initiation of tamoxifen injection). To isolate SMCs and reduce the possibility of contamination from other cell types, we used a dissecting microscope to carefully remove the adventitia and scrape along the inner wall with forceps to remove the endothelium. The aortic media was then digested with a proteinase K lysis buffer. PCR was performed to determine the recombination of floxed SIRT6 alleles. In addition to the P1 and P2 primers used for genotyping, the recombination allele was amplified using primers P1 and P3: 5'-GCGTCCACTTCTCTTTCCTG-3' (Figure 2.1, A).

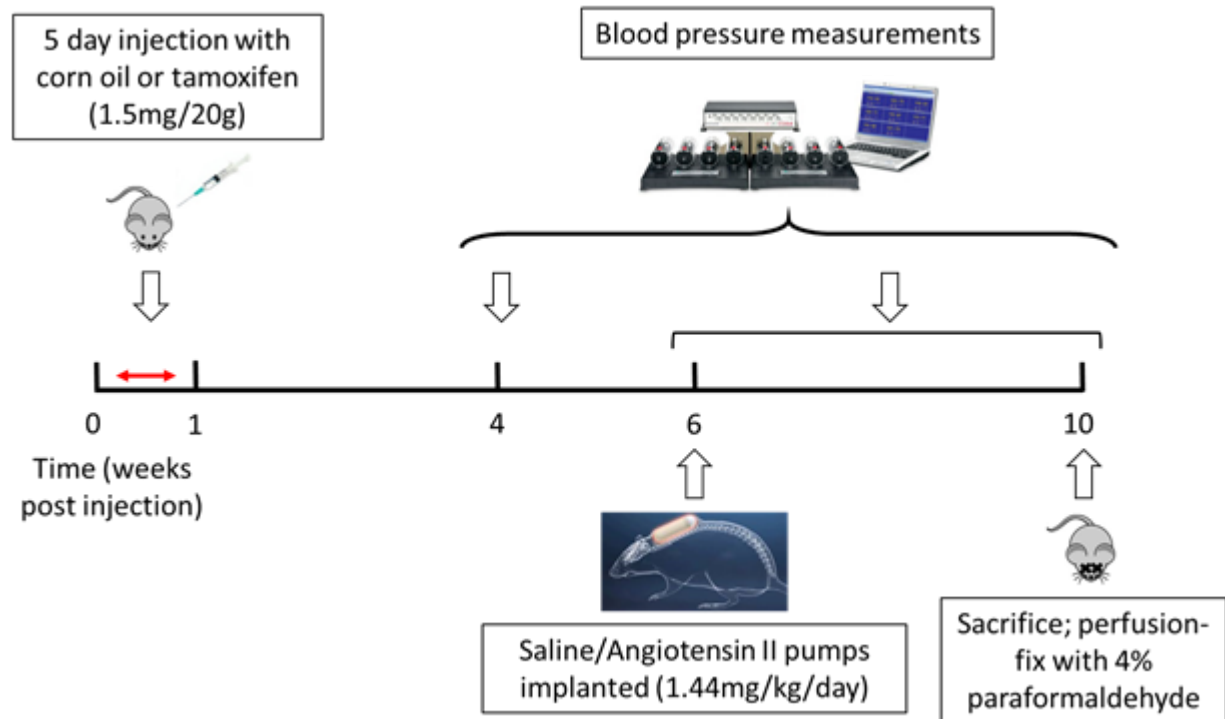


**Figure 2.3 Experimental timeline for Angiotensin II-induced aortic stress.**

Six weeks after injection with vehicle corn oil or tamoxifen, mice were surgically implanted with osmotic pumps that infused saline or Ang II for 28 days. Ang II was infused at a rate of 1.44 mg/kg/day. For blood pressure measurements, a baseline was taken at 4 weeks post injection. Two measurements were taken weekly during the entire course of saline/Ang II-infusion. Aortas were harvested at 4 weeks post saline/Ang II-infusion, i.e. 10 weeks post injection.

## 2.4 Quantitative Real-Time PCR Analysis for Gene Abundance

Control and SIRT6-deficient mice were euthanized at 2 weeks (n=7-13) and 10 weeks (n=4-7) after initial administration of vehicle or tamoxifen. The vasculature was perfused with PBS via the left ventricle at physiological pressure before aortas were dissected. Infrarenal aortic tissue samples were used and both the adventitia and endothelium were removed as previously described.

For RNA extraction, TRIzol® (Life Technologies) and chloroform were added to tissue samples and centrifuged for 15 min at 4°C. The upper aqueous phase was mixed with 100% ethanol before transfer to an RNeasy column. From this point on, the RNeasy Plus Mini Kit protocol (Qiagen) was used to complete RNA extraction. RNA was eluted with 30µl of RNase-free water.

Nano-Drop spectrometry (Wilmington, DE) was used to measure RNA concentrations. RNA was reverse transcribed into cDNA using a High Capacity cDNA Reverse Transcription kit (Applied Biosystems) on an Eppendorf Master cycler Gradient S thermal cycler. Specific mRNA abundances of *Sirt6* and *Rn18S*, as a housekeeping gene, were measured with quantitative real-time PCR. Each 10µl reaction contained 5 ng of cDNA/well and samples were run in triplicates, and the mouse *Sirt6* transcript abundance was normalized to *Rn18S* level and analyzed using  $\Delta\Delta C_t$  method on a ViiA7 PCR system (Life Technologies).

## 2.5 Immunoblotting

Infrarenal aortic media tissue samples were taken from control and SIRT6-deficient mice euthanized at 2 weeks after initial administration of vehicle or tamoxifen. Tissue samples were lysed with RIPA buffer containing protease inhibitor cocktail (Sigma-Aldrich), phosphatase inhibitor cocktail 2 (Sigma-Aldrich), phenylmethanesulfonylfluoride, and nicotinamide (Sigma-Aldrich). Proteins were separated by SDS-PAGE. Total cell lysates isolated from tissue samples were loaded onto a 10% polyacrylamide gel at 20 µg per well.



The gel was run at 80V for 2.5 hrs before the protein was transferred onto a 0.45 $\mu$ m pore polyvinylidene fluoride membrane at 110V for 1h.

The membrane was blocked with 5% skim milk in Tris-buffered saline with 0.1% Tween 20 (TBS/t) for 1h at room temperature. The primary antibodies used were rabbit monoclonal SIRT6 antibody (D8D12, Cell Signaling) and rabbit polyclonal  $\beta$ -actin antibody (4967, Cell Signaling). Both antibodies were diluted 1:1000 in 2.5% skim milk TBS/t buffer before incubation with the membrane overnight at 4°C. The secondary antibody used was an HRP-conjugated donkey anti-rabbit antibody (GE Healthcare Life Sciences) diluted 1:10000 in TBS/t, incubated for 1h at room temperature. ECL chemiluminescence of target proteins was detected and quantified using LI-COR imaging system (LI-COR Fc).

## 2.6 Histology

Control and SIRT6-deficient mice were anesthetized with isoflurane and perfusion-fixed at physiological pressure with 4% paraformaldehyde (PFA). Tissue was kept in 4% PFA overnight and immersed in 70% ethanol the next day for storage. The heart connected to the aorta was dissected and the surrounding fat and tissue were removed. For macroscopic examination, the heart and aorta were imaged with a dissecting microscope (Olympus). Four specific aortic regions were sectioned for histology: one ascending segment (Asc), two descending thoracic segments (Desc 1, Desc 2), and one abdominal segment [199] (Figure 2.4). These were located using the aortic root, left subclavian artery, and superior mesenteric artery as landmarks. Aortic segments were embedded in paraffin and 5 $\mu$ m-thick-transverse sections were stained with hematoxylin and eosin (H&E). Three histological sections per aortic region were measured using ImageJ software ([www.imagej.nih.gov/ij/](http://www.imagej.nih.gov/ij/)) and averaged to obtain aortic lumen measurements.

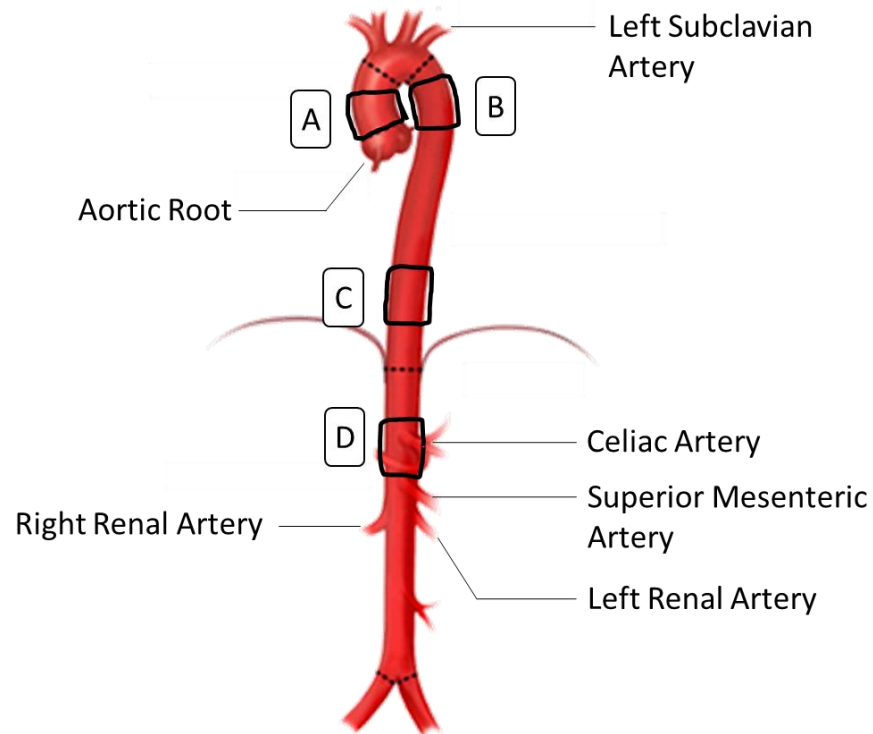


**Figure 2.4 Schematic diagram of aortic regional segments.**

Four regions were sectioned and histologically examined: A) Ascending, B) Descending 1, C) Descending 2, D) Suprarenal. The aortic root, left subclavian artery, and superior mesenteric artery were used as landmarks for standardization among animals.

### 2.6.1 Characterization of Cell Infiltration and Aortic Wall Destruction

To calculate the percentage of medial layers affected by the cellular infiltrate, the number of layers affected was divided by the average number of medial layers usually found in that specific region. For each animal, the percentages of layers infiltrated was measured in three sections per aortic region and averaged.

We developed a grading criteria to assess the varying degrees of aortic wall destruction seen in our mice (Figure 2.5). This criteria took into account the area occupied by the cell infiltrate, SMC degradation, elastin breakage, and neointima formation.

## 2.7 Immunohistochemistry

PFA-fixed, paraffin-embedded 5 $\mu$ m-thick aortic sections were immunolabeled with primary antibodies overnight at 4°C: smooth muscle  $\alpha$ -actin (1:300 M0851, Dako), Ki67 (1:100 ab16667, Cell Signaling), and CD45 (1:100 ab10558, Cell Signaling). To detect smooth muscle  $\alpha$ -actin, an HRP-conjugated sheep anti-mouse secondary antibody (GE Healthcare Life Sciences) was used with 3-3-diaminobenzidine tetrahydrochloride (DAB) (Vector Labs). To detect Ki67, sections underwent antigen retrieval in a 10mM sodium citrate buffer and pre-blocked with an avidin/biotin kit (Vector Labs). To complete detection, a goat anti-rabbit biotinylated secondary antibody (Vector Labs), Vectastain ABC Kit (Vector Labs), and DAB (Vector Labs) were used. For CD45 immunostaining, sections underwent antigen retrieval in a 10mM sodium citrate buffer. An HRP-conjugated donkey anti-rabbit secondary antibody (GE Healthcare Life Sciences) was used with DAB (Vector Labs). All immunohistochemistry sections were counterstained with eosin. Bright-field images were acquired using an Olympus BX51 microscope.

## 2.8 Statistical Analysis

The data were expressed as mean  $\pm$  standard error (SE). A  $p < 0.05$  was considered statistically different. Statistical analysis was determined using Graphpad Prism software version 6.0.

Grade	Criteria
0	No presence cellular infiltrate
1	Minor, local infiltration; limited to outer medial layer
2	Infiltration has spread to half the circumference of the aorta; beginning to expand an individual layer of media
3	Major infiltration; evidence of infiltration in 3+ medial layers
4	Massive infiltration and inflammation in all medial layers

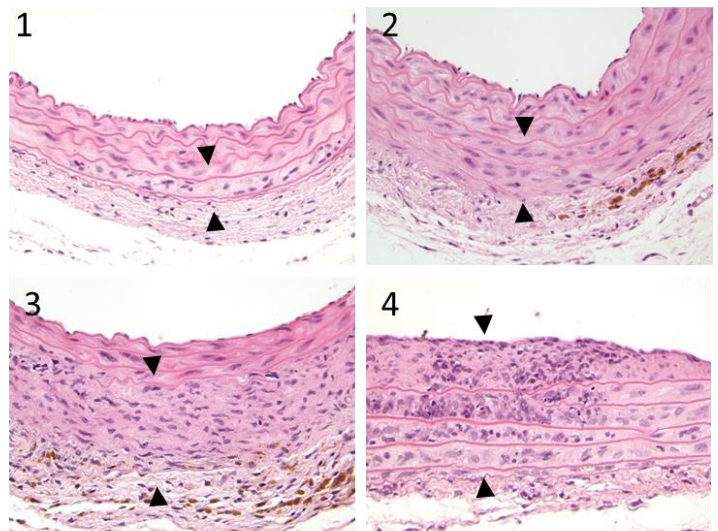


**Figure 2.5 Grading criteria for degree of cell infiltration and aortic wall destruction.**

Outline of grading system used to assess the degree of damage to the aortic wall. H&E images are representative of the four levels of destruction with arrowheads marking the boundaries of the area of cell infiltrate and destruction.

## Chapter 3

### 3 Results

#### 3.1 Confirmation of SIRT6 Knockdown in Aortic Medial DNA, mRNA, and Protein in Novel Mouse Strain

To determine whether SIRT6 was necessary for vascular wall integrity, we first generated a novel mouse model specifically lacking SIRT6 in SMCs. Mice homozygous for the *Sirt6* transcript flanked by *loxP* sites around exons 2 and 3 [171] were bred with mice expressing Cre recombinase fused with a mutated estrogen receptor binding domain (ER<sup>T2</sup>) under control of a smooth muscle myosin heavy chain (SMMHC) promoter [196]. This allowed for spatial and temporal control of *Sirt6* disruption in our experimental mice with the administration of a synthetic estrogen antagonist, tamoxifen. Littermate controls were injected with corn oil.

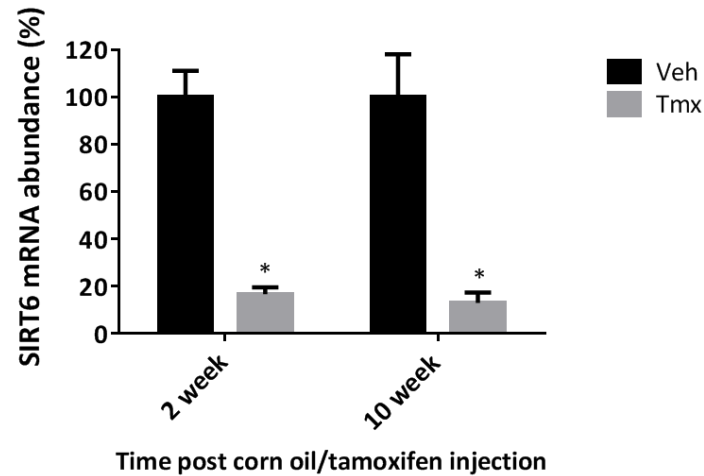
We sought confirmation of SIRT6 knockdown in aortic SMCs with three different methods. First, we sought to show evidence that a recombination event had occurred within the *Sirt6* transcript. Aortic media was isolated from SMMHC-CreER<sup>T2</sup>;SIRT6<sup>+f</sup>, SMMHC-CreER<sup>T2</sup>;SIRT6<sup>f/f</sup>, and SMMHC-CreER<sup>T2</sup>;SIRT6<sup>f/f</sup> mice given tamoxifen. Using three primers, DNA fragments from WT, floxed, and recombination *Sirt6* alleles were amplified (Figure 3.1, A). The heterozygous *Sirt6* mouse produced the WT allele (399 bp) and the heavier floxed allele (453 bp) while the homozygous *Sirt6* mouse yielded the floxed allele alone. The Cre-deleted allele (524 bp) was only found in the homozygous *Sirt6* mouse given tamoxifen; thereby, confirming a recombination event (Figure 3.1, B). The presence of the unmodified floxed allele in homozygous *Sirt6* mouse given tamoxifen may be a result of additional cell types in the aortic tissue that was analyzed.



Next, real time-PCR was used to detect *Sirt6* mRNA levels in aortic SMCs from vehicle (Veh) and tamoxifen (Tmx) injected SMMHC-CreER<sup>T2</sup>;SIRT6<sup>fl/fl</sup> mice (Figure 3.2, A). Robust *Sirt6* mRNA expression was observed in SMMHC-CreER<sup>T2</sup>;SIRT6<sup>fl/fl</sup> mice given corn oil. This result was expected as *Sirt6* mRNA expression is found all mouse tissues tested: heart, brain, spleen, lung, liver, skeletal muscle, kidney, testis, and thymus [151,165]. We confirmed knockdown of *Sirt6* mRNA in Tmx mice at two time points. Compared to Veh, *Sirt6* mRNA was reduced to 16.6% ( $p < 0.0001$ ) in Tmx mice 2 weeks after initial injection with tamoxifen. At 10 weeks after administration of tamoxifen, *Sirt6* mRNA was reduced to 13.1% ( $p < 0.001$ ) in Tmx mice (Figure 3.2, A).

SIRT6 protein has been found in all tissues where its mRNA is expressed [151,165]. Western analysis confirmed the presence of a 37 kDa SIRT6 protein appearing as a doublet in aortic SMCs of Veh mice (Figure 3.2, B). Although Western analysis of most mouse tissues produce a single band for SIRT6 at 37 kDa, SIRT6 is reported as a doublet in MEFs [200]. We also confirmed the deletion of SIRT6 in aortic SMCs 2 weeks after initial injection with tamoxifen. Densitometry revealed a 99.9% knockdown of SIRT6 protein ( $p < 0.0001$ ) in Tmx mice ( $n=3$ ) compared to Veh mice ( $n=3$ ) (Figure 3.2, B).

A



B

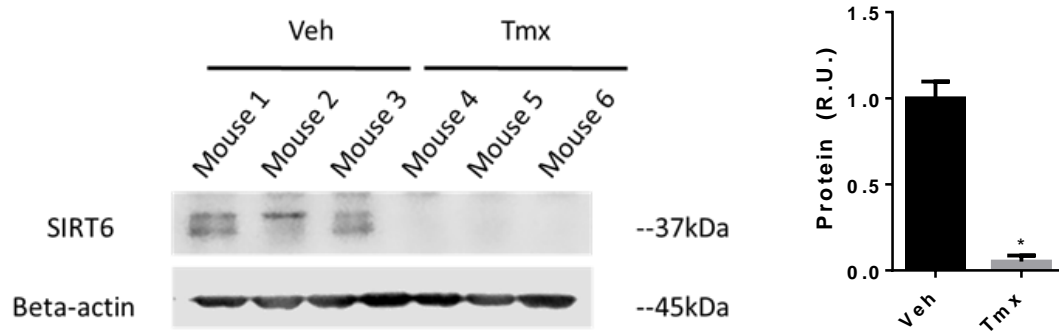


### Figure 3.2 SIRT6 knockdown in mRNA expression and protein in aortic SMCs.

A) Quantitative real time-PCR analysis of aortic media-derived RNA transcripts from SMMHC-CreER<sup>T2</sup>;SIRT6<sup>f/f</sup> mice that were either injected with the vehicle (Veh) or tamoxifen (Tmx). Aortas were harvested at 2 weeks (Veh n=13; Tmx n=7) and 10 weeks; (Veh n=7; Tmx n=4) post injection. *SIRT6* mRNA abundance is presented as a  $\Delta\Delta C_t$  comparison of Tmx expression to Veh; bars represent means $\pm$ SEM. \*Significant compared to Veh (p<0.05), 2-way ANOVA and Sidak's multiple comparisons test. B) Immunoblotting for SIRT6 protein in aortic medial tissue from SMMHC-CreER<sup>T2</sup>;SIRT6<sup>f/f</sup> mice harvested 2 weeks post injection of Veh (n=3) or Tmx (n=3). Band densities were normalized to corresponding  $\beta$ -actin bands and expressed as a fraction of a control value. \*Significant compared to Veh (p<0.05) using *t* test. RU, relative units.



## 3.2 SIRT6-Deficient Aortas Appear Healthy

Vascular characterization of SMC-specific SIRT6 deficiency began with gross examination of perfusion-fixed aortas. The heart and kidneys served as boundaries while various arteries branching off the aorta were used as landmarks (e.g. left subclavian a., intercostal a., renal a.). Six weeks after the initial injection, the ascending, aortic arch, thoracic, and abdominal aortic regions appeared normal and without any obvious signs of damage in both corn oil (control) and tamoxifen (SIRT6KO) injected mice (Figure 3.3, A).

Four regions of the aorta were subjected to histological examination, adapted from Owens 2010 [199]: ascending (Asc), two descending thoracic sections (Desc 1, Desc 2), and abdominal/suprarenal (Supra) (Figure 3.3, B). Distinctions were made between different areas of the aorta because of the regional heterogeneity of aortic SMCs that exists along the length of the aorta. This is attributed to differing embryonic origins of SMCs at anatomical locations. Aside from neuroectoderm-derived SMCs in the aortic root and arch, all other SMCs are mesoderm-derived [201]. Interestingly, one of the typical Ang II effects in the aortic wall, medial thickening, has different regional causes. SMCs from ascending sections were hyperplastic while thoracic and abdominal regions were hypertrophic [199]. This, in addition to varied responses to TGF- $\beta$ 1 [202] affirms aortic regional diversity as an important factor for understanding varied pathologic responses in blood vessels.

H&E stained histological sections of all regions also showed no signs of aortic medial abnormalities or damage in both control and SIRT6KO mice (Figure 3.3, B). We further analyzed aortic morphometry via lumen area measurements for evidence of structural damage (i.e. vessel dilation) and found no differences between control and SIRT6KO mice (Figure 3.3, C).

A

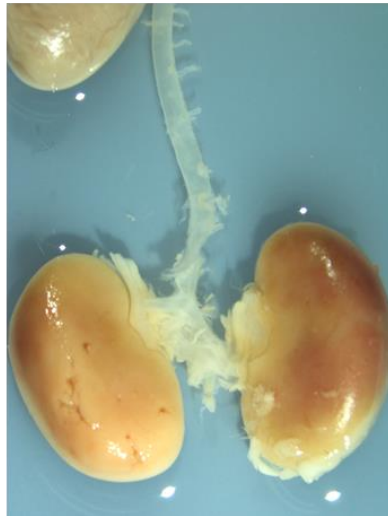
Veh

Tmx

Ascending and  
Descending  
Thoracic Aorta



Abdominal  
Aorta



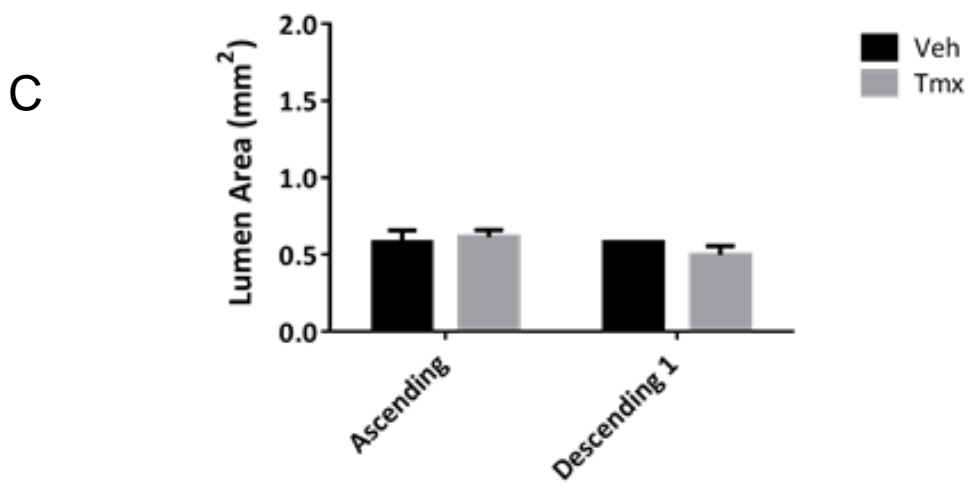
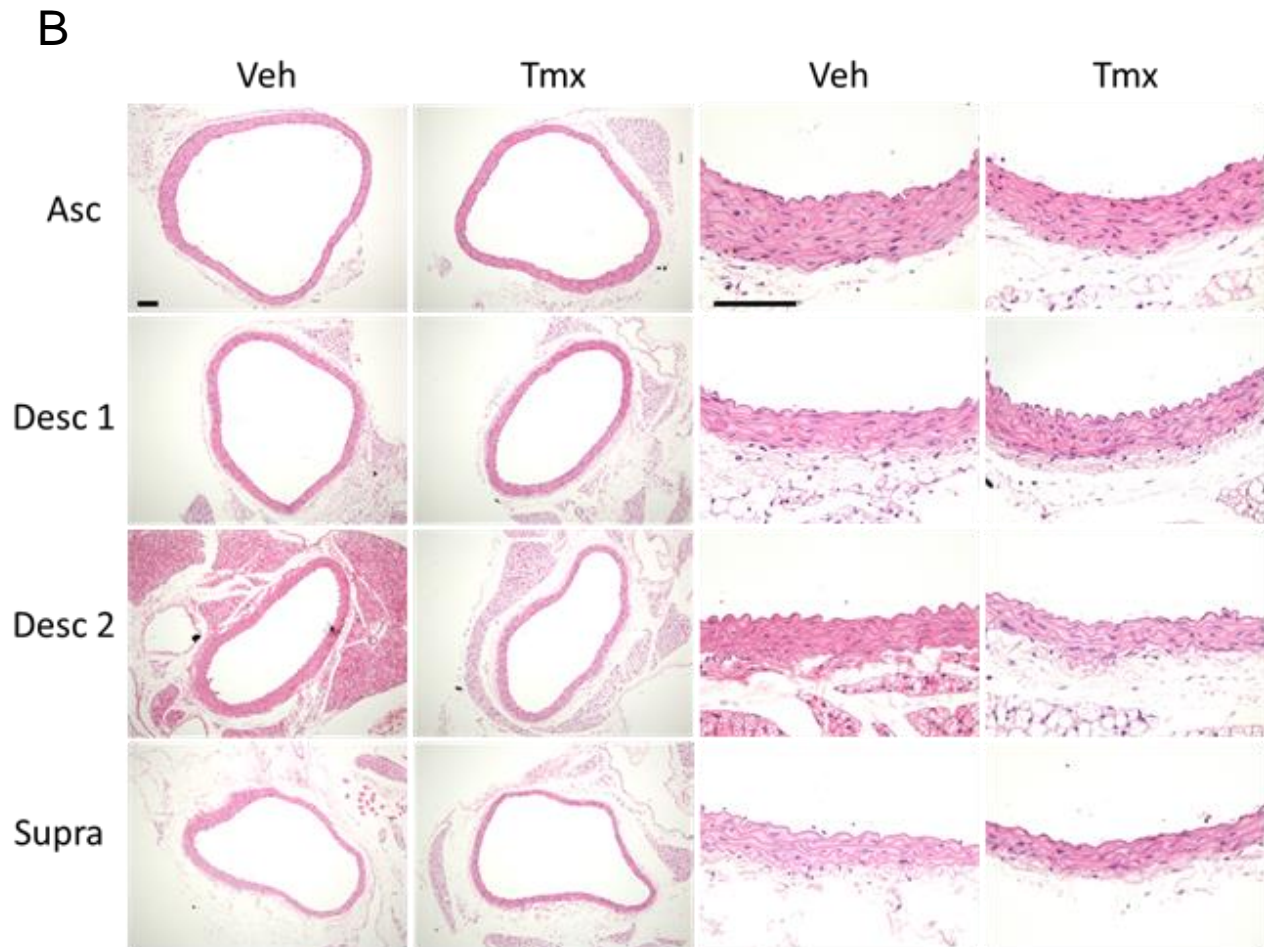


**Figure 3.3 Gross aortic morphology, aortic morphometry, and aortic histology appear normal after induction of SIRT6 knockdown.**

Aortas were dissected from SMMHC-CreER<sup>T2</sup>;SIRT6<sup>f/f</sup> mice at six weeks post vehicle (Veh) or tamoxifen (Tmx) injection. A) Representative gross images of ascending, aortic arch, thoracic, and abdominal aorta; Veh n=4, Tmx n=4. Scale bar: 10 mm. B) Panel of representative H&E stained sections of ascending (Asc), descending thoracic (Desc 1, Desc 2), and suprarenal (Supra) regions of the aorta; Veh n=4, Tmx n=4. Scale bars: 100 $\mu$ m. C) Lumen area measurements of ascending and descending thoracic sections of aorta. Histograms represent means $\pm$ SEM; Veh n=4, Tmx n=4.

### 3.3 Ang II-Infusion Induces Inflammatory Aortic Wall Destruction in SMC-specific SIRT6-Deficient Mice

#### 3.3.1 Saline-Infused Corn Oil and Tamoxifen Injected Mice have Healthy Aortas

To further our understanding of SIRT6 in vascular SMCs, we infused Veh and Tmx injected SMMHC-CreER<sup>T2</sup>;SIRT6<sup>ff</sup> mice with Ang II to create an environment of prolonged exposure to oxidative stress in the vasculature. Ang II-infusion via subcutaneous surgical implantation of osmotic minipumps have been used to study a range of vascular pathologies including atherosclerosis, hypertension, vascular remodeling, and inflammation [17]. Ang II-infusion typically lasts either 7, 14, or 28 days. Saline-infusion is commonly used to control for any stress or damage from surgery. Saline-infused control and SIRT6KO mice had aortas that were normal without any obvious signs of abnormalities or damage (Figure 3.4). Aortic histology of saline-infused mice was identical to that of previous mice without saline-infusion.

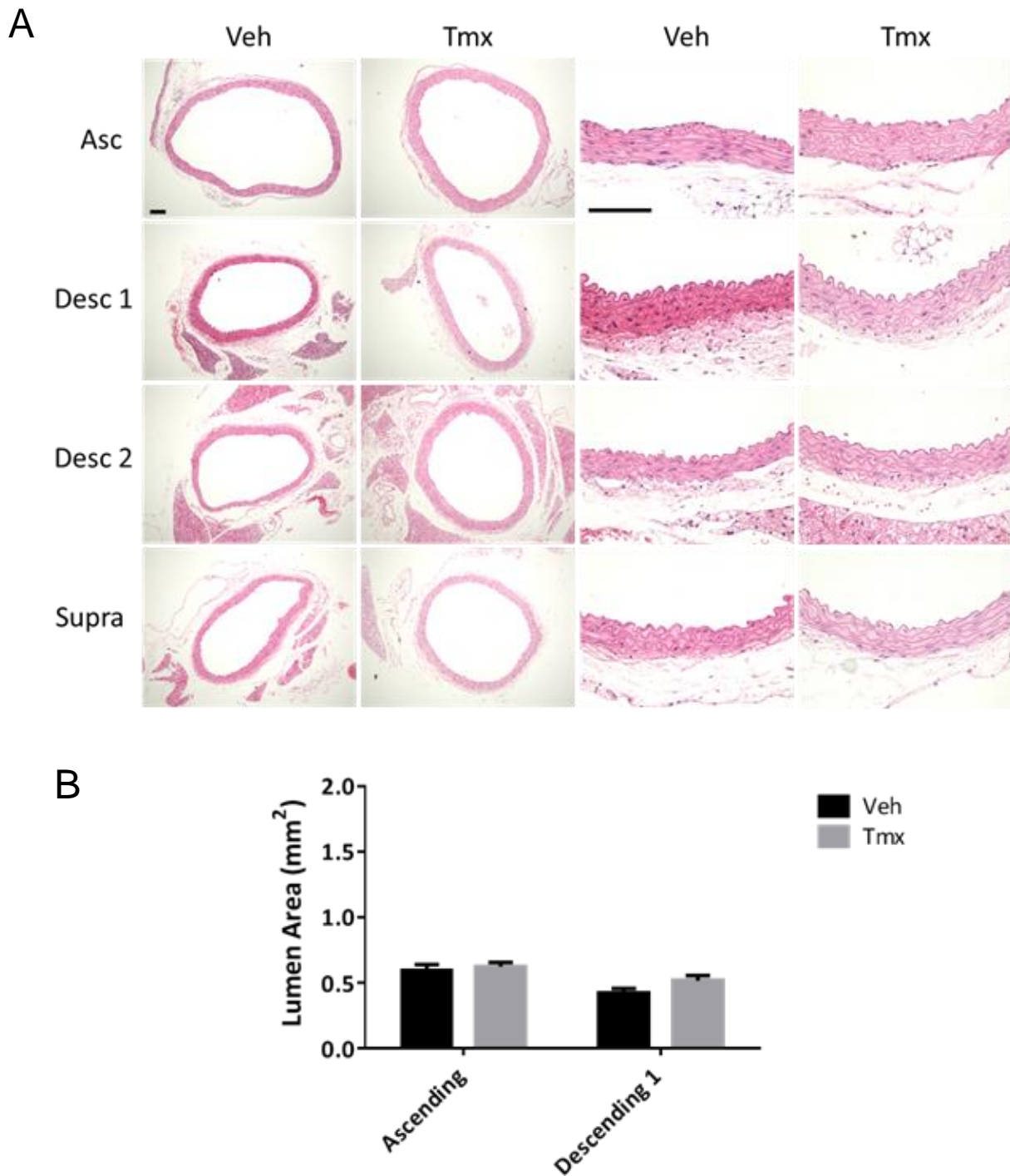


**Figure 3.4 Aortic morphometry and histology appear normal in the saline-infused in SIRT6KD mouse.**

Aortas dissected from Veh and Tmx injected SMMHC-CreER<sup>T2</sup>;SIRT6<sup>f/f</sup> mice after 28 day saline-infusion (i.e. 10 weeks post Veh or Tmx injection). A) Panel of representative H&E stained sections of ascending (Asc), descending thoracic (Desc 1, Desc 2), and suprarenal (Supra) regions of the aorta; Veh n=4, Tmx n=4. Scale bars: 100 $\mu$ m. B) Lumen area measurements of ascending and descending thoracic sections of aorta. Histobars represent means $\pm$ SEM; Veh n=6, Tmx n=6.

### 3.3.2 Ang II-Infusion causes Aortic Petechial Hemorrhage in SMC-specific SIRT6-Deficient Mice

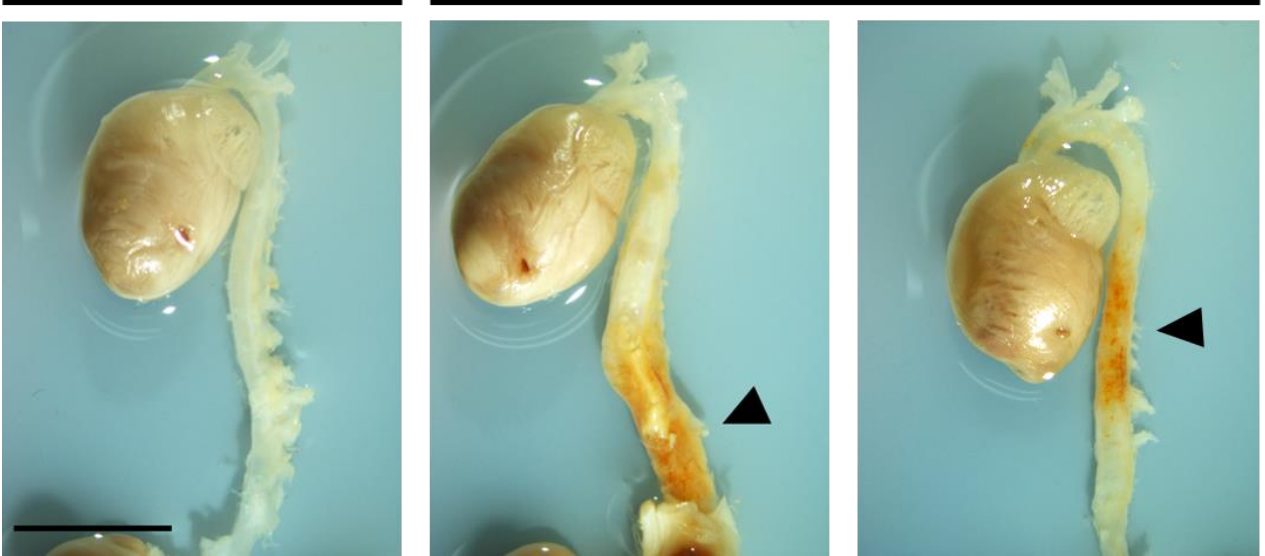
At 6 weeks post Veh or Tmx injection, SMMHC-CreER<sup>T2</sup>;SIRT6<sup>f/f</sup> mice were infused with Ang II over the course of 28 days and then euthanized. Upon gross inspection, we observed marked sites of petechial, or punctate, hemorrhage along the external surface of the aorta in 67% (n=4/6) of SIRT6KO mice (Figure 3.5, A). Though gross abnormalities were absent in the majority of control mice, there was one incident of minor hemorrhaging just inferior to the left subclavian artery that was nominally visible under the dissecting microscope (n=1/8). Hemorrhage sites were patchy in nature and consistently located inferior to the left subclavian artery in the descending thoracic aorta with extension into the abdominal aorta.

Histological examination of these sites revealed an accumulation of hemosiderin within the outer layers of the media and adventitia (Figure 3.5, B). Hemosiderin is an aggregate of ferritin found within cells that often forms after bleeding and subsequent degradation of red blood cells. Histology revealed traces of hemosiderin in aortic regions that were not visible grossly. Hemosiderin was found in all regions (Asc, Desc 1, Desc 2, Supra) of SIRT6KO aortas, while in the control, it was minimally present in the ascending and upper descending thoracic (Asc and Desc 1) regions. The presence of hemosiderin was significantly greater in lower descending thoracic (Desc 2) region of SIRT6KO mice compared to control (Figure 3.5, C). Finding hemosiderin, as opposed to red blood cells, suggests that a significant amount of time has passed since the initial hemorrhage event. Moreover, its location predominately in the peripheral layers of the media and in the adventitia suggests the vasa vasorum as the source of blood and not the lumen.

A

Veh

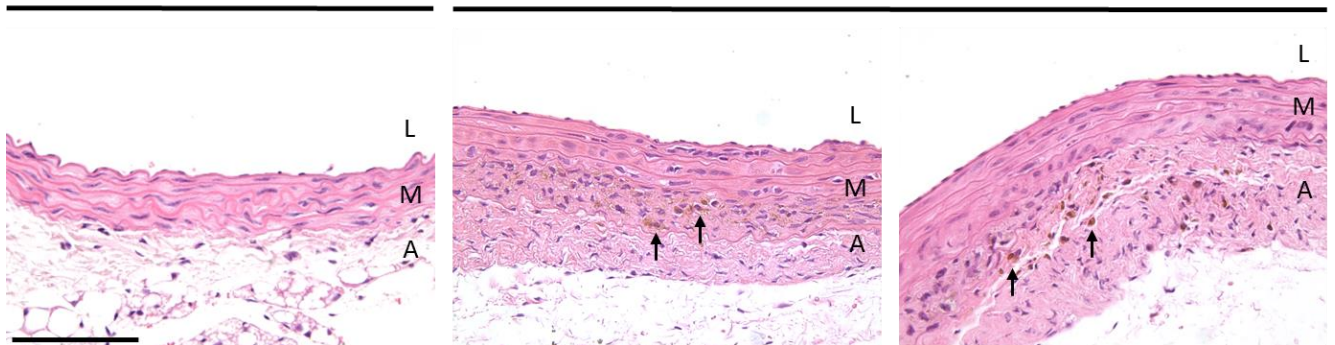
Tmx



B

Veh

Tmx





C

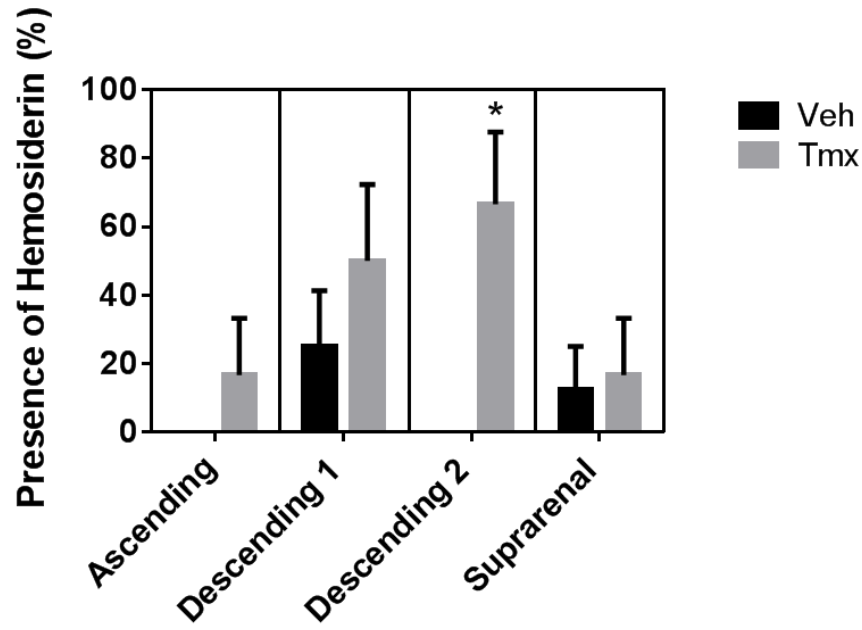


**Figure 3.5 Ang II-infusion causes petechial hemorrhage in SMC-specific SIRT6KO aortas.**

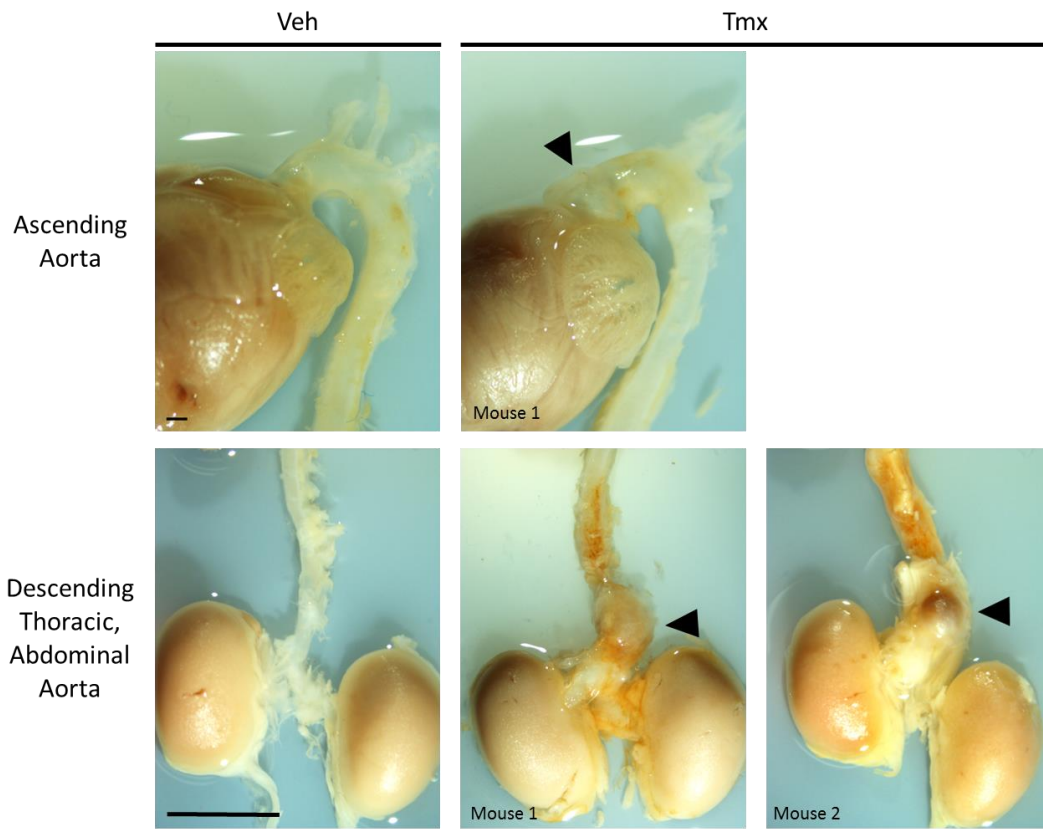
Aortas were harvested from Veh and Tmx-injected SMMHC-CreER<sup>T2</sup>;SIRT6<sup>fl/fl</sup> mice after 28 day Ang II infusion (10 weeks post Veh or Tmx injection). A) Representative gross images of ascending, aortic arch, thoracic, and abdominal aorta; Veh n=8, Tmx n=6. Arrowheads mark gross petechial hemorrhage in descending thoracic and abdominal aorta; Veh n=1/8, Tmx n=4/6. Scale bar: 1cm. B) Representative H&E stained sections of Veh and Tmx-injected descending thoracic aorta. Arrows mark buildup of hemosiderin in the media (middle) and adventitia (right). L, lumen; M, media; A, adventitia. Scale bar: 100 $\mu$ m. C) Presence of hemosiderin in 4 aortic regions; Veh n=8, Tmx n=6. Histobars represent means $\pm$ SEM. \*Significant compared to Veh ( $p < 0.05$ ), Chi-square and Fisher's exact test.

### 3.3.3 Ang II-Infusion causes Aortic Aneurysms in SMC-specific SIRT6-Deficient Mice

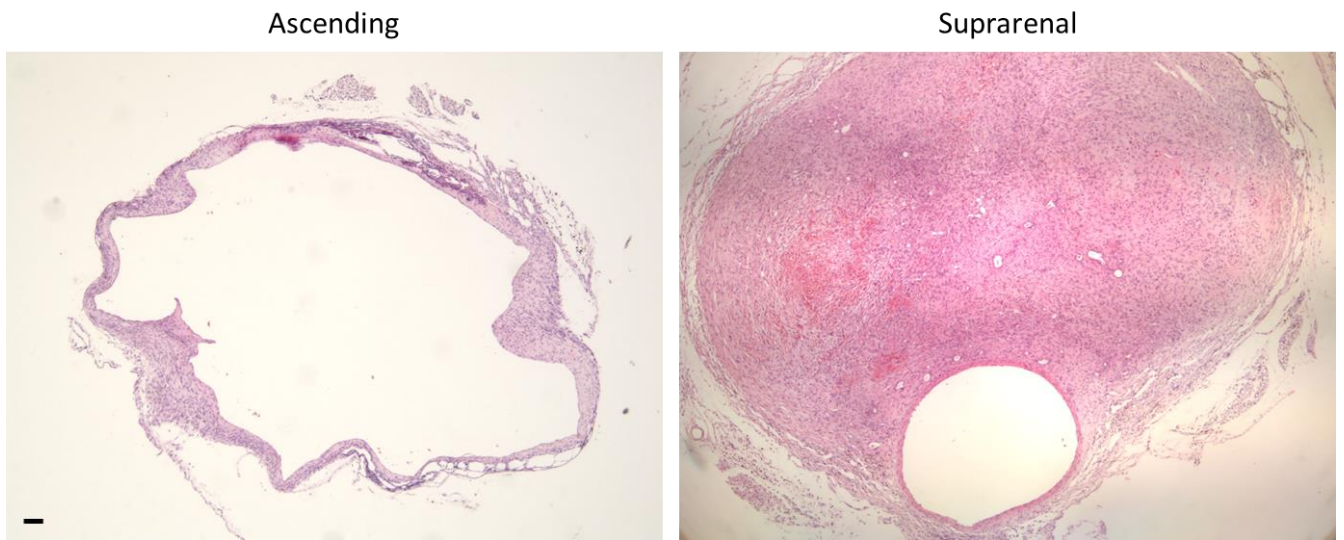
In addition to petechial hemorrhage, gross observation revealed aortic aneurysms in Ang II-infused SIRT6KO mice only, and not in control mice. By definition, an aneurysm is defined as the permanent, localized dilatation of a vessel [203]. We observed aneurysms in 33% (n=2/6) of SIRT6KO mice and located in different regions of the aorta. While one mouse (Mouse 2) had a single aneurysm in the descending thoracic region, the other (Mouse 1) had two (Figure 3.6, A). Mouse 1 had one aneurysm positioned close to the aortic root in the ascending region and another in the suprarenal region (Figure 3.6, A). Histology revealed almost complete loss of media in the ascending aneurysm and massive adventitial reaction in the suprarenal aneurysm (Figure 3.6, B).

After the discovery of aortic aneurysms, we wanted to know if SMC-specific SIRT6KO caused increased aortic dilatation. Measuring the lumen area in four different regions revealed a slight trend of increased dilatation in the ascending (p=0.09), descending 2, and suprarenal sections of SIRT6KO mice (i.e. regions with aneurysm) without statistical significance (Figure 3.6, C).

A



B



C

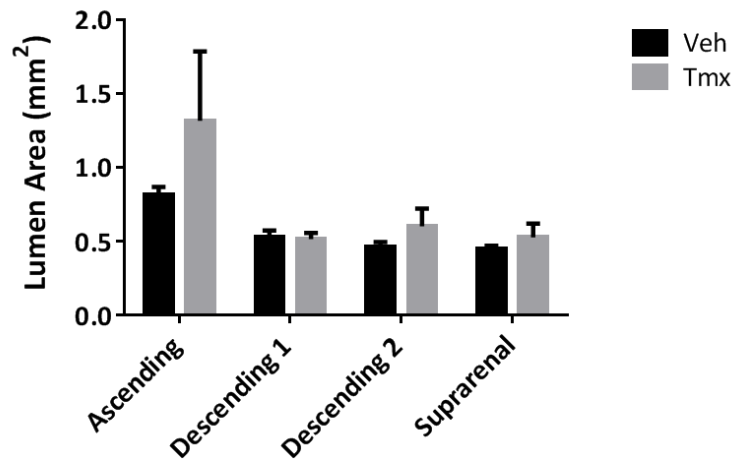


**Figure 3.6 Ang II-infusion causes aortic aneurysms in SMC-specific SIRT6KO mice.**

Aortas were harvested from Veh and Tmx-injected SMMHC-CreER<sup>T2</sup>;SIRT6<sup>f/f</sup> mice after 28 day Ang II-infusion (10 weeks post Veh or Tmx injection). A) Gross images of aneurysms in ascending, descending thoracic, and abdominal aorta of Tmx-injected mouse; Veh n=0/8, Tmx n=2/6. Scale bar: 1cm. B) H&E stained sections of ascending and suprarenal aortic aneurysm in Tmx-injected mouse. Scale bar: 100 $\mu$ m. C) Lumen area measurements of four aortic regions; Veh n=8, Tmx n=6. Histograms represent means $\pm$ SEM.

### 3.3.4 Evidence of an Inflammatory Cell Infiltrate in Ang II-Infused SIRT6-Deficient Mice and Minor Cell Infiltration in the Vehicle Control

Even more striking than hemorrhaging was the deposition of a prominent cellular infiltrate in the aortic media of Ang II-infused SIRT6KO mice (n=6/6). Cell infiltration was also found in vehicle control mice (n=6/8) at a lower degree of severity. H&E staining revealed areas containing high concentration of nuclei that were morphologically different from the conventional elongated SMC nuclei (Figure 3.7, A). In such areas, vascular SMCs were absent and replaced with a cellular infiltrate.

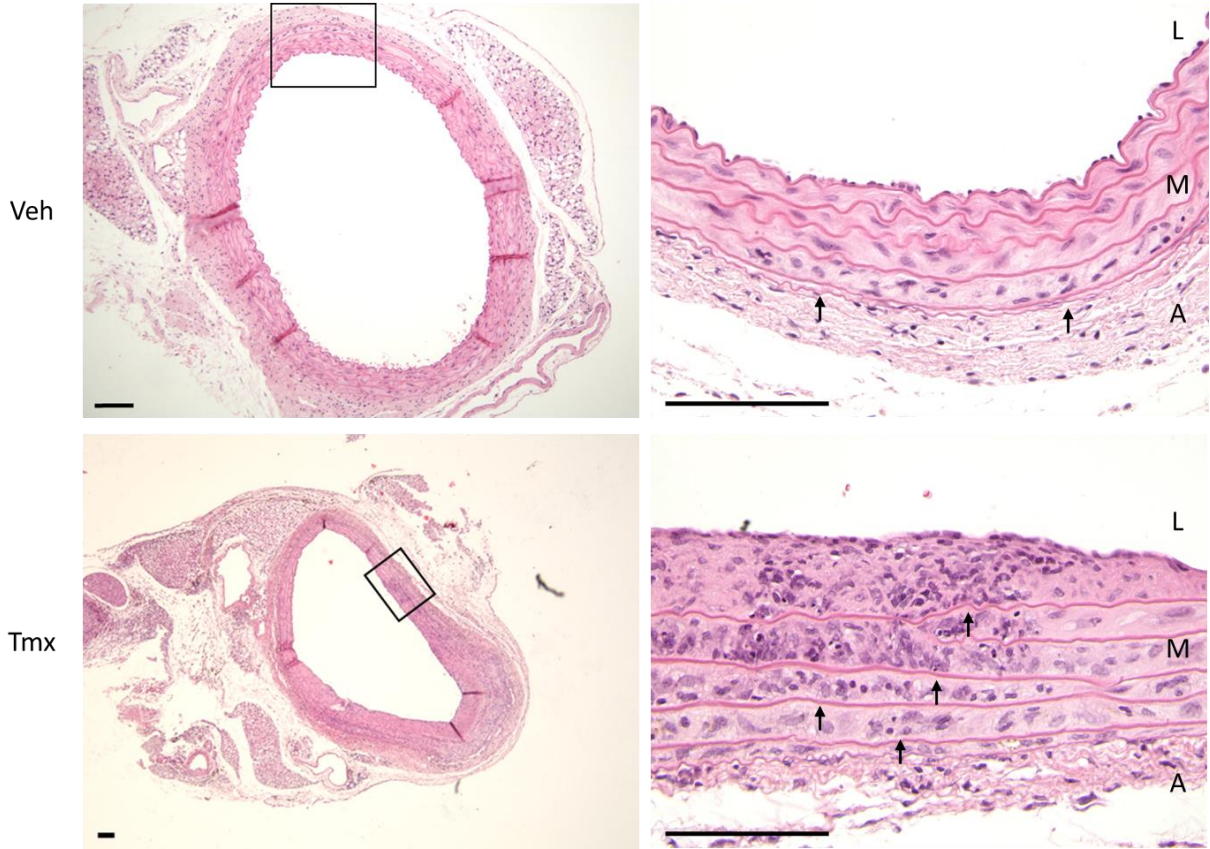
In every case, cell infiltration and loss of SMCs began in the outermost layer of media and gradually progressed towards the lumen. Therefore, we first sought to describe this unique phenotype by calculating the percentage of aortic medial layers penetrated by the cell infiltrate in both control and SIRT6KO mice. Cell infiltrate medial layer permeation was greater in SIRT6KO mice compared to control in all regions: 37±16% in ascending (p<0.05), 32±14% in descending-1 (p<0.05), 31±19% in descending-2 (p=0.12), 32±11% suprarenal (p<0.05) (Figure 3.7, B). Moreover, areas that were infiltrated showed signs of aortic wall destruction such as breaks in the elastic lamella and formation of a neointima. To assess the degree of damage and destruction to the aortic wall, we created a scoring system from 0 being no presence of cellular infiltration to 4 representing massive infiltration penetrating all layers of the aortic wall. Grading was based on criteria that took into account cell infiltrate area, increase in medial thickness, neointima formation, and elastin breakage. Within this system, aortic wall destruction was significantly greater across all aortic regions in SIRT6KO mice compared to control (Figure 3.7, C). Therefore, though cell infiltration was also found in control mice, its severity and damage was to a far lesser extent than SIRT6KO mice.

Next, we sought to identify the cell types that comprised the cell infiltrate. While some nuclei were characteristic of inflammatory cells (i.e. monocytes), round and stained darkly with hematoxylin, the morphology of most nuclei were provided insufficient information for accurate characterization. Histological sections were immunostained with  $\alpha$ -smooth muscle actin ( $\alpha$ -SMA), CD45, and Ki67 to identify constituents of the cell infiltrate (Figure

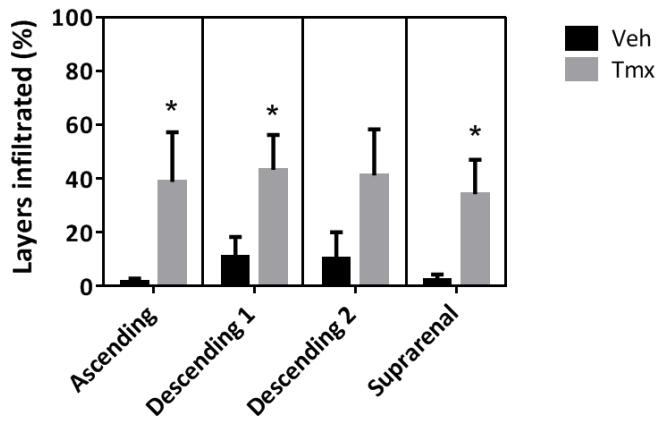
3.7, D). The contractile protein  $\alpha$ -SMA is expressed in both differentiated SMCs and myofibroblasts [6]. Most infiltrated areas stained positive for  $\alpha$ -SMA staining, signifying the presence of myofibroblasts in a wound-healing situation. However, its staining pattern was patchy and integrated with  $\alpha$ -SMA-negative areas. The leukocyte common antigen CD45 is expressed in all hematopoietic cells such as macrophages, monocytes, T, B, dendritic, and natural killer cells. Positive brown staining for CD45 revealed the prominence of inflammatory cells in the cell infiltrate. The marker Ki67 was used to assess proliferative activity at the sites of inflammation. Ki67-positive staining overlapped with CD45-positive areas as opposed to  $\alpha$ -SMA-positive areas. This suggests that the cell infiltrate is not comprised of actively proliferating myofibroblasts or SMCs. Rather, there is a portion of the inflammatory cell infiltrate that is proliferative (e.g. monocytes and in some cases macrophages [204]).

In a different mouse,  $\alpha$ -SMA staining revealed a clear boundaries outlining actin-negative layers sandwiched between actin-positive layers adjacent to either the lumen or the adventitia (Figure 3.7, E). Within the actin-negative layers we see loss of SMCs as well as Ki67 and CD45-positive cells that appear to be invading the remaining inner medial layers that do not show signs of damage. The actin-positive layer adjacent to the adventitia implies the presence of myofibroblasts and a wound healing response following SMC death and inflammation.

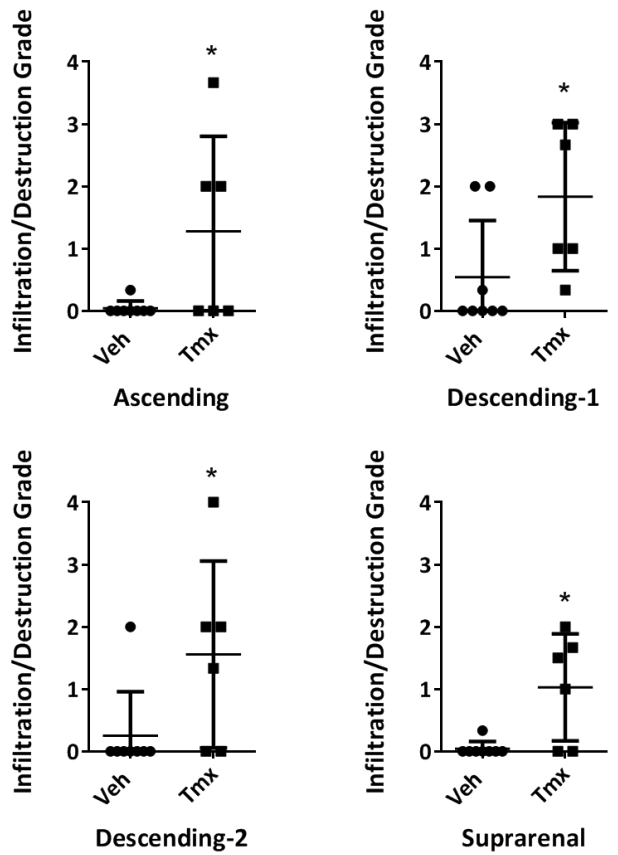
A



B

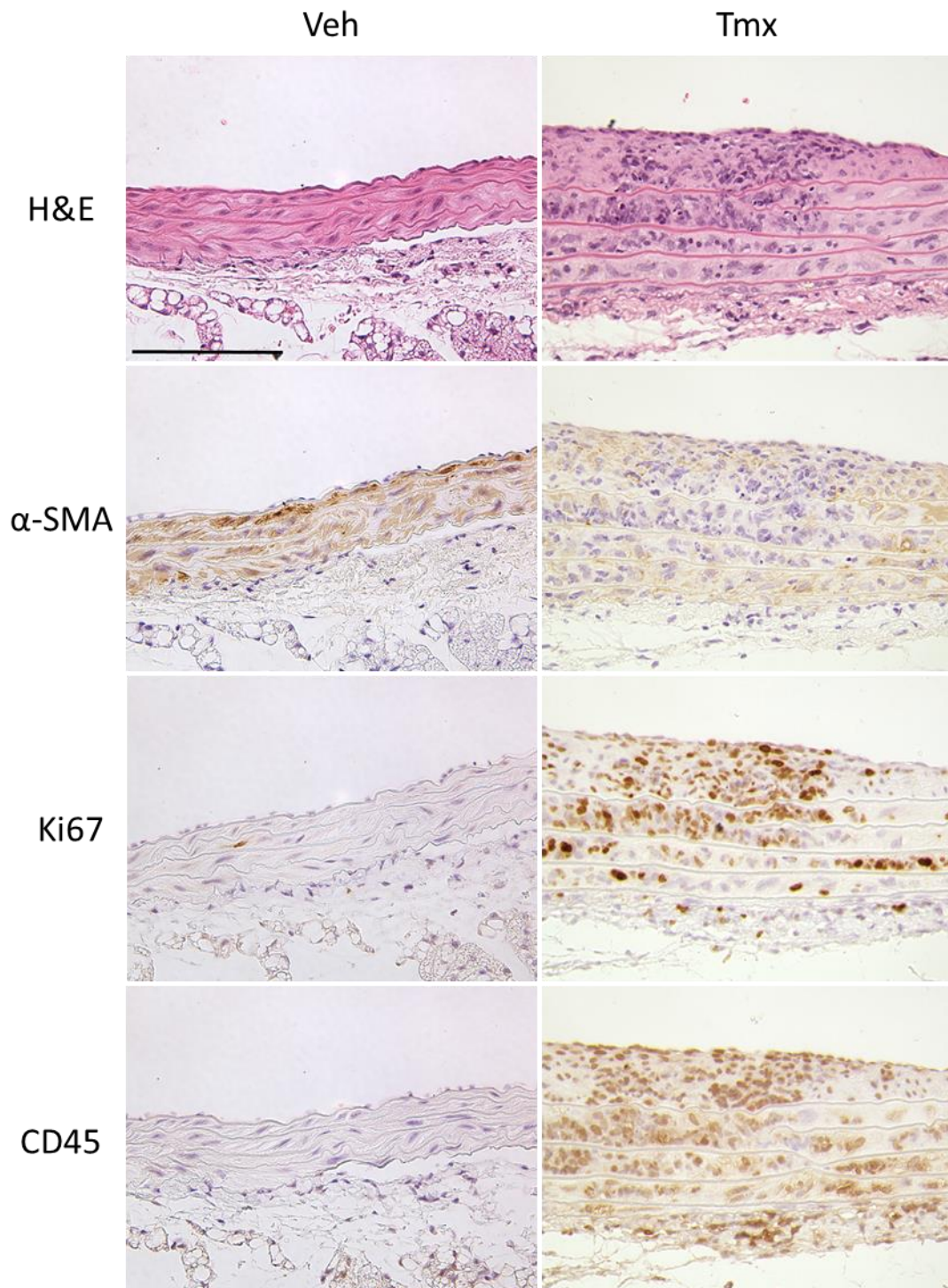


C





D





E

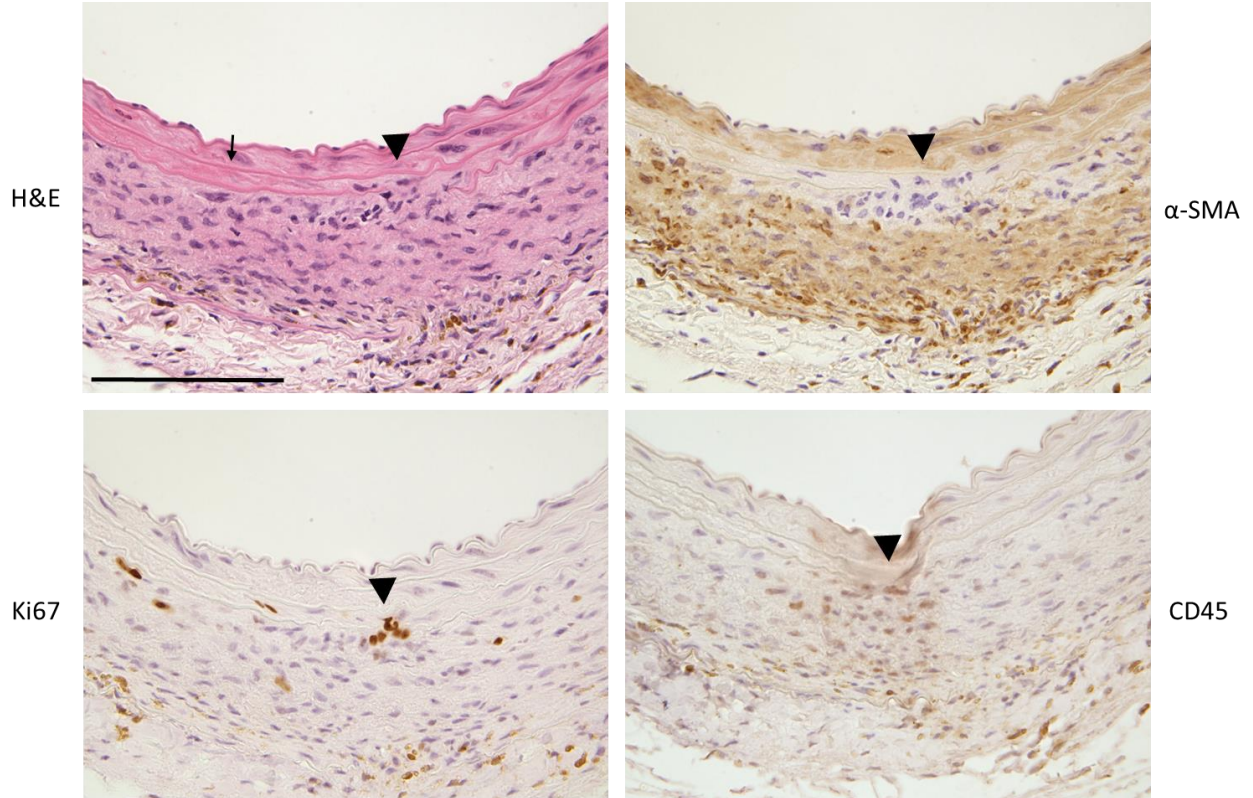


**Figure 3.7 Ang II-infusion of SIRT6KO mouse shows greater degree of inflammatory cell infiltration and aortic wall destruction compared to vehicle-control.**

Aortas were harvested at 10 weeks post Veh and Tmx-injection and 4 weeks post Ang-II infusion; Veh n=8, Tmx n=6. A) Representative H&E stained sections of Veh-injected descending thoracic aorta showing minor cell infiltration in the outer layer of aortic media (n=6/8) and Tmx-injected descending thoracic aorta showing massive cell infiltration affecting all layers of the aortic media (n=6/6). L, lumen; M, media; A, adventitia. Scale bar: 100 $\mu$ m. B) Percentage of aortic medial layers invaded by cell infiltration in four aortic regions. Histobars represent means $\pm$ SEM. \*Significant compared to Veh (p<0.05), *t* test. C) Evaluation of the degree of aortic wall destruction in four aortic regions. Histobars represent means $\pm$ SEM. \*Significant compared to Veh (p<0.05), *t* test. D) Representative histological sections of descending thoracic aorta (Desc-2) of Veh-injected mouse and inflammatory cell infiltrate in Tmx-injected mouse immunostained with Hematoxylin and Eosin (H&E), alpha-smooth muscle actin ( $\alpha$ -SMA), Ki67, and CD45. Scale bar: 100 $\mu$ m. E) Representative histological sections of descending thoracic aorta (Desc-1) of Tmx-injected mice. Arrowheads show inflammatory cells infiltrating the inner medial layers. Arrows show evidence of SMC loss in media. Scale bar: 100 $\mu$ m.

### 3.3.5 Ang II-Induced Hypertensive Response in Vehicles and SIRT6KO Mice

Prolonged Ang II-infusion causes steady increases in blood pressure (BP) and is commonly used to induce hypertension in animal models [18]. We wanted to know whether there was a correlation between high blood pressure and the aortic hemorrhage, aneurysms, and inflammation seen in Ang II-infused SIRT6KO mice. In addition, we wanted to know whether control and SIRT6KO mice differed in their response to Ang II. Measurements were taken 2 weeks prior to saline or Ang II-infusion (i.e. 4 weeks post Veh or Tmx-injection) to establish baseline BP levels. Two measurements per week were taken and averaged as weekly measurements during the 28 day-infusion of saline or Ang II.

With respect to baseline BPs in both control and SIRT6KO mice, no statistical difference was found in mice that were eventually saline-infused (mean difference =  $11.59 \pm 7.54$  mmHg;  $p=0.16$ ). However, in mice that would later receive Ang-II, SIRT6KO mice had significantly higher baseline BP than control (mean difference =  $23.17 \pm 6.92$  mmHg;  $p<0.05$ ) (Figure 3.8, B).

As expected, saline-infusion did not significantly increase mean arterial BP in control ( $n=6$ ) or SIRT6KO mice ( $n=6$ ) (Figure 3.8, A). Ang II-infusion produced a hypertensive response in both control ( $n=8$ ) and SIRT6KO mice ( $n=6$ ) (Figure 3.8, B). Comparing baseline measurements with those taken in the final week of infusion, BP increased by 31.0 and 24.5 mmHg in control and SIRT6KO mice, respectively. Though there was a slight trend towards higher BP in Ang II-infused SIRT6KO mice compared to control, the difference was not statistically different. Another observation made was that in SIRT6KO mice, BP gradually increased from 154.2 mmHg in the first week of Ang II-infusion to 168.7 mmHg in the final week. In the control, BP stayed the same at 151.3 mmHg in the first week to 152.0 mmHg in the final week. Therefore, the hypertensive response appeared to be continually increasing in SIRT6KO while it reached a plateau in control mice by the first week of Ang II-infusion.

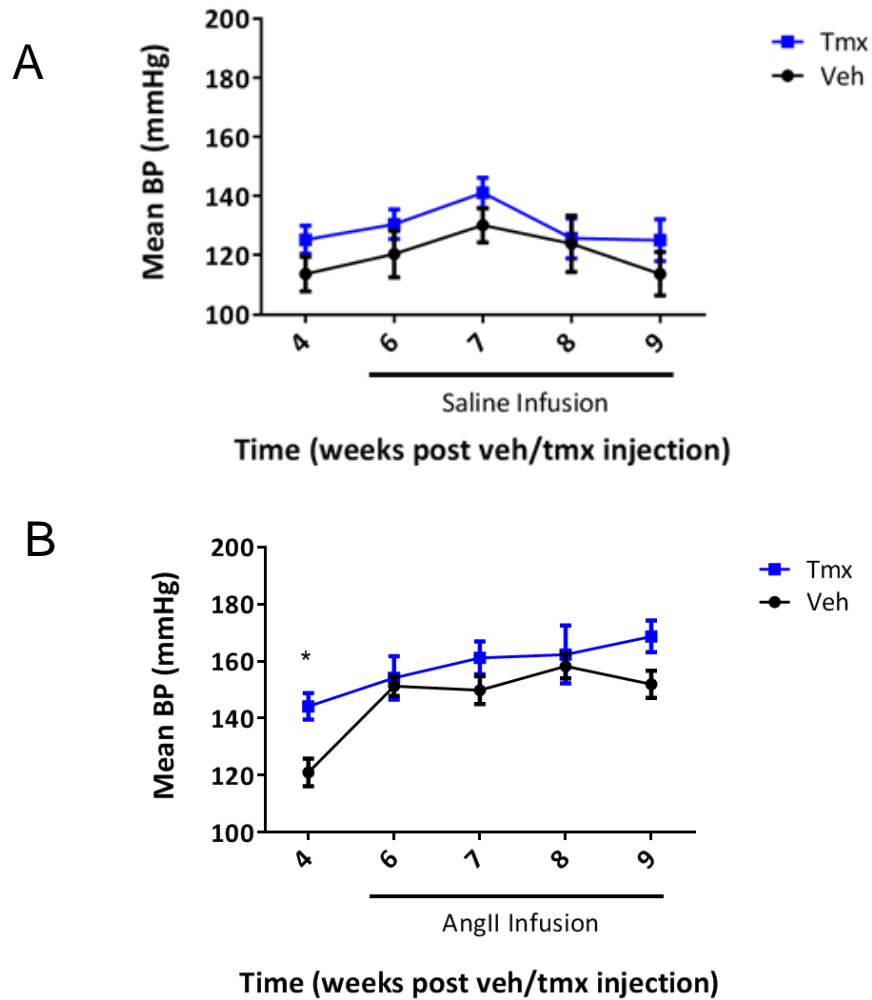


**Figure 3.8 Aortic mean arterial blood pressures of vehicle and tamoxifen-injected mice after saline/Ang II-infusion.**

A) Weekly blood pressure measurements of Veh and Tmx-injected saline-infused mice; Veh n=6, Tmx n=6. Points represent means±SEM. B) Weekly blood pressure measurements of Veh and Tmx-injected Ang II-infused mice; Veh n=8, Tmx n=6. Points represent means±SEM. \*Significant compared to Veh ( $p < 0.05$ ), 2-way ANOVA and Sidak's multiple comparisons test.

## 4 Discussion

In summary, we were able to create a novel SMC-specific SIRT6-deficient (SIRT6KO) mouse model that was inducible upon tamoxifen injection. This was evidenced via SIRT6 knockdown at the DNA, mRNA, and protein level. We showed that aortas in SIRT6KO mice were normal and free from gross and histological signs of damage. In response to Ang II-infusion, SIRT6KO aortas develop petechial hemorrhage and aneurysms. We also found evidence of widespread aortic inflammatory cell infiltration and medial degeneration in SIRT6KO mice. Therefore, we propose a protective role for SIRT6 against oxidative stress-induced inflammation and aortic wall destruction.

### 4.1 Oxidative Stress Causes Aortic Wall Destruction in the Absence of SIRT6

The effect of oxidative stress via Ang II on vascular injuries has been well studied. Ang II is known to initiate and advance pathologies such as aortic dissection, aortic aneurysms, high blood pressure, and vascular inflammation. As discussed previously, most Ang II-induced vascular injuries are mediated via activation of NAD(P)H oxidases and increased ROS levels in SMCs.

#### 4.1.1 Petechial Hemorrhage and Aneurysm

Ang II-infusion has been shown to cause aortic hemorrhages in hyperlipidemic (i.e. apolipoprotein E- and LDL receptor-deficient), older (i.e. 6-12 months), and various KO mouse models, including SMC-specific SIRT1KO mice [84,205,206]. The presence of blood within the vessel wall is primarily presented as an aortic dissection. This disorder occurs when blood enters the media through a break in the intima and propagates longitudinally along the aorta. As blood pools into the media, it creates a “false lumen” that protrudes into the true lumen. Less common are hemorrhages that lack an intimal tear and are classified as intramural hematomas [207]. Blood is thought to be sourced by the vasa vasorum, though, a recent study identified medial tears in aortic arterial branches as the rupture point and source of blood [208]. Upon gross observation, intramural hematomas differ from aortic dissections and present as a crescent-shaped bulge that protrudes outwardly from the aortic wall (Figure 4.1).

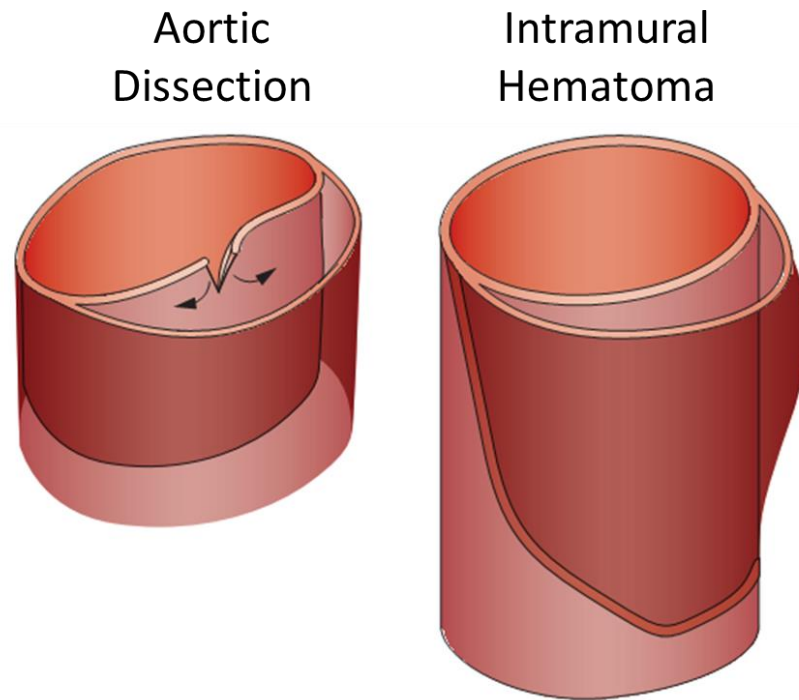


**Figure 4.1** Diagram depicting the difference between aortic dissection and intramural hematoma.

Aortic dissection presents with a false lumen that encroaches upon the intraluminal area while intramural hematoma bulges outward from the aortic wall.

Our finding of petechial hemorrhage in the descending thoracic and abdominal aorta in SIRT6KO mice differed from both aortic dissection and intramural hematoma. The patchy appearance of hemosiderin at both the macro- and microscopic level points toward ruptures in the vasa vasorum as the most probably source of the bleed. Most studies that report aortic dissections present H&E images with red blood cells present in the aorta. In contrast, our histology shows traces of hemosiderin as evidence that a considerable amount of time has passed from when the hemorrhage was initiated to when mice were sacrificed. Though hemosiderin can be found in all cells, it is most commonly found in macrophages. Hemosiderin-laden macrophages may represent the aftermath of a medial and adventitial inflammatory response to wall injury.

In the presence of Ang II, SIRT6KO mice also developed aneurysms in the ascending, descending thoracic, and abdominal aorta. H&E sections revealed substantial loss of both SMCs and elastin, demonstrating complete medial destruction in the ascending aneurysm. On the other hand, aneurysms in the descending thoracic and abdominal aorta presented with massive adventitial reactions. Ang II-infused hyperlipidemic mice have long been used as models of aortic aneurysms, though, aneurysms are also found in normocholesterolemic C57Bl/6 mice at a lower rate [209,210]. Differences between ascending and abdominal aneurysms that have been recognized in the literature were also observed in SIRT6KO mice. Ascending aneurysms have minimal adventitial thickening and diffuse elastin degradation compared to a large adventitial reaction and minor changes in elastin integrity in abdominal aneurysms. Although reasons for these differences are unclear, they are frequently attributed to differences in embryonic cell origins [210].

#### 4.1.2 Aortitis

Although SIRT6KO mice presented with aortic dissections and aneurysms, the most prevalent and striking finding was the presence of an inflammatory cell infiltrate in the aortic media. Moreover, this finding seems to be crucial for understanding the root causes of the gross abnormalities. An inflammatory cell infiltrate was found in the media of at least one aortic region of every SIRT6KO mouse with the highest incidence and severity in the descending thoracic regions. The medial infiltrate in SIRT6KO mice was massive compared to the minor infiltrate seen in the vehicle controls or C57Bl/6 mice in response

to Ang II [211]. Its pervasiveness throughout the aortic media is most similar to aortitis, a pathological term for inflammation localized to the aortic wall. Generally, cases are classified according to the cause of inflammation: infectious aortitis (e.g. infection from *Salmonella*), noninfectious aortitis (e.g. diseases such as giant cell arteritis, Takayasu arteritis), or isolated aortitis (e.g. inflammatory abdominal aortic aneurysm) [212]. The phenotype seen in SIRT6KO mice is best categorized as isolated aortitis. In one human study looking at the prevalence of aortitis among resected thoracic samples, about 75% were isolated cases. Risk factors for aortitis include advanced age, history of connective tissue disease, diabetes mellitus, and heart valve pathology [213]. In mice, inflammatory cell infiltration is most often seen in conjunction with aortic dissection and/or suprarenal aneurysm in Ang II-infused hyperlipidemic mice [205]. Though there was evidence of inflammation at aneurysmal sites in SIRT6KO mice, most incidences of aortitis were found in the absence of aneurysm.

With the information collected via immunostaining, we hypothesize the following progression of events in SIRT6KO mice: increased sensitivity to oxidative damage and possibly cell death in SIRT6-deficient SMCs, heightened pro-inflammatory response, massive infiltration of inflammatory cells from the adventitia into the media, SMC and elastin degeneration, and finally, media remodeling initiated by adventitial myofibroblasts. Our phenotype is consistent with the “outside-in” theory of vascular inflammation whereby adventitial inflammatory cells enter the media through the vasa vasorum [214]. Next, adventitial fibroblasts differentiate into myofibroblasts, migrate to the site of injury, and begin vascular remodeling by synthesizing collagen and ECM proteins (e.g. elastin and fibronectin) [1].

To connect all our findings together, we believe that SIRT6KO-induced aortitis and subsequent medial degeneration (i.e. elastin and medial loss) is the basis for prospective development of hemorrhages and aneurysms. Whether aortitis progresses into those aortic syndromes or not might depend on the balance between medial degeneration by macrophages and the wound healing response by myofibroblasts. A study on aneurysm formation in Ang II-infused hyperlipidemic mice over 56 days identified a similar sequence

of events. Accumulation of macrophages in the media and elastin degradation always preceded aortic dissection and subsequent aneurysm [205].

### 4.1.3 Hypertension

Prolonged Ang II-infusion stimulates vascular remodeling (i.e. SMC hypertrophy and hyperplasia) in SMCs, thereby inducing thickened walls and a consequent hypertension [17]. SIRT6KO mice developed an Ang II-induced hypertensive response that was not significantly different from vehicle controls. SIRT6KO mice blood pressure prior to Ang II-infusion was significantly higher than controls, causing speculation as to whether baseline hypertension was a causal factor in the phenotype seen in SIRT6KO mice. While hypertension is a risk factor for aortic dissection, hyperlipidemic mouse models show that Ang II-induced increases in blood pressure do not account for the development of aortic aneurysms, atherosclerotic lesions, or their associated inflammatory responses [18,203,209,210]. Oxidized LDL in hyperlipidemic mice increase ROS levels and sensitizes the vessel wall to the inflammatory effects of Ang II [206]. We propose that SIRT6 acts in a similar manner, where it plays an anti-inflammatory role in SMCs that prevents aortitis, petechial hemorrhage, and aortic aneurysms. Ultimately, we are persuaded to believe that we see a SIRT6-dependent phenotype in our mice.

We also note that no increase in baseline blood pressure was observed in the same number of SIRT6KO mice (n=6) prior to saline-infusion. Therefore, it is unclear if SMC-specific SIRT6-deficiency induces hypertension in mice.

### 4.1.4 Protective Effect of SIRT6 in SMCs

Our findings provide additional evidence towards an anti-inflammatory role for SIRT6, specifically in SMCs. Pending continued work on this project, we hope to elucidate the molecular mechanisms and signaling pathways behind our phenotypes. SIRT6's anti-inflammatory role through binding of NF- $\kappa$ B and repressing transcription at its target genes has been well described [188]. In arthritis mouse models, SIRT6 overexpression inhibited production of NF- $\kappa$ B downstream proinflammatory cytokines such as TNF- $\alpha$  and IL-6 in injured tissues. Moreover, mRNA expression of MMPs were downregulated [189,190]. Vascular inflammation is also largely mediated by NF- $\kappa$ B signaling pathway. This includes



increased expression of the cytokines IL-6 and monocyte chemoattractant protein (MCP-1), cell adhesion molecules VCAM-1 and ICAM-1, and the major players in collagen degradation, MMPs [17,206]. Therefore, one might expect to find significant increased expression of the aforementioned cytokines and proteins in SIRT6-deficient SMCs in response to Ang II.

## 4.2 Reflections on Vascular Inflammation in Ang II-Infused Vehicle Controls and Cre-lox Technology

As previously discussed, a SMC-specific SIRT1-deficient mouse model was recently generated using a smooth muscle  $22\alpha$  promoter for tissue specificity [84]. For our model, we chose a Cre construct with a SMMHC promoter because it is the marker with the highest specificity for SMCs. In addition to vascular SMCs, SMMHC-CreER<sup>T2</sup> is expressed in the gastrointestinal tract, urinary bladder, and lung bronchial SMCs. The SMMHC-CreER<sup>T2</sup> mouse was given to us by our collaborator, Dr. Offermanns and has been used by others to successfully generate SMC-specific G<sub>q</sub>-G<sub>11</sub>/G<sub>12</sub>-G<sub>13</sub>, PPAR $\gamma$ , and TGF- $\beta$  type II receptor KO mouse models without any reports of “Cre leakage” (i.e. expression of Cre in the absence of tamoxifen) [196,215,216]. Similar to our mice, the PPAR $\gamma$  KO mice had a mixed genetic background (i.e. BALB/c and C57BL/6). To ensure that all our mice maintained a 75% FVB and 25% C57BL/6 background, control and SIRT6KO mice were always generated in the same way as 3<sup>rd</sup> generation FVB backcrosses. Our induction protocol (i.e. tamoxifen dose, treatment length, recovery time prior to examining knockdown efficiency, oil usage as a vehicle control) was also comparable to the aforementioned models.

### 4.2.1 Hypotheses for Aortic Phenotype in Vehicle Controls

Typical Ang II responses in healthy WT mice include increased aortic medial thickness, elevated blood pressure, and low incidence of aortic dissection and aneurysms [209,217]. Ang II also promotes vascular inflammation through NF- $\kappa$ B activation and consequent recruitment of cell adhesion molecules and chemokines [17]. In WT mice, Ang II-induced recruitment of inflammatory cells predominantly occurs in the adventitia where resident immune cells are stored. Some recruitment happens in the intima via leukocyte

extravasation and even fewer are found in the media [211,214]. Therefore, the discovery of minor aortic wall disruption and a low grade inflammatory cell infiltrate in some vehicle control mice was surprising, though both its incidence and degree of severity are considerably less compared to *SIRT6*KO mice. This finding was unexpected because our mRNA and protein data show that no downregulation of *SIRT6* expression could be detected in vehicle control mice, as compared to mice that had not been subjected to intraperitoneal injection. We put forward three hypotheses in an attempt to explain the appearance of mild phenotype in the control: 1) deleterious side effects from intraperitoneal injections of corn oil, 2) mixed genetic background predisposes *SIRT6*<sup>f/f</sup>;SMMHC-CreER<sup>T2</sup> mice to a spontaneous aortic pathology, and 3) leaky SMC Cre expression/activation and subsequent loxP recombination at floxed *SIRT6* in the absence of tamoxifen, leading to minor and/or local *SIRT6* depletion.

Oil is an unlikely culprit because it is used ubiquitously as a vehicle for administering lipophilic chemicals to rodents, including the SMMHC-CreER<sup>T2</sup> models previously mentioned, without any reports of inflammation or vascular defects [218]. With respect to strain related pathologies, while FVB mice have no known strain pathologies that are relevant to this project, spontaneous aortitis was found in Balb/c mice. Though it was initially attributed to femoral artery ligation, incidence rates of aortic root inflammation in controls were comparable to mice that underwent hind limb ischemia [219]. However, because we are using a mixed (i.e. 75% FVB and 25% C57BL/6) background, there is a possibility that we are the first to report Ang II-induced aortitis in mice with this genetic background.

Though Cre-lox technology has been widely used to create knockout and transgenic animal models, recently, its limitations have been highlighted in the scientific community. Studies show that Nestin-Cre, the main construct used for gene deletions in neuronal tissue, causes a metabolic phenotype of decreased linear growth, decreased lean mass, and increased insulin sensitivity in mice [220]. Nonspecific recombination leading to hypopituitarism and decreased growth hormone is thought to be behind this phenotype. Adding to the peculiarity is the fact that not all strains of Nestin-Cre mice will exhibit a metabolic

phenotype. Increased understanding of Cre-lox system shortcomings underscore the need for experiments to use a variety of controls.

In our mouse model, there is a possibility that the phenotype observed in the vehicle controls happened as a result of unintended SIRT6 deletion. Because our mRNA and protein data show that SMC SIRT6 is robustly expressed in controls, aberrant SMC Cre activation might manifest in a mosaic pattern in the aortic media. In general, the minor lesions in controls are more localized and contained compared to SIRT6KO mice. This suggests that there are “hotspots” of SIRT6-deficient SMCs in controls that allow for focal SMC damage while the larger aortic section demonstrates significantly elevated SIRT6 levels compared to SIRT6KO mice.

#### 4.2.2 Creating SIRT6<sup>ff</sup> Cre-negative Controls

To determine whether the phenotype in controls is due to strain background or leaky Cre expression, we chose to create another group of controls. We are currently in the process of generating a line of control mice with the same FVB/C57BL/6 mixed genetic background that lacks SMMHC-CreER<sup>T2</sup>. These Cre-negative controls will be subjected to Ang-II infusion and have their aortas examined. If they are free of an inflammatory cell infiltrate, this would rule out the mixed genetic background as being responsible for the phenotype. We might also consider using the Rosa26lacZ (R26-lacZ) reporter mouse line to profile Cre expression in the aortic media. Crossing a R26-lacZ with a SIRT6<sup>ff</sup>;SMMHC-CreER<sup>T2</sup> will produce mice that express  $\beta$ -galactosidase in all cells where a Cre-mediated recombination event takes place [198]. Cells can then be stained blue with the addition of X-Gal and visualized.

### 4.3 Conclusion

In summary, we created a novel mouse model with SMC-specific SIRT6 deficiency. With these mice, we found that SMC SIRT6 is necessary for vascular wall integrity in response to the potent oxidant and inflammatory stimulus, Ang II. In particular, SIRT6 protects the aorta from aortitis and subsequent development of aortic hemorrhage and aneurysm.

## References

- 1 Stenmark, K.R. *et al.* (2013) The adventitia: essential regulator of vascular wall structure and function. *Annu. Rev. Physiol.* 75, 23–47
- 2 Venkatraman, S. *et al.* (2008) Implanted cardiovascular polymers: Natural, synthetic and bio-inspired. *Prog. Polym. Sci.* 33, 853–874
- 3 Hoffman, G.S. and Calabrese, L.H. (2014) Vasculitis: determinants of disease patterns. *Nat. Rev. Rheumatol.* 10, 454–62
- 4 Pober, J.S. and Sessa, W.C. (2007) Evolving functions of endothelial cells in inflammation. *Nat. Rev. Immunol.* 7, 803–815
- 5 Seidemann, S.B. *et al.* (2014) Development and pathologies of the arterial wall. *Cell. Mol. Life Sci.* 71, 1977–1999
- 6 Owens, G.K. *et al.* (2004) Molecular regulation of vascular smooth muscle cell differentiation in development and disease. *Physiol. Rev.* 84, 767–801
- 7 Rensen, S.S.M. *et al.* (2007) Regulation and characteristics of vascular smooth muscle cell phenotypic diversity. *Neth. Heart J.* 15, 100–8
- 8 Lacolley, P. *et al.* (2012) The vascular smooth muscle cell in arterial pathology: A cell that can take on multiple roles. *Cardiovasc. Res.* 95, 194–204
- 9 Cohen, R. a and Tong, X. (2010) Vascular oxidative stress: the common link in hypertensive and diabetic vascular disease. *J Cardiovasc Pharmacol* 55, 308–316
- 10 Yung, L.M. *et al.* (2006) Reactive oxygen species in vascular wall. *Cardiovasc. Hematol. Disord. Drug Targets* 6, 1–19
- 11 Balaban, R.S. *et al.* (2005) Mitochondria, Oxidants, and Aging. *Cell* 120, 483–495
- 12 Griending, K.K. *et al.* (2000) NAD(P)H Oxidase: role in cardiovascular biology and disease. *Circ. Res.* 86, 494–501

- 13 Papaharalambus, C. a and Griendling, K.K. (2007) Basic Mechanisms of Oxidative Stress and Reactive Oxygen Species in Cardiovascular Injury. *Trends Cardiovasc Med* 17, 48–54
- 14 Wassmann, S. *et al.* (2004) Modulation of oxidant and antioxidant enzyme expression and function in vascular cells. *Hypertension* 44, 381–6
- 15 Montezano, A.C. *et al.* (2014) Angiotensin II and vascular injury. *Curr. Hypertens. Rep.* 16, 431
- 16 Nickenig, G. and Harrison, D.G. (2002) Current Perspective. *Circulation* 105, 393–396
- 17 Mehta, P.K. and Griendling, K.K. (2007) Angiotensin II cell signaling: physiological and pathological effects in the cardiovascular system. *Am. J. Physiol. - Cell Physiol.* 292, C82–C97
- 18 Qin, Z. (2008) Newly developed angiotensin II-infused experimental models in vascular biology. *Regul. Pept.* 150, 1–6
- 19 Touyz, R.M. *et al.* (2002) Expression of a Functionally Active gp91phox-Containing Neutrophil-Type NAD(P)H Oxidase in Smooth Muscle Cells From Human Resistance Arteries: Regulation by Angiotensin II. *Circ. Res.* 90, 1205–1213
- 20 Landmesser, U. *et al.* (2002) Role of p47phox in vascular oxidative stress and hypertension caused by angiotensin II. *Hypertension* 40, 511–515
- 21 Rey, F.E. *et al.* (2001) Novel competitive inhibitor of NAD(P)H oxidase assembly attenuates vascular O<sub>2</sub>(<sup>-</sup>) and systolic blood pressure in mice. *Circ. Res.* 89, 408–414
- 22 Heitzer, T. *et al.* (1999) Increased NAD(P)H oxidase-mediated superoxide production in renovascular hypertension: Evidence for an involvement of protein kinase C. *Kidney Int.* 55, 252–260

- 23 Zalba, G. *et al.* (2000) Vascular NADH/NADPH oxidase is involved in enhanced superoxide production in spontaneously hypertensive rats. *Hypertension* 35, 1055–1061
- 24 Madamanchi, N.R. *et al.* (2005) Oxidative Stress and Vascular Disease. *Arterioscler. Thromb. Vasc. Biol.* 25, 29–38
- 25 Dizdaroglu, M. (2012) Oxidatively induced DNA damage: Mechanisms, repair and disease. *Cancer Lett.* 327, 26–47
- 26 Mahmoudi, M. *et al.* (2006) DNA damage and repair in atherosclerosis. *Cardiovasc. Res.* 71, 259–268
- 27 Fyhrquist, F. *et al.* (2013) The roles of senescence and telomere shortening in cardiovascular disease. *Nat. Rev. Cardiol.* 10, 274–83
- 28 Blasco, M. a (2007) Telomere length, stem cells and aging. *Nat. Chem. Biol.* 3, 640–649
- 29 Wang, J.C. and Bennett, M. (2012) Aging and Atherosclerosis: Mechanisms, Functional Consequences, and Potential Therapeutics for Cellular Senescence. *Circ. Res.* 111, 245–259
- 30 Petersen, S. *et al.* (1998) Preferential accumulation of single-stranded regions in telomeres of human fibroblasts. *Exp. Cell Res.* 239, 152–60
- 31 Moon, S.K. *et al.* (2001) Aging, oxidative responses, and proliferative capacity in cultured mouse aortic smooth muscle cells. *Am. J. Physiol. Heart Circ. Physiol.* 280, H2779–H2788
- 32 Matthews, C. *et al.* (2006) Vascular smooth muscle cells undergo telomere-based senescence in human atherosclerosis: Effects of telomerase and oxidative stress. *Circ. Res.* 99, 156–164
- 33 Houtkooper, R.H. and Auwerx, J. (2012) Exploring the therapeutic space around

- NAD<sup>+</sup>. *J. Cell Biol.* 199, 205–209
- 34 Houtkooper, R.H. *et al.* (2010) The Secret Life of NAD<sup>+</sup>: An Old Metabolite Controlling New Metabolic Signaling Pathways. *Endocr. Rev.* 31, 194–223
- 35 Berger, F. *et al.* (2004) The new life of a centenarian: signalling functions of NAD(P). *Trends Biochem. Sci.* 29, 111–118
- 36 Kugel, S. and Mostoslavsky, R. (2014) Chromatin and beyond: the multitasking roles for SIRT6. *Trends Biochem. Sci.* 39, 72–81
- 37 Garten, A. *et al.* (2015) Physiological and pathophysiological roles of NAMPT and NAD metabolism. *Nat. Rev. Endocrinol.* 11, 535–546
- 38 van der Veer, E. *et al.* (2007) Extension of human cell lifespan by nicotinamide phosphoribosyltransferase. *J. Biol. Chem.* 282, 10841–5
- 39 Ciccia, A. and Elledge, S.J. (2010) The DNA Damage Response: Making It Safe to Play with Knives. *Mol. Cell* 40, 179–204
- 40 Toiber, D. *et al.* (2013) SIRT6 recruits SNF2H to DNA break sites, preventing genomic instability through chromatin remodeling. *Mol. Cell* 51, 454–68
- 41 Sousa, F.G. *et al.* (2012) PARPs and the DNA damage response. *Carcinogenesis* 33, 1433–1440
- 42 Schreiber, V. *et al.* (2006) Poly(ADP-ribose): novel functions for an old molecule. *Nat. Rev. Mol. Cell Biol.* 7, 517–528
- 43 Min, W.K. *et al.* (2010) Deletion of the nuclear isoform of poly(ADP-ribose) glycohydrolase (PARG) reveals its function in DNA repair, genomic stability and tumorigenesis. *Carcinogenesis* 31, 2058–2065
- 44 D'Amours, D. *et al.* (1999) Poly(ADP-ribosyl)ation reactions in the regulation of nuclear functions. *Biochem. J.* 342 ( Pt 2, 249–268

- 45 Rine, J. *et al.* (1979) A suppressor of mating-type locus mutations in *Saccharomyces cerevisiae*: Evidence for and identification of cryptic mating-type loci. *Genetics* 93, 877–901
- 46 Shore, D. *et al.* (1984) Characterization of two genes required for the position-effect control of yeast mating-type genes. *EMBO J.* 3, 2817–2823
- 47 Ivy, J.M. *et al.* (1986) Cloning and characterization of four SIR genes of *Saccharomyces cerevisiae*. *Mol. Cell. Biol.* 6, 688–702
- 48 Rine, J. and Herskowitz, I. (1987) Four genes responsible for a position effect on expression from HML and HMR in *Saccharomyces cerevisiae*. *Genetics* 116, 9–22
- 49 Moretti, P. *et al.* (1994) Evidence that a complex of SIR proteins interacts with the silencer and telomere-binding protein RAP1. *Genes Dev.* 8, 2257–2269
- 50 Strahl-Bolsinger, S. *et al.* (1997) SIR2 and SIR4 interactions differ in core and extended telomeric heterochromatin in yeast. *Genes Dev.* 11, 83–93
- 51 Gottlieb, S. and Esposito, R.E. (1989) A new role for a yeast transcriptional silencer gene, SIR2, in regulation of recombination in ribosomal DNA. *Cell* 56, 771–776
- 52 Smith, J.S. and Boeke, J.D. (1997) An unusual form of transcriptional silencing in yeast ribosomal DNA. *Genes Dev.* 11, 241–254
- 53 Fritze, C.E. *et al.* (1997) Direct evidence for SIR2 modulation of chromatin structure in yeast rDNA. *EMBO J.* 16, 6495–509
- 54 Brachmann CB *et al.* (1995) The SIR2 gene family, conserved from bacteria to humans, functions in silencing, cell cycle progression, and chromosome stability. *Genes Dev.* 9, 2888–2902.
- 55 Tanny, J.C. *et al.* (1999) An enzymatic activity in the yeast Sir2 protein that is essential for gene silencing. *Cell* 99, 735–745



- 56 Imai, S. *et al.* (2000) Transcriptional silencing and longevity protein Sir2 is an NAD-dependent histone deacetylase. *Nature* 403, 795–800
- 57 Lombardi, P.M. *et al.* (2011) Structure, mechanism, and inhibition of histone deacetylases and related metalloenzymes. *Curr. Opin. Struct. Biol.* 21, 735–743
- 58 Tanner, K.G. *et al.* (2000) Silent information regulator 2 family of NAD-dependent histone/protein deacetylases generates a unique product, 1-O-acetyl-ADP-ribose. *Proc. Natl. Acad. Sci. U. S. A.* 97, 14178–14182
- 59 Kaeberlein, M. *et al.* (1999) Saccharomyces cerevisiae by two different mechanisms promote longevity in Saccharomyces cerevisiae by two different mechanisms. *Genes Dev.* 13, 2570–2580
- 60 Frye, R. a (1999) Characterization of five human cDNAs with homology to the yeast SIR2 gene: Sir2-like proteins (sirtuins) metabolize NAD and may have protein ADP-ribosyltransferase activity. *Biochem. Biophys. Res. Commun.* 260, 273–279
- 61 Frye, R. a (2000) Phylogenetic classification of prokaryotic and eukaryotic Sir2-like proteins. *Biochem. Biophys. Res. Commun.* 273, 793–798
- 62 Michishita, E. *et al.* (2005) Evolutionarily conserved and nonconserved cellular localizations and functions of human SIRT proteins. *Mol. Biol. Cell* 16, 4623–4635
- 63 Haigis, M.C. *et al.* (2006) SIRT4 Inhibits Glutamate Dehydrogenase and Opposes the Effects of Calorie Restriction in Pancreatic  $\beta$  Cells. *Cell* 126, 941–954
- 64 Tanno, M. *et al.* (2006) Nucleocytoplasmic Shuttling of the NAD<sup>+</sup>-dependent Histone Deacetylase SIRT1. *J. Biol. Chem.* 282, 6823–6832
- 65 Cheng, H.-L. *et al.* (2003) Developmental defects and p53 hyperacetylation in Sir2 homolog (SIRT1)-deficient mice. *Proc. Natl. Acad. Sci. U. S. A.* 100, 10794–10799

- 66 Mcburney, M.W. *et al.* (2003) The Mammalian SIR2  $\alpha$  Protein Has a Role in Embryogenesis and Gametogenesis The Mammalian SIR2  $\alpha$  Protein Has a Role in Embryogenesis and Gametogenesis. *Mol. Cell. Biol.* 23, 38–54
- 67 Mercken, E.M. *et al.* (2014) SIRT1 but not its increased expression is essential for lifespan extension in caloric-restricted mice. *Aging Cell* 13, 193–6
- 68 Herranz, D. *et al.* (2010) Sirt1 improves healthy ageing and protects from metabolic syndrome-associated cancer. *Nat. Commun.* 1, 3
- 69 Satoh, A. *et al.* (2013) Sirt1 Extends Life Span and Delays Aging in Mice through the Regulation of Nk2 Homeobox 1 in the DMH and LH. *Cell Metab.* 18, 416–430
- 70 Chawla, A. *et al.* (2001) Nuclear Receptors and Lipid Physiology: Opening the X-Files. *Science* (80-. ). 294, 1866–1870
- 71 Purushotham, A. *et al.* (2009) Hepatocyte-Specific Deletion of SIRT1 Alters Fatty Acid Metabolism and Results in Hepatic Steatosis and Inflammation. *Cell Metab.* 9, 327–338
- 72 Gerhart-Hines, Z. *et al.* (2007) Metabolic control of muscle mitochondrial function and fatty acid oxidation through SIRT1/PGC-1 $\alpha$ . *EMBO J.* 26, 1913–1923
- 73 Rodgers, J.T. *et al.* (2005) Nutrient control of glucose homeostasis through a complex of PGC-1 $\alpha$  and SIRT1. *Nature* 434, 113–118
- 74 Picard, F. *et al.* (2004) Sirt1 promotes fat mobilization in white adipocytes by repressing PPAR- $\gamma$ . *Nature* 429, 771–776
- 75 Qiang, L. *et al.* (2012) Brown remodeling of white adipose tissue by SirT1-dependent deacetylation of Ppar $\gamma$ . *Cell* 150, 620–632
- 76 Ho, C. *et al.* (2009) SIRT1 markedly extends replicative lifespan if the NAD<sup>+</sup> salvage pathway is enhanced. *FEBS Lett.* 583, 3081–3085
- 77 Thompson, A.M. *et al.* (2014) Age-related loss of SirT1 expression results in

- dysregulated human vascular smooth muscle cell function. *Am. J. Physiol. Heart Circ. Physiol.* 307, H533–41
- 78 Gorenne, I. *et al.* (2013) Vascular Smooth Muscle Cell Sirtuin 1 Protects Against DNA Damage and Inhibits Atherosclerosis. *Circulation* 127, 386–396
- 79 Takemura, a. *et al.* (2011) Sirtuin 1 Retards Hyperphosphatemia-Induced Calcification of Vascular Smooth Muscle Cells. *Arterioscler. Thromb. Vasc. Biol.* 31, 2054–2062
- 80 Li, L. *et al.* (2011) SIRT1 acts as a modulator of neointima formation following vascular injury in mice. *Circ. Res.* 108, 1180–1189
- 81 Li, L. *et al.* (2011) SIRT1 inhibits angiotensin II-induced vascular smooth muscle cell hypertrophy. *Acta Biochim. Biophys. Sin. (Shanghai)*. 43, 103–109
- 82 Miyazaki, R. *et al.* (2008) SIRT1, a Longevity Gene, Downregulates Angiotensin II Type 1 Receptor Expression in Vascular Smooth Muscle Cells. *Arterioscler. Thromb. Vasc. Biol.* 28, 1263–1269
- 83 Gao, P. *et al.* (2014) Overexpression of SIRT1 in vascular smooth muscle cells attenuates angiotensin II-induced vascular remodeling and hypertension in mice. *J. Mol. Med.* 92, 347–357
- 84 Fry, J.L. *et al.* (2015) Vascular Smooth Muscle Sirtuin-1 Protects Against Aortic Dissection During Angiotensin II-induced Hypertension. *J. Am. Heart Assoc.* 4, 1–16
- 85 Inoue, T. *et al.* (2007) SIRT2, a tubulin deacetylase, acts to block the entry to chromosome condensation in response to mitotic stress. *Oncogene* 26, 945–957
- 86 North, B.J. *et al.* (2003) The Human Sir2 Ortholog, SIRT2, Is an NAD<sup>+</sup> - Dependent Tubulin Deacetylase. *Mol. Cell* 11, 437–444
- 87 Tang, B.L. and Chua, C.E.L. (2008) SIRT2, tubulin deacetylation, and

- oligodendroglia differentiation. *Cell Motil. Cytoskeleton* 65, 179–182
- 88 Vaquero, A. *et al.* (2006) SirT2 is a histone deacetylase with preference for histone H4 Lys 16 during mitosis. *Genes Dev.* 20, 1256–1261
- 89 North, B.J. *et al.* (2014) SIRT2 induces the checkpoint kinase BubR1 to increase lifespan. *EMBO J.* 33, 1438–1453
- 90 Kim, H.-S. *et al.* (2011) SIRT2 Maintains Genome Integrity and Suppresses Tumorigenesis through Regulating APC/C Activity. *Cancer Cell* 20, 487–499
- 91 Gomes, P. *et al.* (2015) Emerging Role of Sirtuin 2 in the Regulation of Mammalian Metabolism. *Trends Pharmacol. Sci.* 36, 756–768
- 92 Jing, E. *et al.* (2007) SIRT2 Regulates Adipocyte Differentiation through FoxO1 Acetylation/Deacetylation. *Cell Metab.* 6, 105–114
- 93 Wang, F. and Tong, Q. (2009) SIRT2 Suppresses Adipocyte Differentiation by Deacetylating FOXO1 and Enhancing FOXO1's Repressive Interaction with PPAR $\gamma$ . *Mol. Biol. Cell* 20, 801–808
- 94 Rothgiesser, K.M. *et al.* (2010) SIRT2 regulates NF- $\kappa$ B dependent gene expression through deacetylation of p65 Lys310. *J. Cell Sci.* 123, 4251–4258
- 95 Lo Sasso, G. *et al.* (2014) SIRT2 Deficiency Modulates Macrophage Polarization and Susceptibility to Experimental Colitis. *PLoS One* 9, e103573
- 96 Wang, F. *et al.* (2007) SIRT2 deacetylates FOXO3a in response to oxidative stress and caloric restriction. *Aging Cell* 6, 505–514
- 97 Liu, J. *et al.* (2013) Global gene expression profiling reveals functional importance of sirt2 in endothelial cells under oxidative stress. *Int. J. Mol. Sci.* 14, 5633–5649
- 98 Hashimoto-Komatsu, A. *et al.* (2011) Angiotensin II induces microtubule reorganization mediated by a deacetylase SIRT2 in endothelial cells. *Hypertens. Res.* 34, 949–956

- 99 Ahn, B.-H. *et al.* (2008) A role for the mitochondrial deacetylase Sirt3 in regulating energy homeostasis. *Proc. Natl. Acad. Sci. U. S. A.* 105, 14447–14452
- 100 Palacios, O.M. *et al.* (2009) Diet and exercise signals regulate SIRT3 and activate AMPK and PGC-1alpha in skeletal muscle. *Aging (Albany, NY)*. 1, 771–783
- 101 Lombard, D.B. *et al.* (2007) Mammalian Sir2 Homolog SIRT3 Regulates Global Mitochondrial Lysine Acetylation. *Mol. Cell. Biol.* 27, 8807–8814
- 102 Cimen, H. *et al.* (2010) Regulation of Succinate Dehydrogenase Activity by SIRT3 in Mammalian Mitochondria. *Biochemistry* 49, 304–311
- 103 Jing, E. *et al.* (2011) Sirtuin-3 (Sirt3) regulates skeletal muscle metabolism and insulin signaling via altered mitochondrial oxidation and reactive oxygen species production. *Proc. Natl. Acad. Sci. U. S. A.* 108, 14608–14613
- 104 Schlicker, C. *et al.* (2008) Substrates and Regulation Mechanisms for the Human Mitochondrial Sirtuins Sirt3 and Sirt5. *J. Mol. Biol.* 382, 790–801
- 105 Hallows, W.C. *et al.* (2011) Sirt3 promotes the urea cycle and fatty acid oxidation during dietary restriction. *Mol Cell* 41, 139–149
- 106 Kim, H.-S. *et al.* (2010) SIRT3 Is a Mitochondria-Localized Tumor Suppressor Required for Maintenance of Mitochondrial Integrity and Metabolism during Stress. *Cancer Cell* 17, 41–52
- 107 Finley, L.W.S. *et al.* (2011) SIRT3 opposes reprogramming of cancer cell metabolism through HIF1 $\alpha$  destabilization. *Cancer Cell* 19, 416–28
- 108 Fan, J. *et al.* (2014) Tyr Phosphorylation of PDP1 Toggles Recruitment between ACAT1 and SIRT3 to Regulate the Pyruvate Dehydrogenase Complex. *Mol. Cell* 53, 534–548
- 109 Qiu, X. *et al.* (2010) Calorie Restriction Reduces Oxidative Stress by SIRT3-Mediated SOD2 Activation. *Cell Metab.* 12, 662–667

- 110 Someya, S. *et al.* (2010) Sirt3 mediates reduction of oxidative damage and prevention of age-related hearing loss under Caloric Restriction. *Cell* 143, 802–812
- 111 Tao, R. *et al.* (2010) Sirt3-Mediated Deacetylation of Evolutionarily Conserved Lysine 122 Regulates MnSOD Activity in Response to Stress. *Mol. Cell* 40, 893–904
- 112 Chen, Y. *et al.* (2011) Tumour suppressor SIRT3 deacetylates and activates manganese superoxide dismutase to scavenge ROS. *EMBO Rep.* 12, 534–541
- 113 Bell, E.L. *et al.* (2011) SirT3 suppresses hypoxia inducible factor 1 $\alpha$  and tumor growth by inhibiting mitochondrial ROS production. *Oncogene* 30, 2986–2996
- 114 Hirschev, M.D. *et al.* (2010) SIRT3 regulates mitochondrial fatty-acid oxidation by reversible enzyme deacetylation. *Nature* 464, 121–125
- 115 Hirschev, M.D. *et al.* (2011) SIRT3 deficiency and mitochondrial protein hyperacetylation accelerate the development of the metabolic syndrome. *Mol. Cell* 44, 177–90
- 116 Sundaresan, N.R. *et al.* (2008) SIRT3 Is a Stress-Responsive Deacetylase in Cardiomyocytes That Protects Cells from Stress-Mediated Cell Death by Deacetylation of Ku70. *Mol. Cell. Biol.* 28, 6384–6401
- 117 Hafner, A. V. *et al.* (2010) Regulation of the mPTP by SIRT3-mediated deacetylation of CypD at lysine 166 suppresses age-related cardiac hypertrophy. *Aging (Albany. NY)*. 2, 914–923
- 118 Sundaresan, N.R. *et al.* (2009) Sirt3 blocks the cardiac hypertrophic response by augmenting Foxo3a-dependent antioxidant defense mechanisms in mice. *J. Clin. Invest.* 119, 2758–2771
- 119 Tseng, A.H.-H. *et al.* (2014) SIRT3 interactions with FOXO3 acetylation, phosphorylation and ubiquitinylation mediate endothelial cell responses to

- hypoxia. *Biochem. J.* 464, 157–68
- 120 Winnik, S. *et al.* (2014) Deletion of Sirt3 does not affect atherosclerosis but accelerates weight gain and impairs rapid metabolic adaptation in LDL receptor knockout mice: implications for cardiovascular risk factor development. *Basic Res. Cardiol.* 109, 399
- 121 Paulin, R. *et al.* (2014) Sirtuin 3 deficiency is associated with inhibited mitochondrial function and pulmonary arterial hypertension in rodents and humans. *Cell Metab.* 20, 827–39
- 122 Herrero-Yraola, a *et al.* (2001) Regulation of glutamate dehydrogenase by reversible ADP-ribosylation in mitochondria. *EMBO J.* 20, 2404–12
- 123 Ahuja, N. *et al.* (2007) Regulation of Insulin Secretion by SIRT4, a Mitochondrial ADP-ribosyltransferase. *J. Biol. Chem.* 282, 33583–33592
- 124 Wise, D.R. and Thompson, C.B. (2010) Glutamine addiction: a new therapeutic target in cancer. *Trends Biochem. Sci.* 35, 427–433
- 125 Jeong, S.M. *et al.* (2013) SIRT4 Has Tumor-Suppressive Activity and Regulates the Cellular Metabolic Response to DNA Damage by Inhibiting Mitochondrial Glutamine Metabolism. *Cancer Cell* 23, 450–463
- 126 Jeong, S.M. *et al.* (2014) SIRT4 protein suppresses tumor formation in genetic models of Myc-induced B cell lymphoma. *J. Biol. Chem.* 289, 4135–4144
- 127 Csibi, A. *et al.* (2013) The mTORC1 Pathway Stimulates Glutamine Metabolism and Cell Proliferation by Repressing SIRT4. *Cell* 153, 840–854
- 128 Nasrin, N. *et al.* (2010) SIRT4 Regulates Fatty Acid Oxidation and Mitochondrial Gene Expression in Liver and Muscle Cells. *J. Biol. Chem.* 285, 31995–32002
- 129 Laurent, G. *et al.* (2013) SIRT4 coordinates the balance between lipid synthesis and catabolism by repressing malonyl CoA decarboxylase. *Mol. Cell* 50, 686–98

- 130 Chen, Y. *et al.* (2014) SIRT4 inhibits cigarette smoke extracts-induced mononuclear cell adhesion to human pulmonary microvascular endothelial cells via regulating NF- $\kappa$ B activity. *Toxicol. Lett.* 226, 320–7
- 131 Matsushita, N. *et al.* (2011) Distinct regulation of mitochondrial localization and stability of two human Sirt5 isoforms. *Genes to Cells* 16, 190–202
- 132 Nakagawa, T. *et al.* (2009) SIRT5 Deacetylates Carbamoyl Phosphate Synthetase 1 and Regulates the Urea Cycle. *Cell* 137, 560–570
- 133 Rardin, M.J. *et al.* (2013) SIRT5 Regulates the Mitochondrial Lysine Succinylome and Metabolic Networks. *Cell Metab.* 18, 920–933
- 134 Yu, J. *et al.* (2013) Metabolic characterization of a Sirt5 deficient mouse model. *Sci. Rep.* 3, 1–7
- 135 Ogura, M. *et al.* (2010) Overexpression of SIRT5 confirms its involvement in deacetylation and activation of carbamoyl phosphate synthetase 1. *Biochem. Biophys. Res. Commun.* 393, 73–8
- 136 Du, J. *et al.* (2011) Sirt5 is a NAD-dependent protein lysine demalonylase and desuccinylase. *Science* 334, 806–9
- 137 Tan, M. *et al.* (2014) Lysine Glutarylation Is a Protein Posttranslational Modification Regulated by SIRT5. *Cell Metab.* 19, 605–617
- 138 Polletta, L. *et al.* (2015) SIRT5 regulation of ammonia-induced autophagy and mitophagy. *Autophagy* 11, 253–70
- 139 Park, J. *et al.* (2013) SIRT5-Mediated Lysine Desuccinylation Impacts Diverse Metabolic Pathways. *Mol. Cell* 50, 919–930
- 140 Nishida, Y. *et al.* (2015) SIRT5 Regulates both Cytosolic and Mitochondrial Protein Malonylation with Glycolysis as a Major Target. *Mol. Cell* 59, 1–13
- 141 Dong, C. *et al.* (2011) Association of the sirtuin and mitochondrial uncoupling



- protein genes with carotid plaque. *PLoS One* 6, 1–8
- 142 Ford, E. *et al.* (2006) Mammalian Sir2 homolog SIRT7 is an activator of RNA polymerase I transcription. *Genes Dev.* 20, 1075–1080
- 143 Kiran, S. *et al.* (2015) Sirtuin 7 in cell proliferation, stress and disease: Rise of the Seventh Sirtuin! *Cell. Signal.* 27, 673–682
- 144 Grob, A. *et al.* (2009) Involvement of SIRT7 in resumption of rDNA transcription at the exit from mitosis. *J. Cell Sci.* 122, 489–498
- 145 Chen, S. *et al.* (2013) Repression of RNA polymerase I upon stress is caused by inhibition of RNA-dependent deacetylation of PAF53 by SIRT7. *Mol. Cell* 52, 303–13
- 146 Barber, M.F. *et al.* (2012) SIRT7 links H3K18 deacetylation to maintenance of oncogenic transformation. *Nature* 487, 114–118
- 147 Shin, J. *et al.* (2013) SIRT7 represses myc activity to suppress er stress and prevent fatty liver disease. *Cell Rep.* 5, 654–665
- 148 Yoshizawa, T. *et al.* (2014) SIRT7 controls hepatic lipid metabolism by regulating the ubiquitin-proteasome pathway. *Cell Metab.* 19, 712–721
- 149 Vakhrusheva, O. *et al.* (2008) Sirt7 increases stress resistance of cardiomyocytes and prevents apoptosis and inflammatory cardiomyopathy in mice. *Circ. Res.* 102, 703–710
- 150 Tennen, R.I. *et al.* (2010) Functional dissection of SIRT6: identification of domains that regulate histone deacetylase activity and chromatin localization. *Mech. Ageing Dev.* 131, 185–92
- 151 Liszt, G. *et al.* (2005) Mouse Sir2 homolog SIRT6 is a nuclear ADP-ribosyltransferase. *J. Biol. Chem.* 280, 21313–20
- 152 Michishita, E. *et al.* (2008) SIRT6 is a histone H3 lysine 9 deacetylase that

- modulates telomeric chromatin. *Nature* 452, 492–496
- 153 Pan, P.W. *et al.* (2011) Structure and biochemical functions of SIRT6. *J. Biol. Chem.* 286, 14575–87
- 154 Michishita, E. *et al.* (2009) Cell cycle-dependent deacetylation of telomeric histone H3 lysine K56 by human SIRT6. *Cell Cycle* 8, 2664–6
- 155 Yang, B. *et al.* (2009) The sirtuin SIRT6 deacetylates H3 K56Ac in vivo to promote genomic stability. *Cell Cycle* 8, 2662–3
- 156 Kaidi, A. *et al.* (2010) Human SIRT6 promotes DNA end resection through CtIP deacetylation. *Science* 329, 1348–53
- 157 Dominy, J.E. *et al.* (2012) The Deacetylase Sirt6 Activates the Acetyltransferase GCN5 and Suppresses Hepatic Gluconeogenesis. *Mol. Cell* 48, 900–913
- 158 Jiang, H. *et al.* (2013) SIRT6 regulates TNF- $\alpha$  secretion through hydrolysis of long-chain fatty acyl lysine. *Nature* 496, 110–3
- 159 Feldman, J.L. *et al.* (2013) Activation of the protein deacetylase SIRT6 by long-chain fatty acids and widespread deacylation by Mammalian Sirtuins. *J. Biol. Chem.* 288, 31350–31356
- 160 Gil, R. *et al.* (2013) SIRT6 exhibits nucleosome-dependent deacetylase activity. *Nucleic Acids Res.* 41, 1–9
- 161 Min, L. *et al.* (2012) Liver cancer initiation is controlled by AP-1 through SIRT6-dependent inhibition of survivin. *Nat. Cell Biol.* 14, 1203–1211
- 162 Sharma, A. *et al.* (2013) The role of SIRT6 protein in aging and reprogramming of human induced pluripotent stem cells. *J. Biol. Chem.* 288, 18439–18447
- 163 Elhanati, S. *et al.* (2013) Multiple regulatory layers of SREBP1/2 by SIRT6. *Cell Rep.* 4, 905–12

- 164 Ronnebaum, S.M. *et al.* (2013) The ubiquitin ligase CHIP prevents SirT6 degradation through noncanonical ubiquitination. *Mol. Cell. Biol.* 33, 4461–72
- 165 Mostoslavsky, R. *et al.* (2006) Genomic instability and aging-like phenotype in the absence of mammalian SIRT6. *Cell* 124, 315–329
- 166 Xiao, C. *et al.* (2010) SIRT6 deficiency results in severe hypoglycemia by enhancing both basal and insulin-stimulated glucose uptake in mice. *J. Biol. Chem.* 285, 36776–84
- 167 Xiao, C. *et al.* (2012) Progression of chronic liver inflammation and fibrosis driven by activation of c-JUN signaling in Sirt6 mutant mice. *J. Biol. Chem.* 287, 41903–41913
- 168 Kanfi, Y. *et al.* (2012) The sirtuin SIRT6 regulates lifespan in male mice. *Nature* 483, 218–221
- 169 Kanfi, Y. *et al.* (2010) SIRT6 protects against pathological damage caused by diet-induced obesity. *Aging Cell* 9, 162–73
- 170 Schwer, B. *et al.* (2010) Neural sirtuin 6 (Sirt6) ablation attenuates somatic growth and causes obesity. *Proc. Natl. Acad. Sci.* 107, 21790–94
- 171 Kim, H.S. *et al.* (2010) Hepatic-specific disruption of SIRT6 in mice results in fatty liver formation due to enhanced glycolysis and triglyceride synthesis. *Cell Metab.* 12, 224–236
- 172 Sundaesan, N.R. *et al.* (2012) The sirtuin SIRT6 blocks IGF-Akt signaling and development of cardiac hypertrophy by targeting c-Jun. *Nat. Med.* 18, 1643–50
- 173 Tao, R. *et al.* (2013) Hepatic SREBP-2 and cholesterol biosynthesis are regulated by FoxO3 and Sirt6. *J. Lipid Res.* 54, 2745–53
- 174 Zhong, L. *et al.* (2010) The histone deacetylase Sirt6 regulates glucose homeostasis via Hif1alpha. *Cell* 140, 280–93

- 175 Zhang, P. *et al.* (2014) Tumor suppressor p53 cooperates with SIRT6 to regulate gluconeogenesis by promoting FoxO1 nuclear exclusion. *Proc. Natl. Acad. Sci. U. S. A.* 111, 1–6
- 176 Anderson, J.G. *et al.* (2015) Enhanced insulin sensitivity in skeletal muscle and liver by physiological overexpression of SIRT6. *Mol. Metab.* 4, 846–856
- 177 Heiden, M.G. Vander *et al.* (2009) Understanding the Warburg Effect : Cell Proliferation. *Science (80-. )*. 324, 1029–1034
- 178 Sebastián, C. *et al.* (2012) The histone deacetylase SIRT6 Is a tumor suppressor that controls cancer metabolism. *Cell* 151, 1185–1199
- 179 Fukuda, T. *et al.* (2015) Putative tumor suppression function of SIRT6 in endometrial cancer. *FEBS Lett.* 589, 2274–2281
- 180 Thirumurthi, U. *et al.* (2014) MDM2-mediated degradation of SIRT6 phosphorylated by AKT1 promotes tumorigenesis and trastuzumab resistance in breast cancer. *Sci. Signal.* 7, ra71–ra71
- 181 Kugel, S. *et al.* (2015) Identification of and Molecular Basis for SIRT6 Loss-of-Function Point Mutations in Cancer. *Cell Rep.* DOI: 10.1016/j.celrep.2015.09.022
- 182 Mccord, A. *et al.* (2009) SIRT6 stabilizes DNA-dependent protein kinase at chromatin for DNA double-strand break repair. *Aging (Albany. NY)*. 1, 109–121
- 183 Mao, Z. *et al.* (2012) Sirtuin 6 ( SIRT6 ) rescues the decline of homologous recombination repair during replicative senescence. *Proc. Natl. Acad. Sci.* 109, 11800–11805
- 184 Xu, Z. *et al.* (2015) SIRT6 rescues the age related decline in base excision repair in a PARP1-dependent manner. *Cell Cycle* 14, 269–76
- 185 Mao, Z. *et al.* (2011) SIRT6 promotes DNA repair under stress by activating PARP1. *Science* 332, 1443–1446

- 186 Van Gool, F. *et al.* (2009) Intracellular NAD levels regulate tumor necrosis factor protein synthesis in a sirtuin-dependent manner. *Nat. Med.* 15, 206–10
- 187 Bauer, I. *et al.* (2012) The NAD<sup>+</sup>-dependent histone deacetylase SIRT6 promotes cytokine production and migration in pancreatic cancer cells by regulating Ca<sup>2+</sup> responses. *J. Biol. Chem.* 287, 40924–37
- 188 Kawahara, T.L. a *et al.* (2009) SIRT6 links histone H3 lysine 9 deacetylation to NF-kappaB-dependent gene expression and organismal life span. *Cell* 136, 62–74
- 189 Lee, H.-S. *et al.* (2013) Overexpression of sirtuin 6 suppresses inflammatory responses and bone destruction in mice with collagen-induced arthritis. *Arthritis Rheum.* 65, 1776–85
- 190 Wu, Y. *et al.* (2015) Overexpression of Sirtuin 6 suppresses cellular senescence and NF-κB mediated inflammatory responses in osteoarthritis development. *Sci. Rep.* 5, 17602
- 191 Yu, S.-S. *et al.* (2013) Sirtuin 6 protects cardiomyocytes from hypertrophy *in vitro* via inhibition of NF-κB-dependent transcriptional activity. *Br. J. Pharmacol.* 168, 117–128
- 192 Maksin-Matveev, A. *et al.* (2015) Sirtuin 6 protects the heart from hypoxic damage. *Exp. Cell Res.* 330, 81–90
- 193 Cardus, A. *et al.* (2013) SIRT6 protects human endothelial cells from DNA damage, telomere dysfunction, and senescence. *Cardiovasc. Res.* 97, 571–9
- 194 Yao, Q.-P. *et al.* (2014) The role of SIRT6 in the differentiation of vascular smooth muscle cells in response to cyclic strain. *Int. J. Biochem. Cell Biol.* 49, 98–104
- 195 Li, S. *et al.* (1999) Evidence from a novel human cell clone that adult vascular smooth muscle cells can convert reversibly between noncontractile and contractile phenotypes. *Circ. Res.* 85, 338–348

- 196 Wirth, A. *et al.* (2008) G12-G13-LARG-mediated signaling in vascular smooth muscle is required for salt-induced hypertension. *Nat. Med.* 14, 64–8
- 197 Jaisser, F. (2000) Inducible gene expression and gene modification in transgenic mice. *J. Am. Soc. Nephrol.* 11 Suppl 1, S95–S100
- 198 Feil, S. *et al.* (2014) Mouse Genetics. In *Methods in Molecular Biology* 1194 (Singh, S. R. and Coppola, V., eds), pp. 113–139, Springer Science+Business Media
- 199 Owens, a P. *et al.* (2010) Angiotensin II induces a region-specific hyperplasia of the ascending aorta through regulation of inhibitor of differentiation 3. *Circ. Res.* 106, 611–9
- 200 Simeoni, F. *et al.* (2013) Proteomic analysis of the SIRT6 interactome: novel links to genome maintenance and cellular stress signaling. *Sci. Rep.* 3, 1–6
- 201 Majesky, M.W. (2007) Developmental basis of vascular smooth muscle diversity. *Arterioscler. Thromb. Vasc. Biol.* 27, 1248–1258
- 202 Topouzis, S. and Majesky, M.W. (1996) Smooth muscle lineage diversity in the chick embryo. Two types of aortic smooth muscle cell differ in growth and receptor-mediated transcriptional responses to transforming growth factor-beta. *Dev. Biol.* 178, 430–45
- 203 Goldfinger, J.Z. *et al.* (2014) Thoracic aortic aneurysm and dissection. *J. Am. Coll. Cardiol.* 64, 1725–1739
- 204 Helming, L. (2011) Inflammation: Cell Recruitment versus local proliferation. *Curr. Biol.* 21, R548–R550
- 205 Saraff, K. *et al.* (2003) Aortic dissection precedes formation of aneurysms and atherosclerosis in angiotensin II-infused, apolipoprotein E-deficient mice. *Arterioscler. Thromb. Vasc. Biol.* 23, 1621–1626

- 206 Tieu, B.C. *et al.* (2009) An adventitial IL-6/MCP1 amplification loop accelerates macrophage-mediated vascular inflammation leading to aortic dissection in mice. *J. Clin. Invest.* 119, 3637–3651
- 207 Dudzinski, D.M. and Isselbacher, E.M. (2015) Diagnosis and Management of Thoracic Aortic Disease. *Curr. Cardiol. Rep.* 17, 1–6
- 208 Trachet, B. *et al.* (2015) Dissecting abdominal aortic aneurysm in Ang II-infused mice: suprarenal branch ruptures and apparent luminal dilatation. *Cardiovasc. Res.* 105, 213–222
- 209 Daugherty, A. and Cassis, L.A. (2004) Mouse Models of Abdominal Aortic Aneurysms. *Arterioscler. Thromb. Vasc. Biol.* 24, 429–434
- 210 Rateri, D.L. *et al.* (2014) Angiotensin II induces region-specific medial disruption during evolution of ascending aortic aneurysms. *Am. J. Pathol.* 184, 2586–2595
- 211 Bush, E. *et al.* (2000) CC chemokine receptor 2 is required for macrophage infiltration and vascular hypertrophy in angiotensin II-induced hypertension. *Hypertension* 36, 360–363
- 212 Gornik, H.L. and Creager, M. a. (2008) Aortitis. *Circulation* 117, 3039–3051
- 213 Pipitone, N. and Salvarani, C. (2011) Idiopathic aortitis: an underrecognized vasculitis. *Arthritis Res. Ther.* 13, 119
- 214 Mulligan-Kehoe, M.J. and Simons, M. (2014) Vasa vasorum in normal and diseased arteries. *Circulation* 129, 2557–2566
- 215 Marchesi, C. *et al.* (2013) Protective role of vascular smooth muscle cell PPAR?? in angiotensin II-induced vascular disease. *Cardiovasc. Res.* 97, 562–570
- 216 Li, W. *et al.* (2014) Tgfbr2 disruption in postnatal smooth muscle impairs aortic wall homeostasis. *J. Clin. Invest.* 124, 755–767
- 217 Gavazzi, G. *et al.* (2007) NOX1 Deficiency Protects From Aortic Dissection in

Response to Angiotensin II. *Hypertension* 50, 189–196

- 218 Sato, M. *et al.* (2000) Influence of corn oil and diet on reproduction and the kidney in female Sprague-Dawley rats. *Toxicol. Sci.* 56, 156–164
- 219 Ramot, Y. *et al.* (2009) Spontaneous aortitis in the Balb/c mouse. *Toxicol. Pathol.* 37, 667–671
- 220 Harno, E. *et al.* (2013) Metabolic pitfalls of CNS cre-based technology. *Cell Metab.* 18, 21–28



## Appendices

### **Appendix A: Statement of permission for the use of animals for experimental research**

All animal experimentation was conducted in compliance with the animal use protocol 2010-244 held by Dr. J. Geoffrey Pickering, principal investigator at the Schulich School of Medicine and Dentistry and the Department of Biochemistry at the University of Western Ontario in London, Ontario, Canada.

## Curriculum Vitae

**Name:** Sharon Leung

**Post-secondary Education and Degrees:** The University of Western Ontario  
London, Ontario, Canada  
2008-2012 BMSc

The University of Western Ontario  
London, Ontario, Canada  
2012-2015 MSc Biochemistry

**Honours and Awards:** CIHR Strategic Training Fellow in Vascular Research  
2012-2014

Western Graduate Research Scholarship  
2012-2014

Dean's Honour List  
2008-2012

UWO In-course Scholarship Year III  
2009-2010

**Related Work Experience** Research Assistant  
Robarts Research Institute (Dr. Pickering's lab)  
2012

**Publications:**